ABSTRACT

OXIDATION OF POLLUTANTS IN A BATCH RECIRCULATION BIOREACTOR WITH IMMOBILIZED MICROORGANISMS

by
Jongtai Jung

The purpose of this work was to study bio-oxidative destruction of several substrates in an immobilized cell batch bioreactor in recirculation configuration. This system was used in three cases: a series of substrates usually used as monomers, ethylene glycol and its tetramer, and phenol under magnetic irradiation. In addition, kinetic studies were performed and experimental versus predicted results compared.

The substances styrene, methyl methacrylate (MMA), and β-hydroxybutyric acid (HBA), common monomers, were biologically treated using an acclimated mixed microbial community immobilized in calcium alginate gel. A comparison of biodegradation rates (3.3, 9.4, and 15 ppm/hr for styrene, MMA, and HBA, respectively, at 75 ppm starting concentration, with essentially constant biomass concentration) indicates the scale of difficulty in biodegrading these monomers. The results show that styrene, which has a ring structure, as opposed to an open chain structure, is relatively more difficult to biodegrade. These results indicate that biodegradability of a substrate is related to its structure.

Biodegradation of ethylene glycol and tetraethylene glycol was also studied. During the biodegradation of ethylene glycol, qualitative analysis showed that the fairly stable intermediates were formed. One of them was identified as being formaldehyde, which is more toxic than ethylene glycol. Therefore monitoring of the parent compound concentration alone does not always provide adequate information regarding complete mineralization of an oligomer.

Studies on the effect of magnetic fields on the rate of biodegradation were also conducted. It was observed that by applying a magnetic South polar field to the process, biological oxidation is enhanced. A magnetic North field was found to inhibit oxidation.

It was also observed that by acclimating the free microorganisms to the South magnetic field prior to immobilization and by subsequently further applying the South polar field to the gel immobilized microorganisms during oxidation, biodegradation is enhanced to a greater degree. Enhancement of oxidation by up to one order of magnitude was obtained after 10 days when a magnetic South field of 0.15 tesla was applied to the bioreactor. The rate of biodegradation was observed to be a function of magnetic field strength and time of exposure.

A preliminary mathematical model describing the process is presented, along with recommendations for improvement of this bioreactor system.

OXIDATION OF POLLUTANTS IN A BATCH RECIRCULATION BIOREACTOR WITH IMMOBILIZED MICROORGANISMS

by
Jongtai Jung

A Dissertation
Submitted to the Faculty of
New Jersey Institute of Technology
in Partial Fulfillment of the Requirements for the Degree of
Doctor of Philosophy

Department of Chemical Engineering,
Chemistry and Environmental Science

May 1994

APPROVAL PAGE

OXIDATION OF POLLUTANTS IN A BATCH RECIRCULATION BIOREACTOR WITH IMMOBILIZED MICROORGANISMS

Jongtai Jung

2-1-94

Dr. Samir S. Sofer, Thesis Adviser — Date
Professor of Chemical Engineering, NJIT

2/1/94

Dr. Ching R. Huang, Committee Member — Date
Professor of Chemical Engineering, NJIT

Feb. 1, 1994

Dr. Piero M. Armenante, Committee Member — Date
Professor of Chemical Engineering, NJIT

2/1/94

Dr. Basil C. Baltzis, Committee Member — Date
Professor of Chemical Engineering, NJIT

1/14/94

Dr. Peter F. Strom, Committee Member — Date
Associate Professor of Environmental Science,
Cook College, Rutgers University

BIOGRAPHICAL SKETCH

Author: Jongtai Jung

Degree: Doctor of Philosophy in Chemical Engineering

Date: May, 1994

Undergraduate and Graduate Eduation:

- Doctor of Philosophy in Chemical Engineering, New Jersey Institute of Technology, Newark, NJ, 1994
- Master of Science in Chemical Engineering, Stevens Institute of Technology, Hoboken, NJ, 1988
- Bachelor of Science in Chemical Engineering, Inha University, Incheon, Korea, 1981

Major: Chemical Engineering

Publications and Presentations:

1. Jung, J., Lakhwala F. and Sofer S., "Biodegradation of Selected Monomers: Effect of Structure", Hazardous Waste and Hazardous Materials, Vol.10 (1993), pp.3-11

2. Jung, J., Sanji, B., Godbole, S. and Sofer, S., "Effects of Magnetic Poles on Biodegradation of Phenol", Journal of Chemical Technology and Biotechnology Vol. 56 (1993), pp.73-76, Presented at AICHE-SAMPE 1st Mini-Tech. Conference, April 1990 Newark, N.J.

3. Lakhwala, F., Jung, J. and Sofer, S., *Comparative Assessment of Wastewater Treatment by Bioremediation vs Charcoal Adsorption*, Presented at Hazmat Conference/South Oct. 1991 Atlanta,GA.

4. Jung, J. and Sofer, S., *Biodegradation of Monomers Using Immobilized Microorganisms*, Presented at ACS meeting April 1991 Atlanta, GA,

5. Jung, J. and Sofer, S., *Biodegradation of Styrene, MMA, and HBA in a Recirculating Batch Reactor*, Presented at the AICHE-SAMPE 2nd Mini-Tech. Conference, April 1991, Newark, N.J. (Award Winning paper)

6. Godbole, S., Jung, J. and Sofer, S., *Evaluation of Polymer Biodegradation Using Immobilized Microorganism*, Presented at the ACS/Mid-Atlantic Regional meeeting Madison, N.J. May 1990, Published in Conference Proceedings.

This dissertation is dedicated to
my mother

ACKNOWLEDGMENT

I wish to express my sincere appreciation to Professor Sam Sofer for his guidance, friendship and moral support throughout this research, and during my stay at the NJIT Biotechnology Laboratory.

I also thank the members of my doctoral committee, Drs. Ching Huang, Basil Baltzis, Piero Armenante, and Peter Strom for their time and effort in serving on my committee. I am especially grateful to Dr. Baltzis for guiding me through detailed oxygen consumption calculations.

I am grateful for support from the National Science Foundation, Biotechnology Chair Funds at NJIT, the Hazardous Substance Management Research Center, and the Department of Chemical Engineering, Chemistry, and Environmental Science at NJIT.

Among my colleagues, I have special regards for Dr. Fayaz Lakhwala, Emilia Rus and Timothy Roche, including all past and present members at the NJIT Biotechnology Laboratory for their help and contribution.

It will be proper to put on record, my thanks to the Stock Room personnel Yogesh Gandhi and Ram Patel for their help.

Among my family I thank my mother for encouraging me throughout my long academic career with sacrifices and perseverance. I also thank my wife, Yoojin and Ziyoon for their indirect contributions to the work have meant a lot to me.

I also express my gratitude for all church members who pray and counsel for my American life.

Finally I believe this work is due to All Mighty God's grace, I attribute it to His Glorification.

TABLE OF CONTENTS

TABLE OF CONTENTS
(Continued)

LIST OF TABLES

LIST OF FIGURES

LIST OF FIGURES
(Continued)

Figures **Page**

LIST OF FIGURES
(Continued)

CHAPTER 1

INTRODUCTION

Activated sludge from wastewater treatment is exposed to many different types of organics. These microbes are easy to acclimate and also show a fast response when challenged with an organic compound. Therefore, they are ideally suited for bio-oxidation studies.

Determination of oxygen transfer capacities and oxygen uptake rates plays an important role in biological treatment of wastewater. Oxygen uptake measurement is the most recognized method for characterization of wastewater and evaluation of kinetic parameters that determine the rate of substrate bio-oxidation.

1.1 Partial Oxidation

Partial oxidation reactions catalyzed by the surface of transition metal oxides are some of the most widely applied processes for converting hydrocarbons into valuable chemical intermediates, such as those incorporating the group -COOH, -CHO, and -CN. Similarly, partial oxidation reactions catalyzed by metal-containing enzymes such as cytochromes are involved in the sequences of reactions responsible for metabolism and efficient energy conversion in living organisms.

A catalyst for a partial-oxidation process is designed to provide a limited amount of oxygen to a reactant, allowing formation of the desired product but restricting further oxidation that would give CO and CO_2. The industrial catalysts which are successful in this way are usually complex oxides, the surfaces of which donate oxygen to adsorbed hydrocarbon reactants. During the course of thesis work, the familiar pungent odor of formaldehyde was observed, and a short qualitative study was pursued.

1.2 Batch Recirculation Reactor

Batch reactors are vessels which operate without inlet or outlet streams. Thus, a steady state cannot be reached, and changes in concentrations and/or temperature occur continuously as a function of time. Batch reactors are seldom employed on a commercial scale for gas phase reactions because the quantity of product that can be produced in a reasonably sized reactor is small. However, batch reactors are often used for liquid phase reactions. Batch reactors are generally more expensive to operate than continuous units but can provide more flexibility and control. Alternatively, the initial cost of a continuous steady state system may be higher owing to the instrumentation required. Therefore for relatively high priced products (such as pharmaceuticals) where operating expense is not a predominant factor in the total cost, batch reactors are commonly employed. They are most often used for low production capacities, in short term productions where the cost of labor and other aspects of the operations are less than the capital costs of new equipment, and constitute a small fraction of the production cost.

Since the batch reactor is always working in a transient state, it is important to ask how it should be scheduled. Batch reactors also are sometimes used to model shallow lakes that are mixed completely.

The configuration of the recirculation flow reactor enables continuous measurement of the rate of DO consumption. Thus, biodegradation of the compound in question can be assayed in terms of oxygen consumption. The recirculation batch mode with immobilized biomass is a convenient configuration for obtaining oxidation rate data. In reactions involving solid/liquid interactions, the mass transfer across the solid/liquid interface often becomes the rate limiting parameter. Linear velocity is the parameter which determines the optimum condition for operation in a region not limited by this mass transfer resistance. The batch recirculation reactor configuration enables us to determine this parameter before designing a continuous system.

1.3 Immobilization

Several techniques of cell immobilization on the surfaces of solid inert supports, and inside semipermeable polymeric membranes are in use. In general, enzymes and microbes can be immobilized in two major ways. One is by entrapment in a gel or polymer matrix (like alginate, carageenan, and polyurethane) which is permeable to the nutrients, oxygen, and the substrates. A second is by attachment on the surface of inert supports such as diatomaceous earth, glass beads, and polymeric membranes [1,2,3].

Use of immobilized microorganisms has numerous advantages over free microorganisms [4,5]. Washout of biomass is one of the most common problems encountered in the biological treatment process using suspended cultures. The recovery and subsequent re-use of biomass is easily accomplished when the biomass is immobilized. Choice of different operating modes for reactors is possible, and most important, upon immobilization there may be a desirable change in biological and chemical activity of the biomass [6]. When the biomass is entrapped, the external matrix may protect it from high concentrations of compounds which are inhibitory. When biomass is attached on the external surface of a support, the system can provide better biodegradation rates due to the reduction of external mass transfer resistance compared to biobeads, especially in a lower substrate concentration regime. On the other hand, the matrix, such as a gel, can increase overall mass transfer resistance by its presence.

1.4 Polymer Biodegradation

The annual production of plastics in the United States has increased from 30 to 60 billion lbs in the last ten years [7]. Economic and safe disposal of plastic has been a major solid waste management issue. Plastics are not inherently biodegradable and scientists historically have sought ways to make them more resistant to other kinds of degradation.

Recently, methods have been discovered which accelerate the degradation of some plastics, and they have been adopted commercially on a limited scale.

Polymers can degrade via physical, chemical, or biological reactions. They may be physically stressed, chemically attacked or consumed by microbes. All three mechanisms have been studied in efforts to accelerate natural degradation of plastics.

Photodegradation is degradation resulting from exposure to light [8,9,10]. There are three basic photodegradation technologies currently in use. The first uses an additive of Ethylene Carbon Monoxide (ECO). This carbonyl additive is sensitive to ultraviolet light, thus making the material with which it is mixed photodegradable [11]. A second additive is ketone carbonyl. This carbonyl group absorbs ultraviolet radiation, thus breaking down the long molecules found in plastics [12]. The third additive is a phenolic compound that similarly weakens the strong plastic molecules. Due to its dependency on availability of a source of light, photodegradation can be expensive. Also it cannot occur naturally in places like underground where no light source is available. On the other hand biodegradation may be less expensive and can occur naturally.

Biodegradation is assimilation or consumption of substances by living organisms. These microorganisms secrete enzymes which require a very moist environment to reach the food source. With plastics, the enzyme must break down the polymer molecules to products small enough to be taken up by the microorganism for digestion [13]. Efforts to make plastics biodegradable have pursued two ways, one to make the polymer itself susceptible to enzyme attack, and the other to incorporate biodegradable additives [14]. A starch additive or filler becomes the food for microorganisms that devour the starch, reducing long polymer molecules to smaller pieces. There are several factors such as the linkage between the individual monomer molecules, molecular weight of polymer, and the structure of monomer that may influence biodegradation rates of polymers.

Unfortunately very little is known about the mode and mechanism of biodegradation of polymers by microorganisms. A systematic study of the degradation of monomers can help understand and predict degradability of its polymers. Complete polymer biodegradation is dependent on mineralization of the monomers. Some monomers degrade faster than others, and specific rates can be measured. Therefore a series of numbers can be assigned, and this constitutes a test for biodegradation of monomers.

1.5 Magnetic Effect on Biological Systems

It is known from some studies that magnetic fields enhance biological activities [15]. Biomagnetics is the study of the effects of a magnet's energies on biological systems. It is not associated with any radio frequency or instrumental method of producing radio waves.

One view is that a magnet's two poles, the North and the South, radiate two different forms of energy. When applied to a biological system these energies may have opposite effects on biological activity.

It is therefore possible that by applying the correct type of magnetic field to the biological processes, biodegradation (biological oxidation) can be enhanced and this can prove useful in speeding up the process of degradation. The experimental direction taken for this work was to evaluate magnetic irradiation as a potential enhancer of oxidative biodegradation. It is recognized, however, that magnetic fields may have a negative impact on the safety of humans.

CHAPTER 2

LITERATURE SURVEY

2.1 Immobilized Microorganisms

Activated sludge has been recognized as one of the most versatile tools for hazardous waste treatment. Beginning from the "gestation period" to the development of "aerated lagoons and ditches", Sawyer [17] has discussed the complete evolution process in terms of 12 milestones.

The technique of using immobilized microorganisms for treatment of hazardous and toxic wastes has also been recognized by others as a promising method [18,19,20].

Westmeier and Rehm [21] studied the biodegradation of 4-chlorophenol by calcium alginate entrapped *Alcaligenes sp A7-2.* When they compared the degradation rates of free and immobilized cells, they found that calcium alginate protects the cell against the high concentration of 4-chlorophenol and allows rapid degradation.

Sofer *et al.* [22] studied the biodegradation of 2-chlorophenol using activated sludge immobilized in calcium alginate gel and on a celite carrier. They found that higher concentrations (>150 ppm) of the substrate (2-chlorophenol) had an inhibitory effect on the rate of biodegradation. They also reported that the optimum concentration of substrate was 56 ppm for biodegradation and that the total removal rate fits the Monod kinetics.

Klein *et al.* [23] investigated the kinetics of phenol degradation by free and immobilized *Candida tropicalis.* In both cases, the reaction was zero order with respect to phenol concentration over the range tested (<1g/L). Dissolved oxygen concentration was a major factor in controlling degradation rate. An attempt was made to model this effect within the beads. The radius, number of cells per bead, specific activity of each cell, bulk oxygen concentration and oxygen diffusivity within the matrix were found to be the important variables.

The diffusion characteristics of several substrates into and out of calcium alginate gel beads has been studied in detail by Tanaka *et al.* [24]. They found that the diffusion coefficients of most of the substrates (with molecular weight less than 20,000) into and from calcium alginate gel beads were the same as that of water systems. These results suggest that these substrates can diffuse easily into and out of calcium alginate gel beads. They found that the diffusion of high molecular weight substrates was limited more strongly by the increase of calcium alginate concentration in the gel beads than by the increase in calcium chloride concentration used in curing the beads.

Chien and Sofer [25] studied the performance of immobilized yeast cell reactors. They studied a number of parameters such as flow rate, yeast growth rate, bead size and type of medium. It was found that variation in these parameters had a pronounced effect on the fermentation rate. The paper presented typical ranges of the above parameters for the production of ethanol and demonstrated the pattern of changes that take place when bead size and reaction medium were varied. Different flow rates and bead sizes were used to optimize the productivity of *Saccharomyces cerevisiae* yeast cells which were immobilized in the calcium alginate gel.

One of the major concerns while using immobilized cell technology has been the transfer of oxygen across the biofilm. Due to high cell density, the requirements of DO are more than that required for a conventional free cell system. In conventional technology oxygen is often supplied by bubbling air, or occasionally pure oxygen, or hydrogen peroxide. Adlercreutz and Mattiasson [26] studied the use of hemoglobin or emulsions of perfluoro chemicals to carry oxygen to immobilized cells. Here the role of hemoglobin is not very different from its role in animals. Perfluoro chemicals are nonpolar and chemically inert organic compounds in which gases like carbon dioxide and oxygen have high solublities. Both methods have their advantages and disadvantages, but to make the process economically more realistic the authors concluded that perfluoro chemicals

were better than hemoglobin. Another way to generate oxygen *in situ* is to co-immobilize oxygen consuming organisms with oxygen producing organisms, for example, algae.

Even though the oxygen carrying capacity is increased, factors like bioparticle or pellet size can limit the availability of oxygen to the cell entrapped systems. Chen and Humphrey [27] investigated the effect of various parameters on the critical radius for the gel particle, where critical was defined as some limiting value of oxygen concentration at the center of the pellet. The parameters used were cell density respiration rate, molecular diffusivity, Michaelis-Menten constant, bulk concentration and critical concentration of dissolved oxygen. By solving for zero and first order approximations of Michaelis Menten kinetics they determined the critical radius for given conditions of biomass density, diffusivity, and specific respiration.

The specific oxygen uptake rate of entrapped microorganisms was examined by Gosmann and Rehm [28]. With increasing cell concentration in the gel, oxygen was consumed faster than it could diffuse into the biobeads. At this point the cells had to compete for oxygen and diffusion became the limiting factor for the oxygen uptake. The drawback of this study was that oxygen measurements were done in the Warburg apparatus with essentially no mixing. Hence it is likely that external diffusion (from the bulk to the surface of the bead) was also a limiting factor. By using the recirculation and small bead size we tried to elimate the external diffusion resistance.

2.2 Biodegradation of Polymers

Biodegradation of polymers still remains a relatively new and unexplored field. Presently, municipal solid waste being placed in landfills consists of nearly 30 percent inorganics and plastic [29] which are not biodegradable and, therefore, will occupy some of the volume for a long time. Taylor [30] demonstrated in his experiments that in the presence of certain enzymes, plastics break down to products small enough to be assimilated by the

microorganisms for digestion. An extensive study and review by Potts [8] reveals that some synthetic polymers support microbial growth.

The use of starch as a biodegradable filler in plastics was reported by Griffin [31]. Griffin claimed that the addition of an autooxidant would lead to degradation of buried synthetic polymer. It was reported that following burial, a polyethylene film containing fifteen percent starch decomposed in six months and the one with six percent starch required from three to five years.

PHBV is an acronym for polyhydroxybutyrate-valerate. This is an aliphatic polyester copolymer produced by some microorganisms during fermentation of sugars. Holmes [32] stated that this polymer is biodegradable and resembles polypropylene in properties. Delafield *et al.* [33] reported that poly-β-hydroxybutyrate (PHB), which is formed as a storage product by many microorganisms, is biodegradable. Brandl *et al.* [34] and Lageween *et al.* [35] recently reported the synthesis of novel biodegradable poly-β-hydroxyalkanoates (PHAs), but their biodegradability has yet to be determined. Macre *et al.* (36) and Slepechy *et al.* (37) have established the physiological role of PHB. The regulation of PHB metabolism and its physiological significance among different species has been studied. Studies on the effects of intermediates formed during biodegradation have been performed by Nakata [38]. Lusty *et al.* [39] showed that some microorganisms like *Pseudomonas lemognei* produce an extracellular depolymerase enzyme system which hydrolyzes PHB to hydroxybutyrate and the dimeric ester of the acid.

Biodegradation of intracellular PHB has been demonstrated by many workers [40,41]. The most detailed study on extracellular PHB biodegradation has been carried out on a cell free system that utilizes *Bacillus megaterium* KM negative PHB granules as substrate and soluble depolymerizing enzymes from *Rhodospirillum rubrum* by Griebel and Merrick [42]. A combined effort by some other researchers has shown that a multi-enzyme system can break down PHB to some oligomers, and the oligomers to the

monomer β-hydroxybutyrate [43,44]. In an interesting study, Dawes and Senior have proposed that PHB degradation may be regulated at the step catalyzed by β-hydroxybutyric dehydrogenase. Here, it is envisaged that competitive inhibitors of the enzyme, pyruvate and a-ketoglutarate would be at high concentrations to inhibit metabolism of PHB. This indicates that the metabolism of intermediates can play an important role in establishing degradation of the parent compound. Biodegradation of β-hydroxybutyrate has been studied by many researchers, but only with pure strains of bacteria or their enzymes [45].

Styrene monomer is a widely used, important material for synthetic resins, and solvent in polymer processing. Microbial degradation of styrene, however, is not well understood as described by Omori *et al.* [46]. They reported that isolated bacteria utilizing aromatic hydrocarbons did not grow on styrene when it was provided as a sole carbon source. In another study, Sielicki *et al.* [47] obtained a mixed community of bacteria which could utilize styrene from a landfill soil. The mixed populations provide a wide range of microbes in coexistence and can help in degrading the organic compounds through different metabolic pathways. In another study Katsuhisa and Kenichi [48] used a pure strain of *Pseudomonas 305-str-1-4* to produce β-phenethyl alcohol by hydroxylation of styrene.

Mammalian metabolism of styrene has been studied quite extensively in view of its intensive use and possible toxic and carcinogenic properties [49]. The first step in the pathway of mammalian metabolism is its oxidation to styrene oxide which is even more toxic. Microbial degradation of styrene may follow the same pathway and due to the accumulation of styrene oxide the microbial activity may be inhibited [50].

Hartmans and coworkers [51] have shown that both styrene and styrene oxide can be degraded with cell extracts having a high styrene oxide isomerase activity. These extracts were obtained by growing three pure cultures incubated with styrene.

Methylmethacrylate monomer is used extensively for the manufacture of acrylate or Plexiglass (R), and surface coating resins. MMA may be emitted or released in wastewater during its production and use in the manufacture of resins and plastics. MMA has been confirmed to degrade significantly in the biodegradability tests conducted by Slave *et al.* [52], and Pahren and Bloodgood [53].

In recent years Structure Activity Relationships (SARs) have been widely applied in the prediction of toxicity, bioaccumulation, and the distribution of chemicals released into the environment. SARs can provide qualitative information as to how modifications of chemical structures result in changes in chemical or biological activity. Quantitative Structure Activity Relationships (QSARs) are mathematical relationships usually found between the biological activity of chemicals and quantitative descriptors derived either experimentally or based on the structure of the chemical.

Several studies have attempted to correlate some physicochemical or structural property of a chemical with its tendency to be biodegraded. Geating [54] developed an algorithm to predict biodegradability based on type and location of substituent groups. Wolfe *et al.* [55] correlated the second-order alkaline hydrolysis rate constant and biodegradation rate constant for selected pesticides and phthalate esters. Vaishnav *et al.* [56] correlated biodegradation of 17 alcohols and 11 ketones with octanol/water coefficients using 5-day BOD. Boethling [57] correlated biodegradation rate constants with molecular connectivities for dialkyl esters, carbamates, dialkyl ethers, dialkyl phthalate esters and aliphatic acids.

None of the above investigators studied common monomers used in plastics as the model compound which was one of the objectives of this study.

2.3 Reactor Models

Livingston and Chase [58] modeled phenol degradation in a three phase fluidized bed bioreactor. The model described simultaneous diffusion and reaction of phenol and oxygen in the reactor packed with calcined diatomaceous earth particles to which the bacteria were attached. The model predicted a transition from phenol to oxygen limiting kinetics.

Lau, Strom, and Jenkins [59] studied filamentous activated sludge bulking attributable to low DO concentration. They developed a mathematical model which incorporated the diffusion and utilization of both substrate and DO in a floc composed of a single strain of a floc-forming microorganism (*Citrobacter sp.*) and a single strain of a filamentous microorganism (*Sphaerotilus. natans*).

De Gooijer *et al.* [60] observed and modeled a series of stirred tank reactors containing immobilized biocatalyst beads, and obeying Michaelis-Menten kinetics to obtain an optimum design. They defined optimum as the smallest total reactor volume needed to accomplish a specific conversion. They demonstrated that a cascade of reactors gave optimum design over one single reactor to achieve a given conversion.

In the above studies, diffusion models were used to evaluate reactor performance. Alternatively we have tried to eliminate diffusion barriers by using small bead size and high linear velocities. Thus, reducing mathematical description of the process to a simple kinetic model is decribed in Chapter 6. The recirculation reactor has been described by Chambers *et al.*[61]. Recirculation is a tool designed to determine a regime of operation with respect to specific kinetic parameters. This helps in determining accurate operating windows while optimizing with respect to reaction rate. Since oxygen is a cosubstrate in aerobic biodegradation, the importance of monitoring oxygen concentration is evident. Other advantages of the recirculation reactor have been described in the literature [62].

2.4 Oxygen Uptake

Biochemical oxygen demand (BOD) is a measurement of the amount of dissolved oxygen required to oxidize an organic chemical by microorganisms. It is one of the important indices which show the chemical concentration in a waste stream. An experimental procedure which has gained popularity and which is intimately related to the BOD principle, is the use of electrolytic respirometers to monitor the progression of biodegradation reaction in terms of oxygen uptake [63,64,65].

Among the techniques for respirometeric and direct oxygen uptake measurements, the ones most often used are the manometric and the direct oxygen uptake measurements using galvanic cells oxygen probes or polarographic electrodes. The Warburg manometric technique is probably the most widely used throughout the world [66]. The major disadvantage of this technique is that it is slow and not suitable for continuous measurements. On the other hand the polarographic technique which uses a galvanic cell oxygen probe is a better and simpler technique which when used properly can provide quick measurements of oxygen uptake rates. It has been shown in an earlier study that it is possible to determine the biochemical oxygen demand of a substrate based on short period oxygen consumption measurements [67].

On-line oxygen uptake measurements are of interest in the context of the dynamics of the process under real time conditions as well as for the control of aeration. Knowledge of the actual oxygen demand allows for optimization of aeration and determination of system performance under varied influent conditions. In an interesting study Sollfrank and Gujer [68] have demonstrated the importance of the on-line measurement method in determining oxygen uptake rate and oxygen transfer coefficients in an activated sludge system.

Determination of dissolved oxygen uptake is often done by measuring the BOD_5 values. The conventional BOD_5 value is the sum value of various biochemical processes

e.g., degradation of organic substances, mineralization of organic particles, including the biomass and nitrification. The inaccuracy of BOD_5 measurements varies between 15 to 50% [69], and does not give a correct indication of the oxygen demand warranted due to the presence of the organic substance in question. The on-line oxygen uptake measurement setup used this study minimizes these errors.

2.5 Biomagnetism

Various studies have indicated that magnetic fields enhance biological activity [70,71]. Magnetotactic bacteria have stimulated great interest among scientists interested in the field of magnetism. Blakemore [72] showed some of the aquatic magnetotactic bacteria orient themselves within magnetic fields. These organisms have intracellular chains of magnetite (Fe_3O_4) particles or magnetosomes around 40 ~ 100 nm in diameter. Since each iron particle is a tiny magnet, the bacteria use their magnetosomes chain to determine northward and downward direction, and swim down to nutrient-rich sediments.

Maugh [73] has observed that magnetosomes are also present in the heads of birds, tuna, dolphins, green turtles, and other animals presumably as an aid in navigation.

One of the most intriguing groups of organisms are those which respond to polar magnetism. Highly motile microaerophilic spirilla have been isolated from freshwater habitats that demonstrate a dramatic directed movement in a magnetic field referred to as magnetotaxis [74].

Lowenstam [75] and Mann [76] studied how magnetite is produced by microorganisms. They showed that there are two biomineralization processes which are called BIM (Biologically Induced Mineralization) and BOM (Boundary Organized Biomineralization).

Other research has demonstrated that cultures of the slime mold, *Physarum polycephalum*, respond to continuous EMF (electromagnetic field) with a lengthened

mitotic cycle and reduction in ATP levels [77,78]. There are also reports that EMF facilitates healing of bone fractures [79].

An interesting review presented by Davis and Rawls [16] states that there are two types of magnetic energy effects: one that arrests life, growth and development (north pole or negative energies), and one that increases life, growth and development (south pole or positive energies).

An important aspect of magnetic field studies involves the effect on cell membranes. Certain physiological effects such as a decrease in oxygen uptake have been observed in tissue cultures subjected to magnetic fields [80]. The decrease of body temperature of mice exposed to magnetic fields for prolonged periods of time and the delay of body temperature restoration of the hypothermic mouse by a magnetic field have been postulated to be due to a magnetic field induced alteration of mitochondria membrane permeability [81].

Gerencser *et al.* [82] showed that bacterial growth was inhibited in a field of high paramagnetic strength. Barnwell and Brown [83] conducted experiments to determine whether living organisms (mud snails) could perceive differences in strength and direction of the horizontal vector of very weak artificial magnetic fields. Their results indicate that the snails did respond to the change in direction and strength of the magnetic field. This was determined by the angle and distance of their movement from the line of applied magnetic field.

All of the above citations do indicate that magnetic fields can influence biological activity in an either positive or negative way. Most studies were done under the influence of alternating north and south pole magnetic fields. This does not clearly indicate the difference between two. No study has been reported on the effect of seperately applied north and south magnetic fields on microbes such as bacteria used in environmental biodegradation. Such a study was undertaken during the work reported in this thesis.

CHAPTER 3

OBJECTIVES

The objective of this work is to study bio-oxidative destruction of several substrates in an immobilized cell batch bioreactor in recirculation configuration. Specific objectives are to:

1. Determine the relative oxidative biodegradability of styrene, MMA, and HBA, which are used as monomers in the polymer industry,
2. Compare biodegradation based upon oxygen consumption as well as substrate disappearance,
3. Compare the relative degradation rates of ethylene glycol and its tetramer,
4. Determine the formation of any partially oxidized intermediates,
5. Observe and quantify the relative influence of various magnetic fields upon oxidation using phenol as a model compound,
6. Derive kinetic expressions describing the biodegradation of MMA, HBA, ethylene glycol, and phenol,
7. Calculate the amount of oxygen consumed for the degradation of each compound, and compare this to the theoretical requirements, and
8. Examine if a simple kinetic model involving Monod expressions can adequately describe the process.

CHAPTER 4

MATERIALS AND EXPERIMENTAL METHODS

4.1 Microorganisms, Nutrient Medium, and Substrates

Activated sludge was obtained from the Parsippany Troy Hills Water Pollution Control Plant (NJ). The sludge was sieved through a 297 μm opening screen, and washed three times with 0.5% saline solution. The sludge was then acclimated with 100 ppm/day of styrene, MMA, HBA, EG, TEG, or phenol, each as a sole carbon source for five days. At the end of the acclimation period the sludge was centrifuged, and the pellets so obtained were stored at 4°C to be used later in making the immobilized beads.

Dry biomass content (dry weight of cells) of the pellets was determined by drying a small sample of pellets overnight at 110°C. In this case the dry biomass concentration was found to be 50 - 55 mg dry biomass/g pellets. In all the experiments 3.5 g dry biomass (as 100 g wet beads) was used.

The nutrient medium used was developed in an earlier study [10], and consisted of magnesium chloride (100 mg), manganese sulfate (10 mg), ferric chloride (0.5 mg), potassium phosphate (10 mg), and tap water (100 ml), all diluted to 1000 ml by adding distilled water. Fixed nitrogen was excluded from the medium to minimize the growth of biomass during the experiments. The substrates used included styrene, phenol, HBA, MMA, EG, and TEG. The properties of these substrate are shown in Table 1.

4.2 Calcium Alginate Biobead Reactor

For a given 50 g batch of pellets a typical procedure for making beads was as follows. Wet bacterial pellets and 0.5% saline solution were taken in a ratio of 2:5 by weight in a blender. Sodium alginate (0.75% w/w) about 1.31g was then added slowly to the mixture with continuous stirring over a period of 2 to 3 minutes to obtain a homogeneous cell

Table 1. Properties of Selected Monomers and Oligomer

Chemicals	Formula	Structure	Molecular weight	Uses
Styrene	C_6H_5-CH=CH_2	Ring with a double bond	104	Polystyrene Butadiene Rubber
Phenol	C_6H_5OH	Ring compound	94	General disinfection
Methyl methacrylate (MMA)	$H_2C=C(CH_3)CO_2CH_3$	Branched chain with a double bond	100	Acrylate Plexiglass
Hydroxybutyric acid (HBA)	$CH_3CH(OH)CH_2CO_2H$	Straight chain	104	Polyhydroxybutyrate Human bone repair
Ethylene glycol	$HOCH_2CH_2OH$	Straight chain	62	Antifreeze in cooling and heating system
Tetraethylene glycol	$O(CH_2CH_2OCH_2CH_2OH)_2$	Straight chain	194	Extraction of aromatics from petroleum

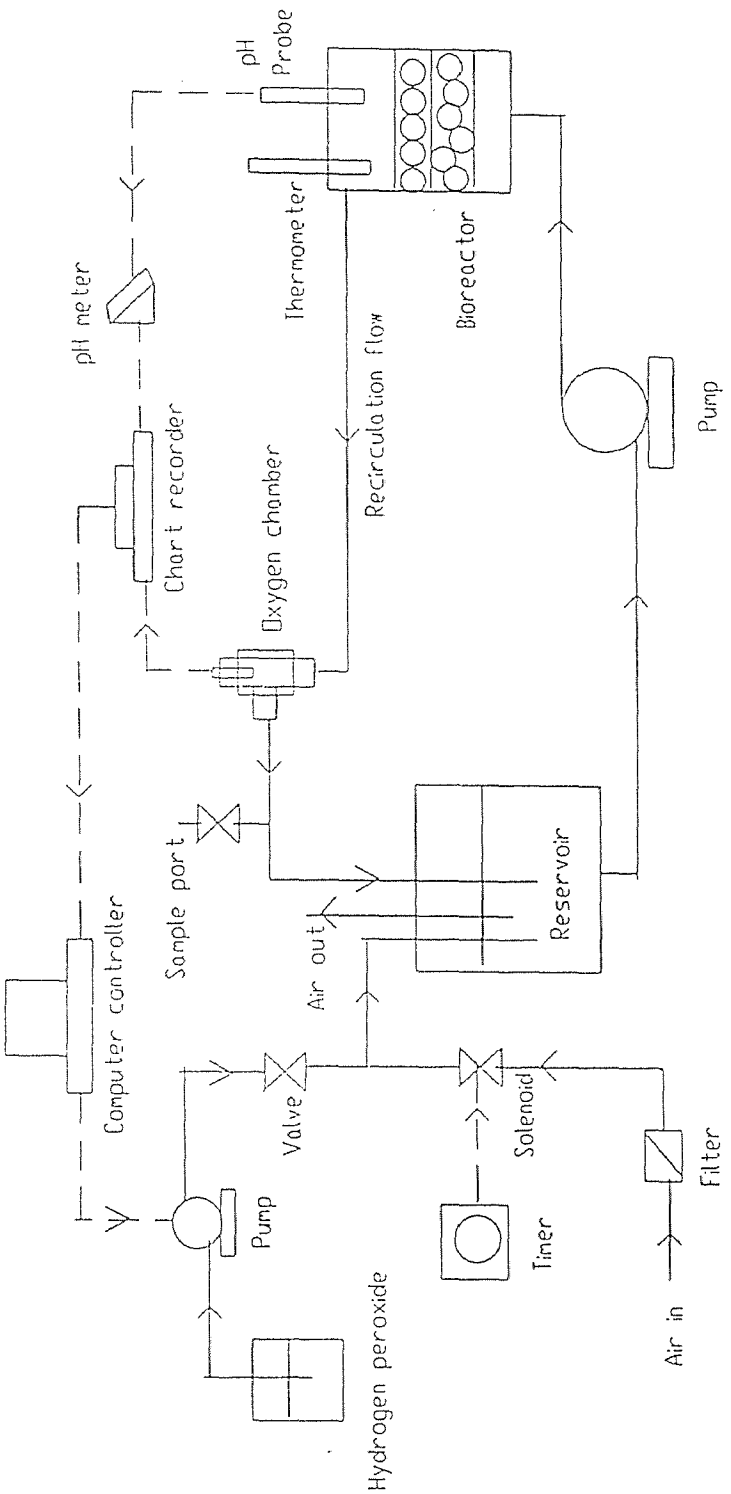

Figure 1. Experimental Set-up of the Bioreactor

suspension. With the help of a syringe pump (Model 351, Sage Instruments, Cambridge, MA) the homogeneous cell suspension was then extruded as discrete droplets into a slowly stirred solution of 0.1M calcium chloride. On contact with calcium chloride, the droplets hardened to form beads about 3.4 to 3.8 mm in diameter. The beads were then cured in calcium chloride for 24 hours at 4 ^{o}C before use.

The experimental setup of the batch recirculation reactor is shown in Figure 1. The reactor is 6 cm in diameter and 21 cm long. The reservoir is 11 cm in diameter and 22.5 cm long. The total reaction volume, excluding bead volume, is set at 2 liters by controlling reservoir level. The reaction medium is circulated between the reservoir and the reactor using a centrifugal pump. The linear velocities were maintained high enough to overcome the solid/liquid film resistance to mass transfer by recirculating the stream at 325- 350 ml/min.

The reactor contained a thermometer to monitor temperature and a pH probe (Orion Cat. No 91-04) which was connected to pH (Corning Model 250 New York) meter. All experiments were done at room temperature, and DO levels were maintained by air or injecting 1 % H_2O_2. Carbon filtered and moist air was sparged into the reservoir at the rate of 1.5 ml/min. An impingement flow Clark-type dissolved oxygen probe (YSI Inc., Yellow Springs, OH) was used to monitor the concentration of dissolved oxygen. Supply of DO to the reactor was set by timer or by on/off computer control. In computer control the DO levels were maintained by reading the sensor and setting "on" and "off" levels.

The controller has capabilities to perform A/D conversion, do real time graphing of input variables, and to do data logging. The microprocessor based controller was obtained from Omega Engineering, Stamford, CT.

4.3 Analytical Methods

Both MMA and styrene were analyzed on a Perkin Elmer Model 8500 (Norwalk, CT) Gas Chromatograph. A 6 ft x 1/8 inch stainless steel column (Supelco, Bellefonte, PA) packed with 1.75 % Bentone 34 with 100/120 Supelcoport mesh, and 5% SP-1200 was used. The detector used was a flame ionization detector (FID), and helium was used as a carrier gas.

Hydroxybutyric acid was analyzed on a Perkin Elmer HPLC with a diode array detector at a wavelength of 215 nm. The mobile phase was 65 % acetonitrile, and 35 % water (v/v). The column used to elute HBA was Spherisorb CN (250 mm x 46 mm).

Ethylene glycol was analyzed on a Perkin Elmer Model 8500 Gas Chromatograph. A 6 ft x 1/8 inch stainless steel column (Supelco) packed with 10 % SP-2100, 100/120 Suppelcoport was used at an oven temperature of 110^{o}C.

Dissolved oxygen consumption was monitored using a Clark type dissolved oxygen probe and a chart recorder. Calibration was done by equilibrium with air at various temperatures for all substrates.

For phenol concentration, periodically 1 ml of liquid sample was taken from the reservoir and analyzed using a Varian 3300 Gas Chromatograph, equipped with an FID . A stainless steel column (183 cm length x 0.32 cm O.D), packed with 10 % SP-2100, 100/120 Suppelcoport was used at an oven temperature of 140^{o}C.

Daily, 1 ml of medium from the system was analyzed for secreted extracellular proteins by using the standard Lowry test, based on color response measurement [87]. Bovine serum albumin (SIGMA Chemicals, St. Louis, MO) was used as a protein standard.

Carbon analyzer (O.I. Analytical Inc. Model 500, College station, Texas) was used to measure total organic carbon (TOC) and total inorganic (TIC) of ethylene glycol and tetraethylene glycol.

4.4 Effect of Magnetic Fields

Experiments were performed using a specially designed and fabricated recirculation flow-type bioreactor. Phenol was used as the substrate in this study. Phenol concentrations in the range of 50 to 200 ppm were studied. The material used for fabrication of the reactor was non-magnetic (largely plastic) in nature. The magnets, either the south or the north pole, were attached using non-magnetic tape to the reactor. The reservoir, the pump and the oxygen probe were located away from the effects of the magnet. The magnets used were rectangular blocks of dimensions 5 x 15 x 1 cm.

These solid state magnetic fields were applied to the reactor containing 100 g of alginate immobilized activated sludge. These experiments were conducted over a period of 1200 hours of continuous operation. Different experiments performed were as follows:

1) control experiment without applying magnetic field,

2) experiments with magnetic south pole applied to the reactor,

3) experiments with magnetic north pole applied to the reactor, and

4) experiments with alternating magnetic north and south poles.

The strength of the magnetic fields used was 0.45 tesla.

For quantitative study the magnets, 0.15 and 0.35 tesla south pole, were attached to the reactor body so that only the reactor stayed in the range of the magnetic field. The magnets used rectangular blocks in dimensions 5x15x0.3 cm and 5x15x0.5 cm for 0.15 and 0.35 tesla respectively. Different experiments performed were:

Run	Acclimation of free cells to magnetic field	Magnetic field during run with immobilized cells
1	no	no
2	yes	no
3	yes	yes (0.15 tesla south pole field)
4	yes	yes (0.35 tesla south pole field)

Acclimation was conducted by exposure to 0.35 tesla for 3 days, 0.49 tesla for the next 3 days, and 0.63 tesla for a final 3 days. This was followed by immobilization and subsequent placement in the recirculation bioreactor.

CHAPTER 5

RESULTS AND DISCUSSION

5.1 The Typical Pattern of Oxidation and Basic Approach

Appendix A shows the typical bio-oxidation pattern of many organic compounds in raw form. The pattern of the DO curve shows an increase in oxygen depletion rate which forms upon injection of substrate. Oxidation continues at length until the curve returns to a baseline plateau. From these slopes the oxidation rates of organic compounds in question can be estimated readily. This can be incorporated in any oxidative biodegradation process, thus eliminating the need for continuous analysis of the substrate, provided it is earlier established that complete mineralization occurs.

Table 2 summarizes the response as measured in terms of oxygen uptake when the microbes are met with various organic compounds. It is observed that the higher the ratio of initial oxidation rate with substrate to baseline oxidation rate without substrate, the higher the biodegradation rate. Baseline oxidation rate is defined as the oxygen uptake in the absence of any external organic substrate. It is a measure of the endogeous respiration rate.

Figure 2 indicates the DO profile and phenol concentration profile in an experiment to study phenol biodegradation. Section AB shows the baseline DO consumption rates in the absence of substrate. The ups and downs in the DO profile are due to an intermittent supply of air which is turned on and off by a timer. By doing this the rate of DO consumption can be monitored at several points in time on a continuous basis.

At point B, 60 ppm of phenol was injected, which initiated a sharp consumption of DO (BC). In the next 5 hours the reaction proceeds as seen by the decrease in phenol concentration as well as that in the overall DO level. After 5 hours the DO level returns to

Table 2. Bio-oxidation and Biodegradation Rates of Organic Compounds. ROC : Rate of oxygen consumption, ROB : Rate of biodegradation, A : Baseline oxidation rate without substrate (nmol O_2/ml*min.). This is an indication of intial biomass activity. B : Initial oxidation rate with substrate (nmol O_2/ml*min.), C : Ratio of B to A.

Compound	Formula	Starting concentration (ppm)	ROC			ROB (ppm/hr/g biobead)
			A	B	C	
Tetraethylene glycol	$HO(CH_2CH_2O)_3$ CH_2CH_2OH	200	1.42	2.76	1.94	0.21
Crotonic acid	$CH_3CH=CHCOOH$	200	1.68	2.97	1.77	0.238
Butyric acid	$CH_3CH_2CH_2COOH$	200	1.35	2.74	2.03	0.399
Citric acid	$HOC(COOH)$ $(CH_2COOH)_2$	200	1.07	2.45	2.29	0.428
Tetrahydrofuran	C_4H_8O	1000	1.15	2.16	1.87	0.44
Ethanol	C_2H_5OH	500	1.08	2.17	2.01	0.45
Acetic acid	CH_3COOH	200	0.76	2.88	3.79	0.50
Acetonitrile	CH_3CN	1000	0.69	2.84	4.12	0.595
Ethylene glycol	$HOCH_2CH_2OH$	600	0.84	4.12	4.91	0.84

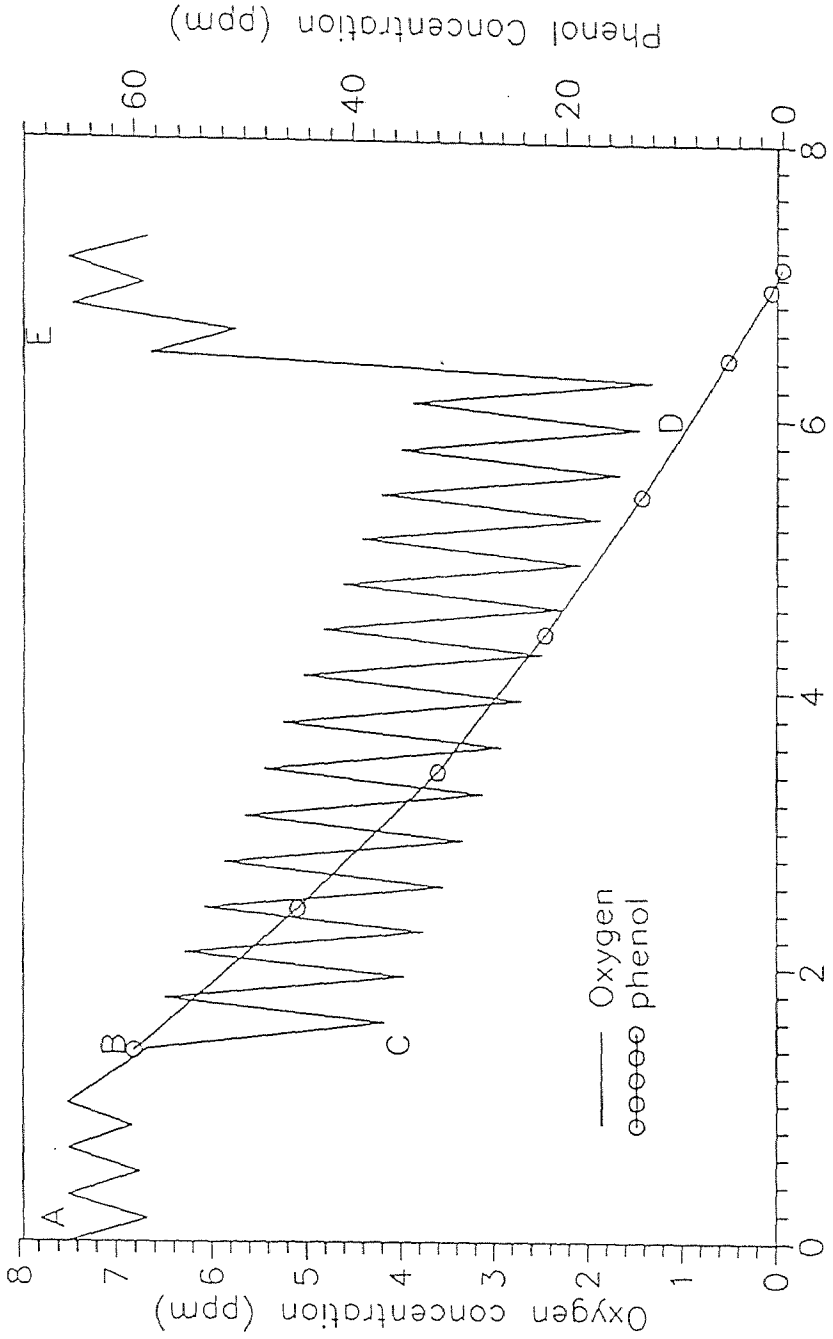

Figure 2. Biodegradation of Phenol with Time Based Addition of DO Supply (Air). AB: baseline, B: injection, BC: initiation, CD: reaction, DE: completion.

the original level and phenol concentration at this time had dropped to around 5 ppm. Section DE indicates completion of the reaction with normal DO levels.

The remainder of this chapter is divided as follows. First, the studies on styrene, MMA, and HBA are presented. The effects of different starting concentrations, typical DO patterns, and corrected oxidation rates at different concentrations are observed. A comparison of the required amount of oxygen as calculated versus the amount measured is made.

Next, the same approach is taken with ethylene glycol and its tetramer, and with phenol under the influence of magnetic fields. Finally, a comparison of biodegradation rates is made.

5.2 Studies with the Monomers

Table 1 shows the physical and chemical characteristics of the chosen chemicals. Figure 3 shows the disappearance of styrene as a function of time at different starting concentrations. From the controls without biomass, it can be seen that while abiotic losses are relatively high, biological oxidation dominates. Oxygen is supplied by supplying H_2O_2, and air which is converted to water and O_2 by catalase.

It needs to be addressed that hydrogen peroxide has a short half-life in the presence of the enzyme catalase. The possibility of a chemical reaction between hydrogen peroxide and the monomers (styrene or MMA) is less likely due to the very low H_2O_2 concentrations, especially in the presence of catalase.

Figure 4 describes the oxidation rate history and Figure 5 shows the corrected oxidation rates during biodegradation of styrene at three different concentrations (50, 75, 150 ppm). These rates has been determined from the DO profiles obtained during a typical biodegradation experiment as shown in Figure 4. Here corrected rate is defined as the ratio of oxygen uptake rate at any time after the injection of the organic substrate to a unit activity giving a baseline oxygen uptake rate (in absence of the organic substrate) of 1.0

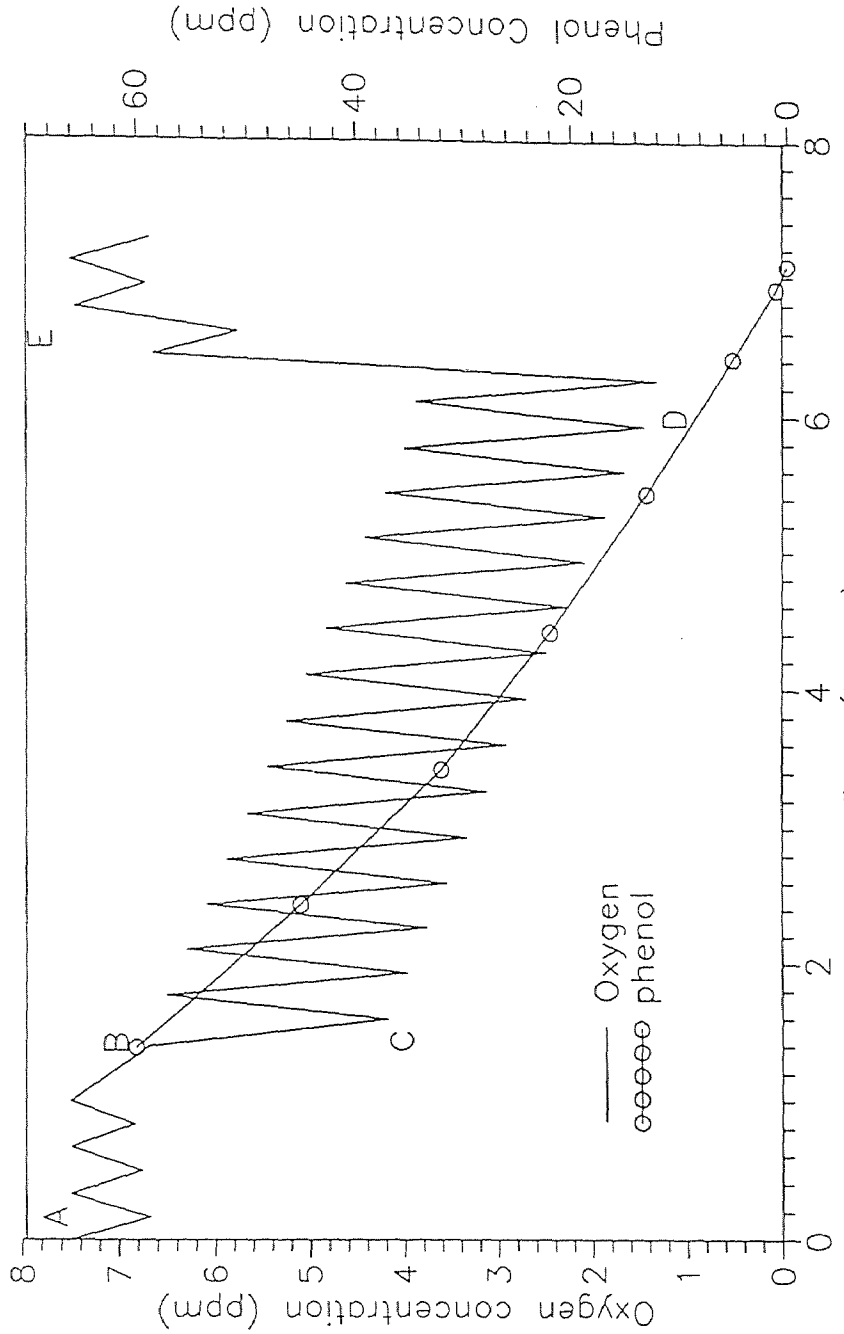

Figure 2. Biodegradation of Phenol with Time Based Addition of DO Supply (Air). AB: baseline, B: injection, BC: initiation, CD: reaction, DE: completion.

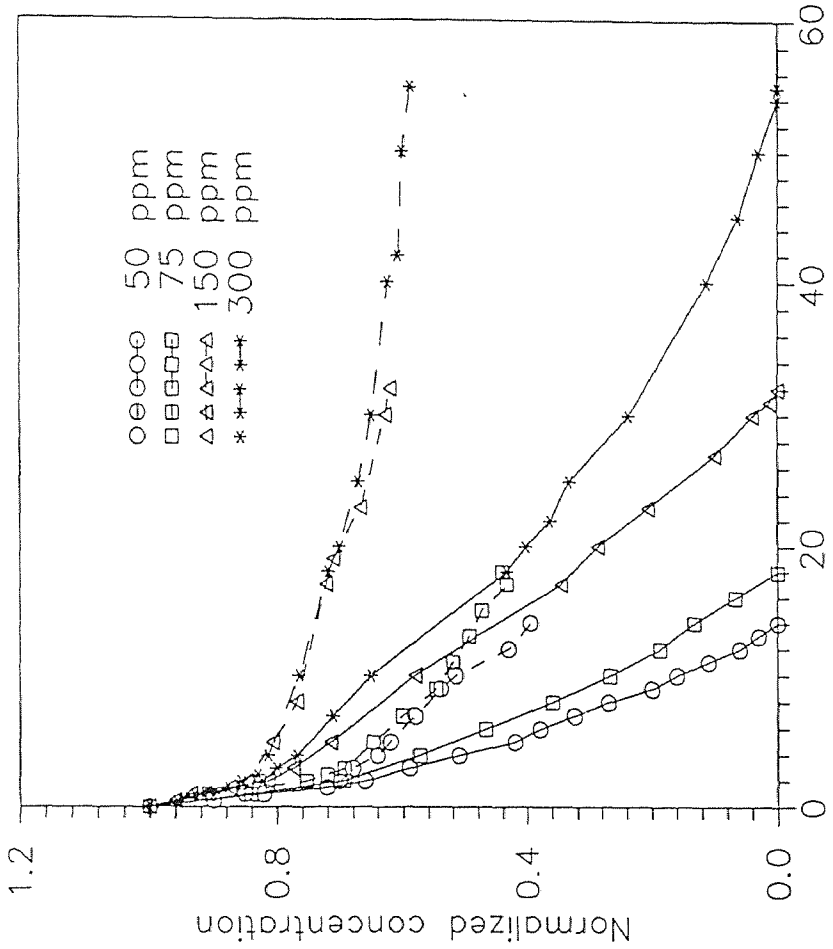

Figure 3. Biodegradation of Styrene at Different Starting Concentrations, solid line: with biomass; dashed line: control (without biomass). DO supplied by hydrogen peroxide.

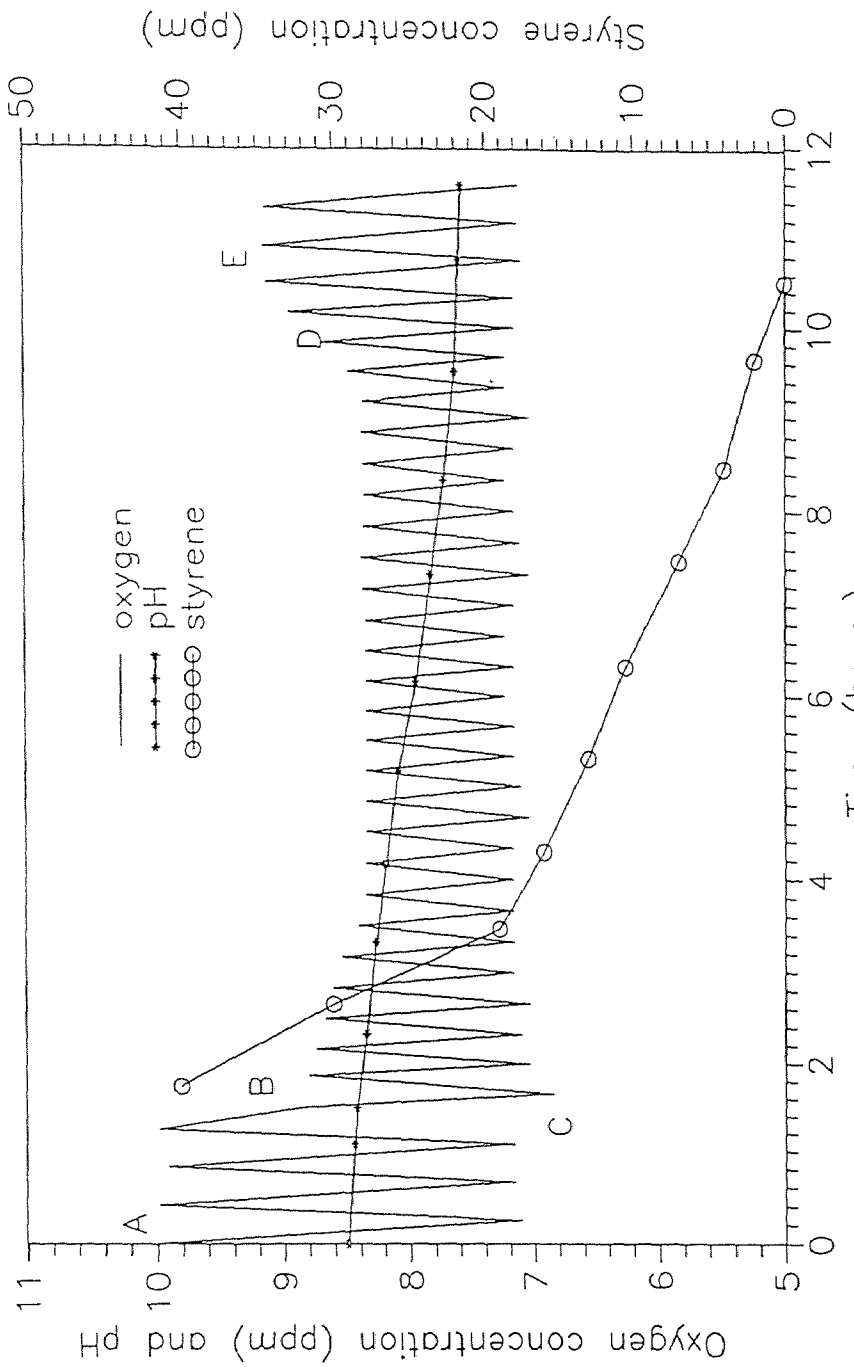

Figure 4. Biodegradation of 40 ppm Styrene Using Batch Feeding of Hydrogen Peroxide. On at DO 7.5 ppm, Off at DO 7.7 ppm
AB: Baseline; B: injection; BC: initiation; CD: reaction; DE: completion.

nmols/(ml-min). These rates can be correlated to the increase in oxygen uptake observed due to the presence of the organic substrate. As seen in Figure 5, the corrected oxidation rates increase as soon as the organic substrate is injected, which indicates that oxygen is used to either completely or partially mineralize the organic substrate that was injected. Later the rates reach a maximum plateau and then decrease rapidly to the original value. At this point it has been found by experience with GC verification that the substrate has been depleted. The extent of mineralization achieved can be predicted by comparing the total oxygen consumed in a typical experiment, to that required theoretically to mineralize the same amount of the organic substrate.

5.2.1 Experimental Determination of Oxygen Required

The total amount of oxygen consumed in any experiment was determined by integrating the area under the curves shown in Figure 5. This area was calculated using a simple graphic method as follows.

First the total area under the curve was determined by counting squares. The absolute value of oxygen used was then determined by multiplying the total number of squares with the coefficients of the x-axis (time, minutes) and the y-axis (oxygen consumption rate , nmols oxidzed/min-ml-unit activity).

Using styrene as an example, the amounts of O_2 required to degrade styrene at concentrations of 50, 75, 150 ppm were thus determined to be 150.55, 220.8, and 412.256 mg with 2 liter reaction volume. Once again the abiotic losses of styrene were taken into account in determining these values. A sample calculation for styrene at 75 ppm is presented in Appendix E.

5.2.2 Theoretical Determination of Oxygen Required

The theoretical quantities were determined as follows. Complete mineralization of the organic compounds containing C, H, and O, assuming that all carbon goes to CO_2 and all H goes to H_2O follows the equation

$$C_xH_yO_z + \frac{y+4x-2z}{4} O_2 \longrightarrow x\,CO_2 + \frac{y}{2} H_2O. \qquad (6.3)$$

(The coefficients for O_2, CO_2 and H_2O were determined by balancing the two sides of the equation.) In this case there is no biomass formation. Based on this the O_2 required to degrade for example styrene follows the equation

$$C_8H_8 + 10\,O_2 \longrightarrow 8\,CO_2 + 4\,H_2O. \qquad (6.4)$$

From equation (6.4) the amount of O_2 required for 50, 75, 150 ppm styrene were determined to be 207.23, 332.22 and 740.57 mg (see line A in Figure 6).

In reality only 34, 54 and 121 ppm of styrene were available for biodegradation due to some abiotic losses. These losses were determined from control experiments as explained earlier (see Figure 3).

The equation that theoretically describes mineralization of an organic compound with cocurrent biomass growth is as follows [85].

$$C_xH_yO_z + a\,O_2 + b\,NH_4^+ \longrightarrow e\,C\,H_{1.8}\,O_{0.5}N_{0.2} + f\,CO_2 + g\,H_2O + h\,H^+. \qquad (6.5)$$

Due to lack of enough experimental data, coefficients a, b, e, f, g, and h in the above equation were determined based on some correlations given by Roels [85]. These

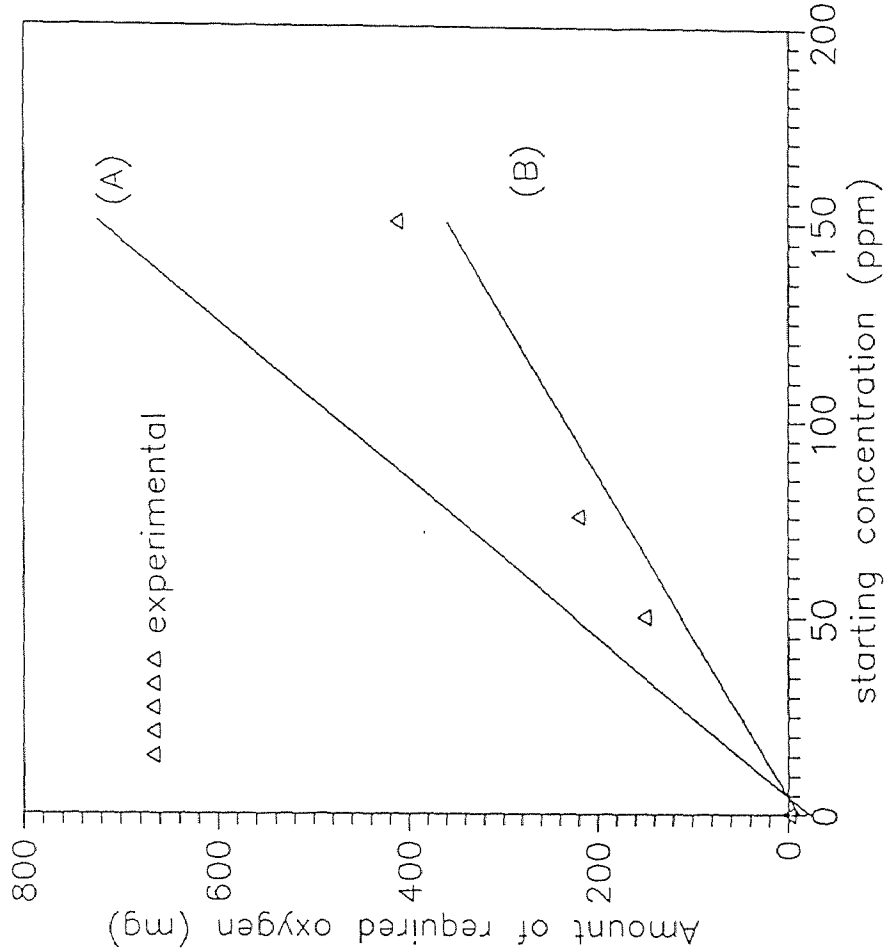

Figure 6. Comparison of the Required Oxygen Amount in Styrene Biodegradation with 2 liter reaction volume. Line (A): respiration; Line (B): with biomass growth.

correlations are based on the degree of reduction (DR) of the substrate. The degree of reduction of a compound can be calculated as follows.

The sum of (total number of carbon atoms × valence of carbon) + (total number of hydrogen atoms × valence of hydrogen) + (total number of oxygen atoms × valence of oxygen) was divided by total number of carbon atoms. Substituting the appropriate numbers for styrene in the above equation, we get

Total number of carbon atoms	= 8
Valence of carbon	= 4
Total number of hydrogen atoms	= 8
Valence of hydrogen	= 1
Total number of oxygen atoms	= 0
Valence of oxygen	= -2

which gives

$$DR_{styrene} = \frac{(8\times 4)+(8\times 1)+\{0\times(-2)\}}{8}$$

For styrene this number is 5. If DR>4.67 then 60 % carbon goes to biomass, if DR < 4.67 then DR×0.83 carbon goes to biomass [85].

These quantities are calculated as follows by substituting the coefficient for CO_2 as 0.4 and for biomass as 0.6 because of $DR_{styrene} > 4.67$ in the equation (6.5).

$$C_xH_yO_z + \left(\frac{1.48x+y-2z}{4}\right) O_2 + 0.12x\ NH_4^+ \longrightarrow$$

$$0.6xCH_{1.8}O_{0.5}N_{0.2} + 0.4x\ CO_2 + \left(\frac{y-0.72x}{2}\right)H_2O + 0.12x\ H^+. \qquad (6.6)$$

For the styrene, Equation (6.6) will be

$$C_8H_8 + 4.96\ O_2 + 0.96\ NH_4^+ \longrightarrow 4.8\ CH_{1.8}ON_{0.2} + 3.2\ CO_2 + 1.12\ H_2O + 0.96\ H^+. \qquad (6.7)$$

Using these calculations the theoretical amount of O_2 required with biomass growth to degrade styrene at 50, 75, 150 ppm concentration and for the reactor volume of the system used, were determined to be 102.79, 163.25, 367.32 mg (see line B in Figure 6). The same procedure was adopted for MMA, HBA, EG and phenol. Table 3 summarizes the degree of reduction, yield coefficient, and the coefficients for biomass and CO_2.

5.2.3 Comparison of Experimental Determination to Theoretical Requirement of Oxygen

The extent of mineralization can be determined by comparing the theoretical and experimental quantities of oxygen required during biodegradation. The three sets of values (two theoretical and one experimental) are plotted as shown in Figure 6. The area underneath each curve in Figure 5 represents oxygen consumed, summarized in Figure 6. The points fall between Line A (respiration or total oxidation) and Line B (oxygen going to biomass growth).

Figures 7-10 go through the same progression for MMA, with Figure 11 indicating similar results for MMA as with styrene. Figures 8 and 9 use H_2O_2 and air, respectively. Air may be used with MMA because MMA is not volatile, as is styrene. The method of oxygen supply does not vary significantly for air and H_2O_2 in so far as MMA disappearance is concerned.

HBA (Figures 12-14) follows a similar progression. However, the measured oxygen consumption (Figure 15) follows a direction of greater oxidation (line A) as opposed to biomass growth (line B). The greater relative oxidation for HBA than for styrene or MMA may be due not only to factors such as volatility or abiotic loss, but also possibly to a small extent by absence of enzymic activity. Yun Tang [84] from our laboratory has shown that while the oxidase isolated from this mixed culture shows activity with phenol, styrene, methylene chloride, and chlorophenol, oxidase activity with

Table 3. Values of Degree of Reduction, Yield Coefficient, Coefficient of Biomass and Coefficient of CO_2
The value of yield coefficient were determined experimentally as explained in section (6.4).

Compound	Degree of reduction	Y_{exp} (mg biomass/mg substrate)	Coefficient for biomass	Coefficient for CO_2
MMA	4.8	0.537	0.6	0.4
HBA	4.25	0.336	0.55	0.45
Ethylene glycol	5.0	0.52	0.6	0.4
Phenol without magnetic field	4.67	0.337	0.6	0.4
Phenol with magnetic field	4.67	0.312	0.6	0.4

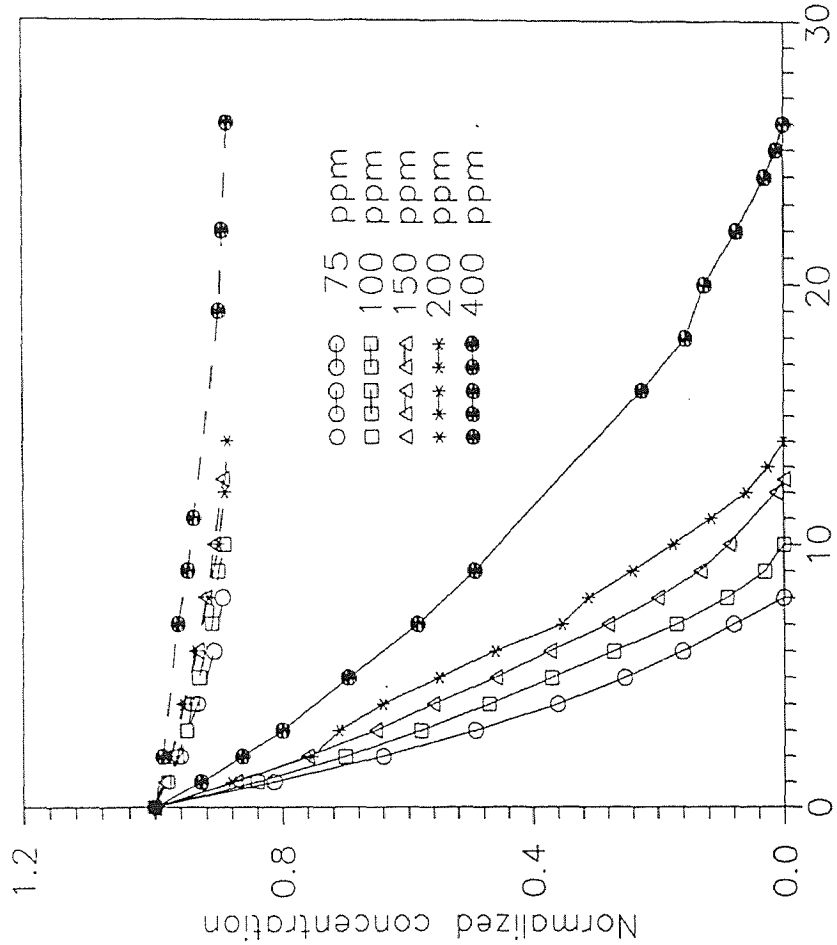

Figure 7. Biodegradation of MMA at Different Starting Concentrations. Solid line: with biomass; Dashed line: control (without biomass). DO supplied by hydrogen peroxide.

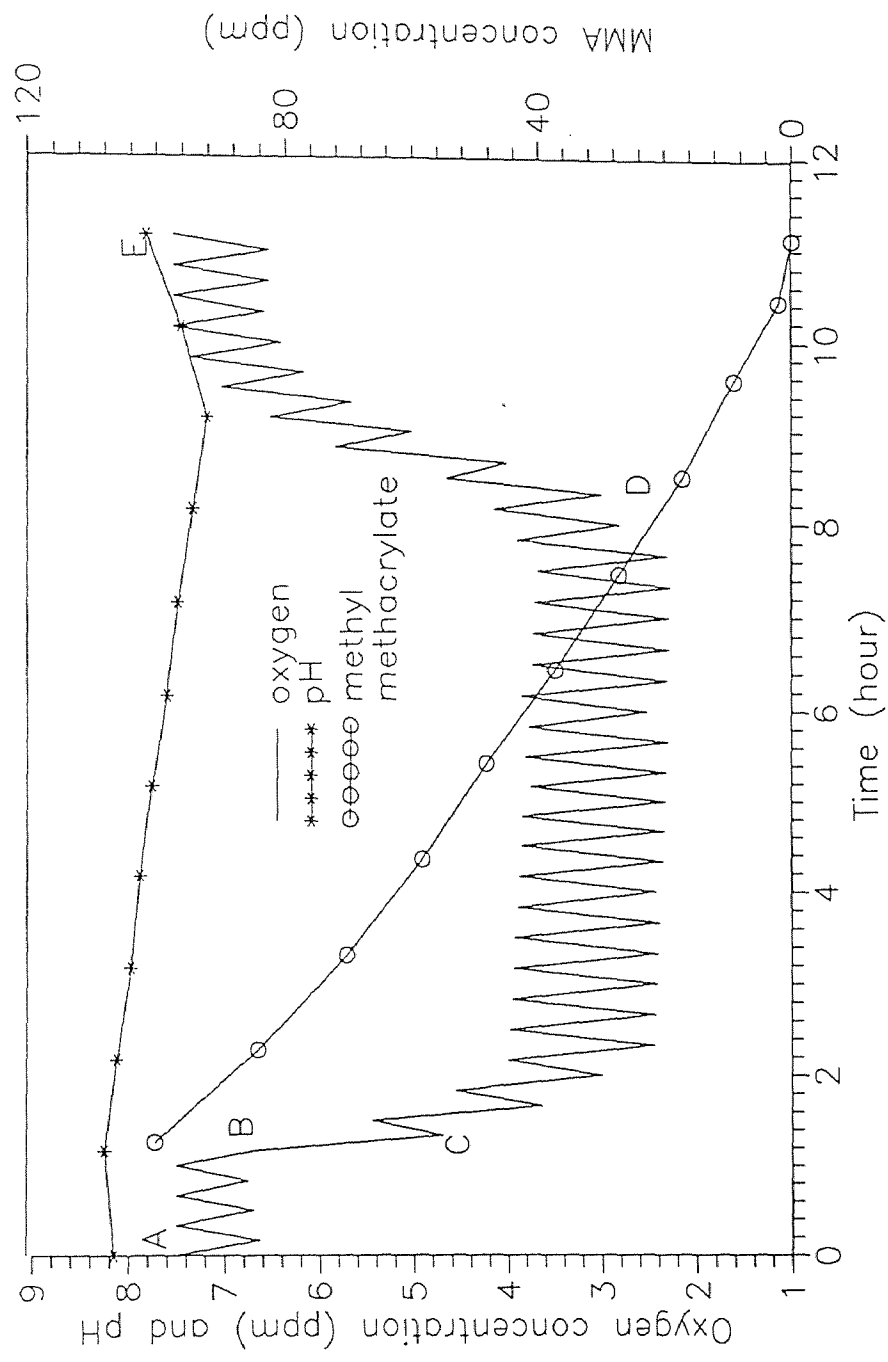

Figure 8. Biodegradation of Methyl Methacrylate (100 ppm) with Time Based Addition of DO Supply (Air). AB: baseline, B: injection, BC: initiation, CD: reaction, DE: completion.

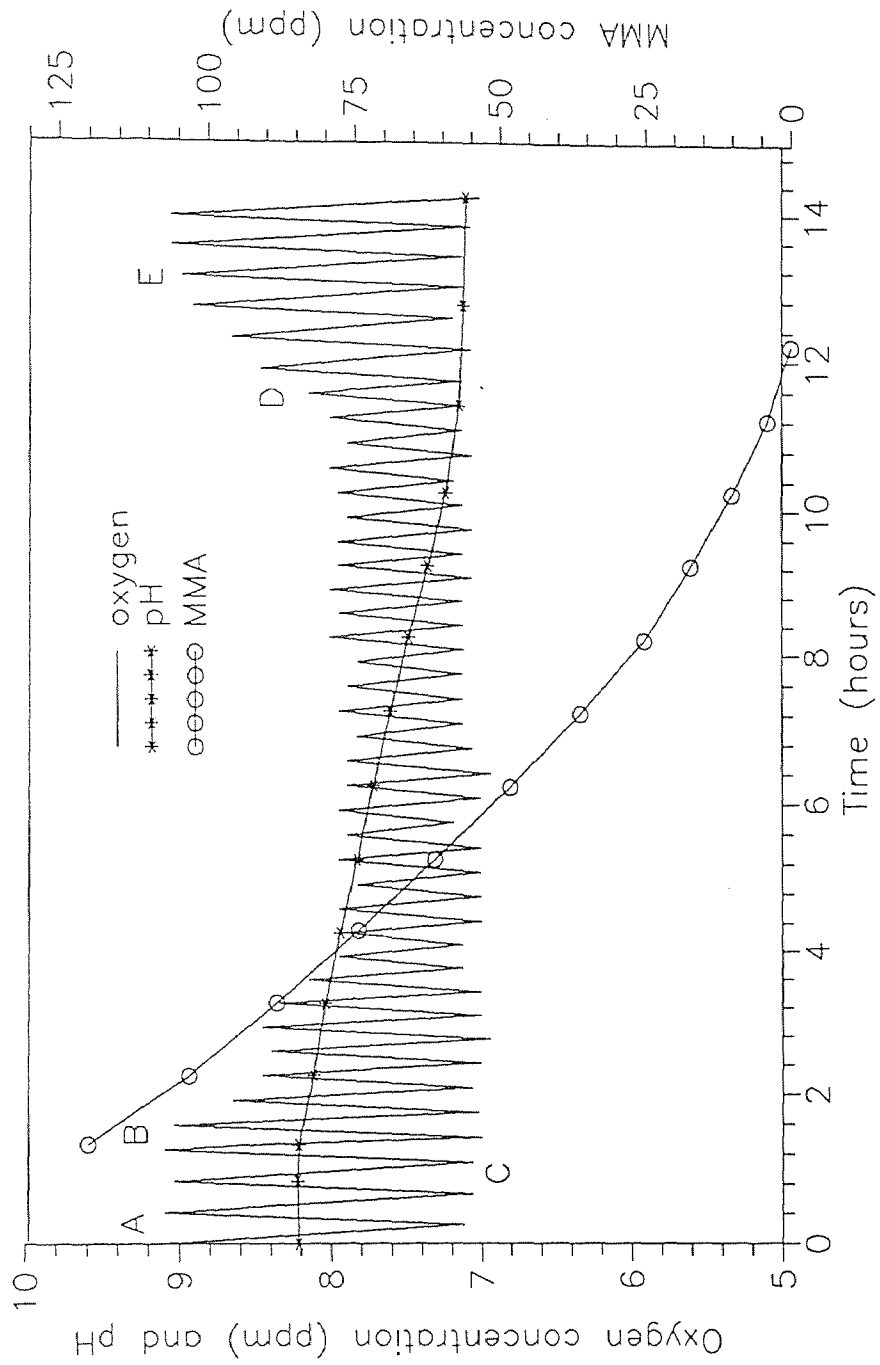

Figure 9. Biodegradation of MMA (120 ppm) Using Batch Feeding of Hydrogen Peroxide. On at DO 7.5 ppm, Off at DO 7.7 ppm. AB: baseline, B: injection, BC: initiation, CD: reaction, DE: completion.

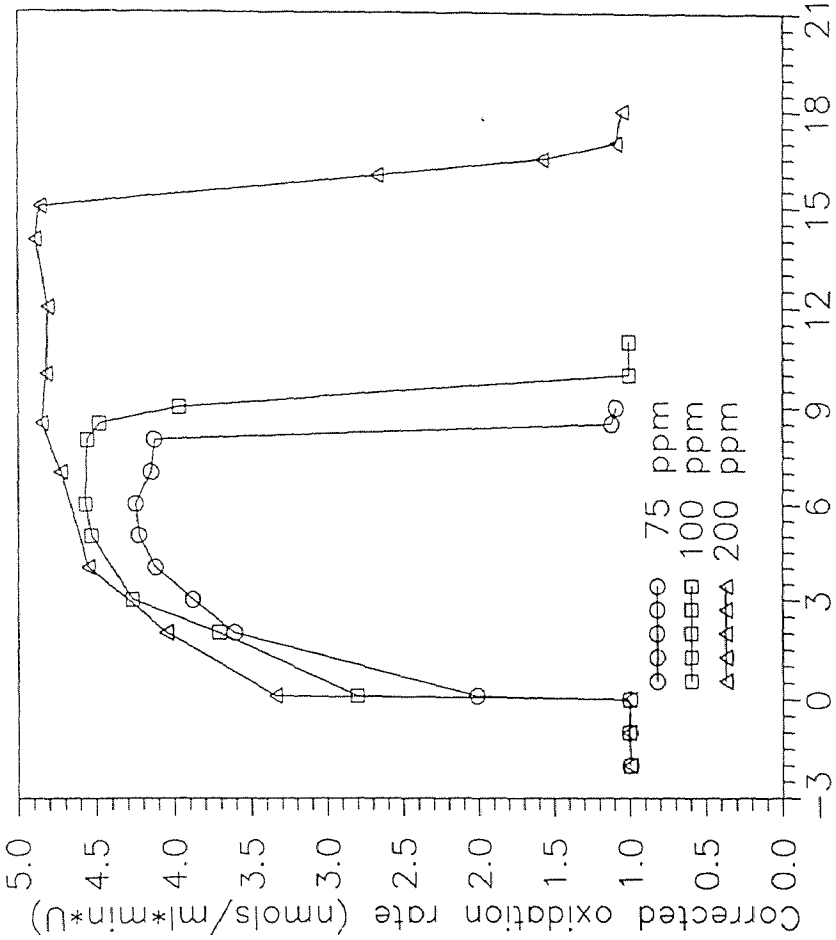

Figure 10. Corrected Oxidation (with H_2O_2) Rate of MMA As a Function of Time. Corrected oxidation rate = oxidation rate/U. U is defined as a unit activity giving a baseline respiration rate of 1.0 nmols/ml*min.

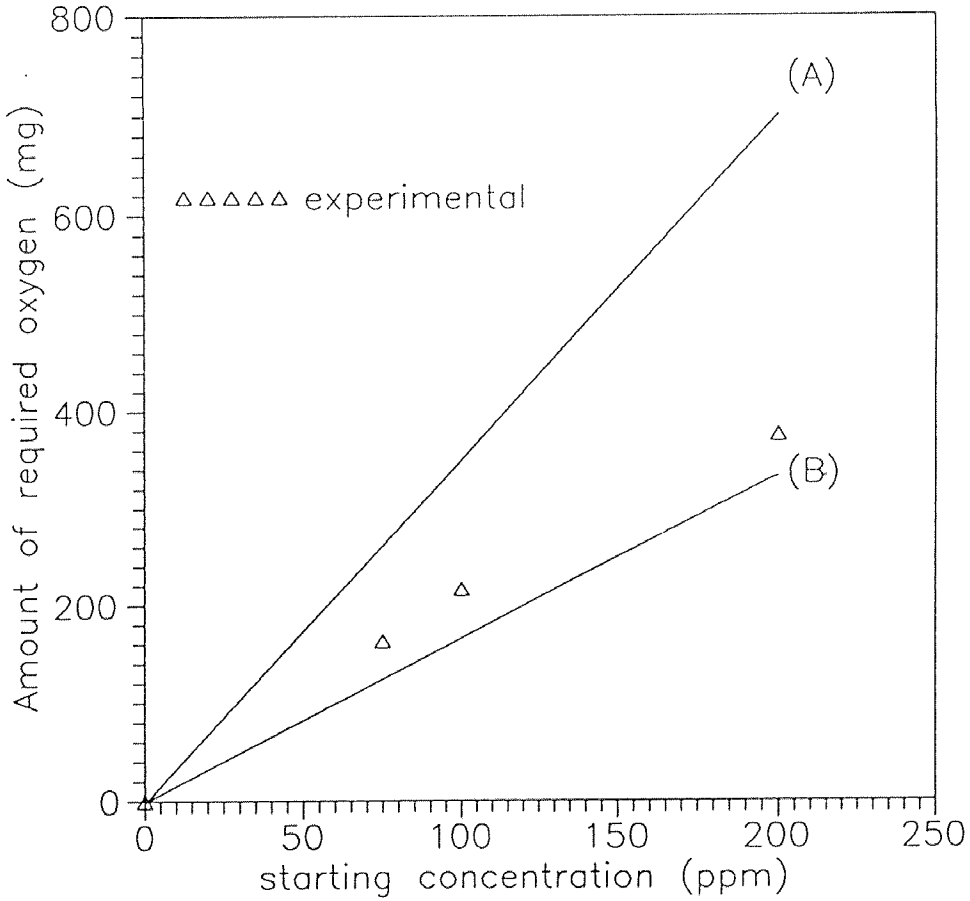

Figure 11. Comparison of the Required Oxygen Amount in MMA Biodegradation with 2 liter reaction volume. Line (A): respiration; Line (B): with biomass growth

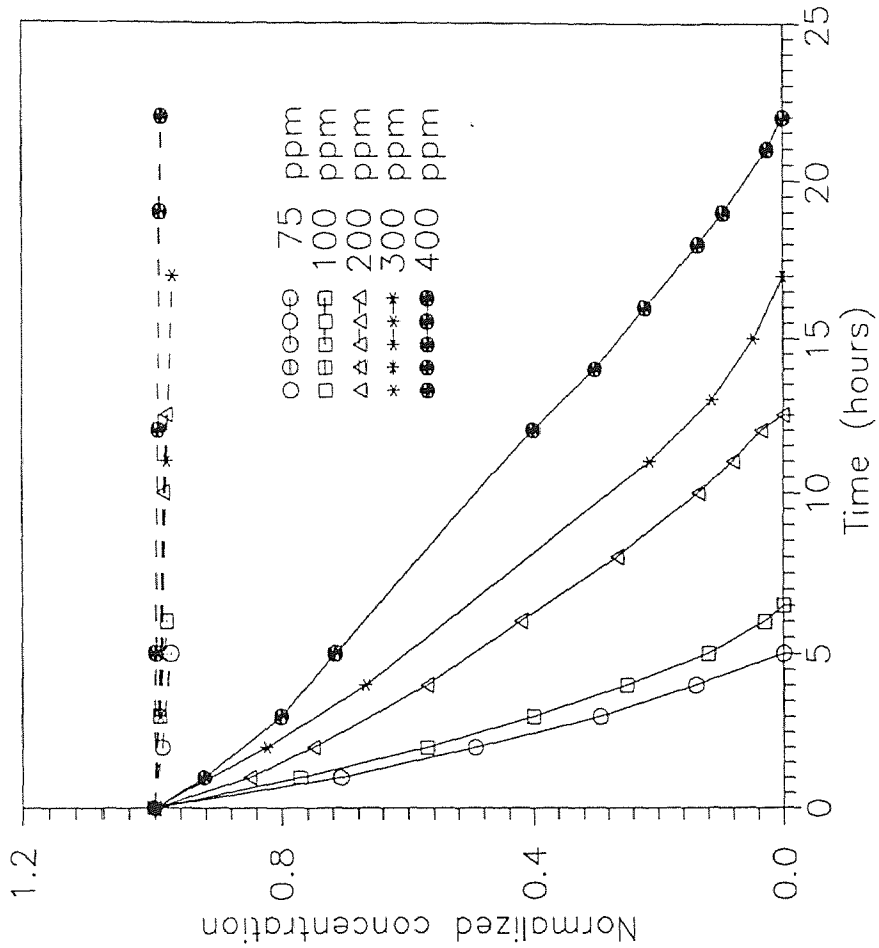

Figure 12. Biodegradation of HBA at Different Starting Concentrations. Solid line: with biomass; dashed line: control (without biomass).

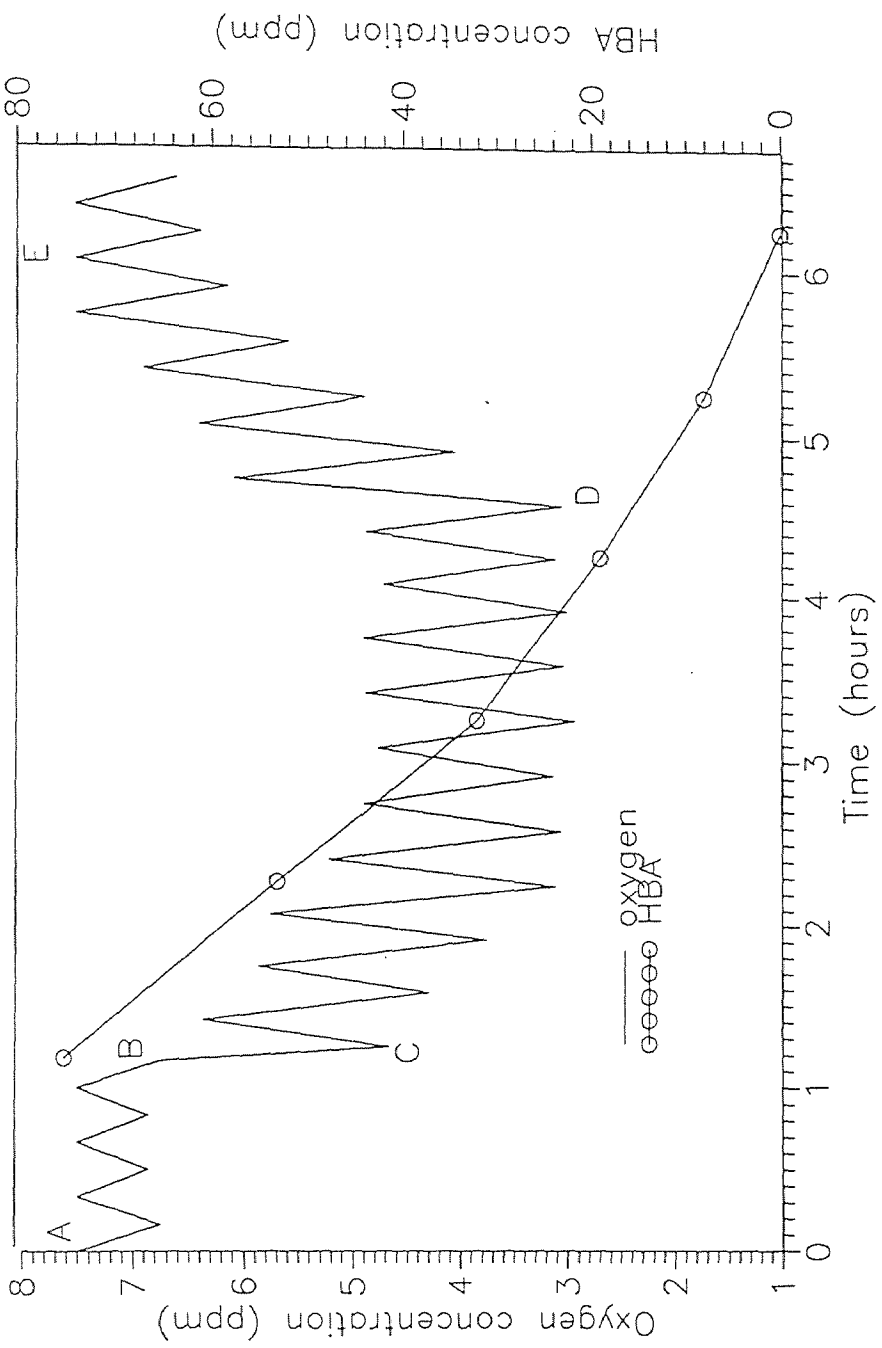

Figure 13. Biodegradation of Hydroxybutyric Acid with Time Based Addition of DO Supply(Air). AB: baseline, B: injection, BC: initiation, CD: reaction DE: completion.

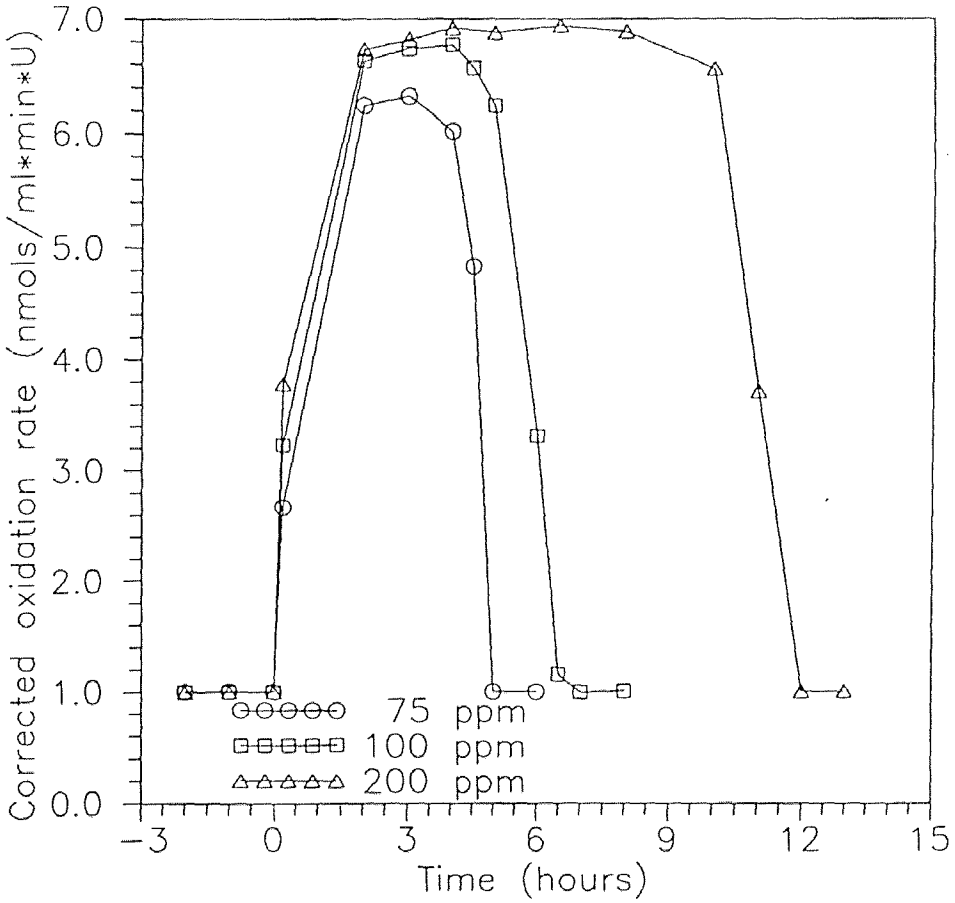

Figure 14. Corrected Oxidation Rate of HBA As a Function of Time. Corrected oxidation rate = oxidation rate/U. U is defined as a unit activity giving a baseline respiration rate of 1.0 nmols/ml*min.

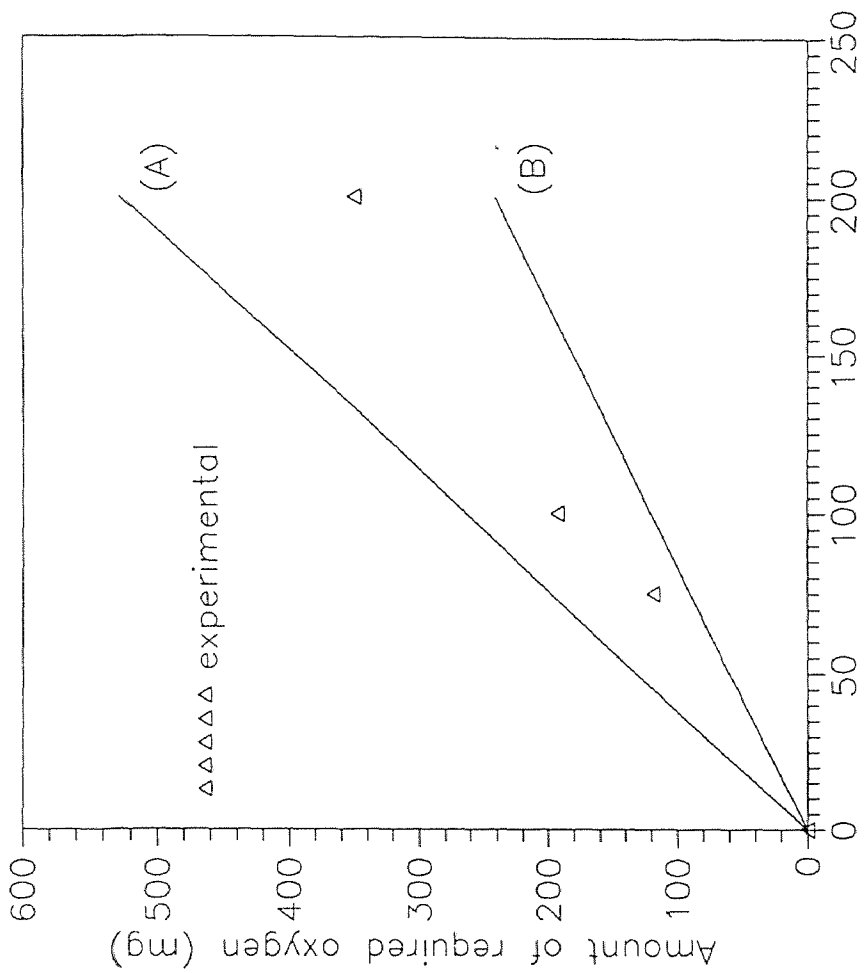

Figure 15. Comparison of the Required Oxygen Amount in HBA Biodegradation with 2 liter reaction volume. Line (A): respiration; Line (B): with biomass growth.

HBA is zero. This means that the oxygen concentration measured is not lowered by enzymes in solution and hence more accurate cellular oxidation is observed.

Figure 16 shows the relative rates of substrate disappearance at various concentrations. The rates approach a plateau at higher concentrations. No substrate inhibition is observed in this region since the rates do not show any decreases at the highest concentrations. This logic also holds true for Figure 17, in which the monitoring is by oxidation rates instead of substrate disappearance. Changes in oxidation rates are actually induced by the injection of the organic substrate.

In Figure 18, the reaction was started with 75 ppm substrate concentration for each substrate. Upon return of the baseline to normal, a new injection of 75 ppm was made. This means that more injections were made for HBA than for MMA and styrene. Thus the pH change is higher for HBA, then MMA, and finally styrene, as expected. HBA was in the form of its sodium salt, so the resulting sodium carbonate increased the pH. Also, air was used for HBA, stripping CO_2 and raising the pH, whereas H_2O_2 was used for MMA and styrene.

Figure 19 and Table 4 show that initial oxidation rates increase as the number of substrate injections increase. The biomass is more acclimated upon repeated injections and the rate increases. A fresh batch of biomass was used with each substrate. Even though the microbes were acclimated in the free cell phase, acclimation continued the immobilized state. Therefore, the data in this dissertation were collected after each batch was fully acclimated in immobilized form. Baseline oxygen consumption also increases, so that this corrected ratio changes little after the first injection.

Results from these experiments indicate that styrene, MMA, and HBA can all be biodegraded using immobilized, acclimated activated sludge.

A comparison of average biodegradation rates (3.3, 9.3, and 15 ppm/hr for styrene, MMA, and HBA, respectively at 75 ppm starting concentration) indicates the scale of difficulty in biodegrading the above monomers. The biodegradation trend

Table 4. Bio-oxidation Response of Monomers with 75 ppm Each Injections.
A : Baseline oxidation rate without substrate (nmol O_2/ml*min), B : Initial oxidation rate with substrate (nmol O_2/ml*min),
C: Ratio of B to A (This ratio represents the relative change during any injection.)

Test #	Styrene			MMA			HBA		
	A	B	C	A	B	C	A	B	C
1	1.26	1.29	1.02	0.98	2.30	2.35	0.88	1.77	2.00
2	1.60	1.72	1.08	1.20	2.80	2.33	0.93	4.18	4.50
3	1.88	2.17	1.15	1.40	3.50	2.50	1.04	4.69	4.51
4	2.22	2.43	1.09	1.80	4.20	2.28	1.17	5.32	4.55
5	2.55	2.95	1.15	2.00	4.90	2.45	1.13	5.26	4.66

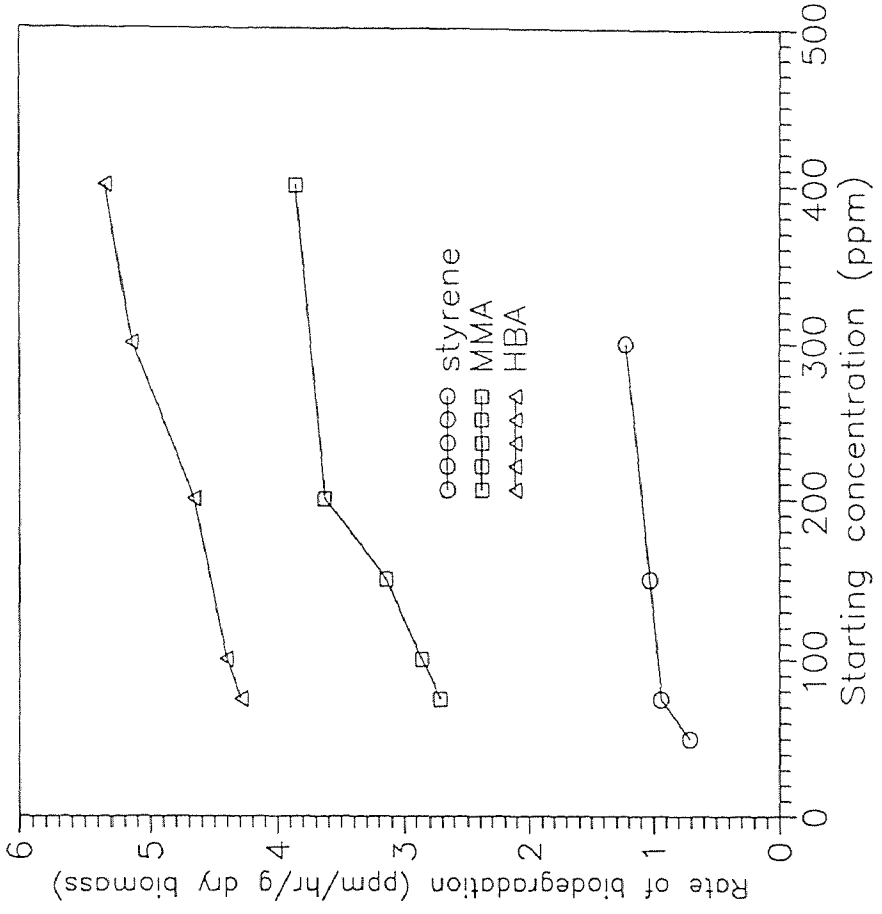

Figure 16. Rate of Monomer Disappearance at Different Starting Concentrations.

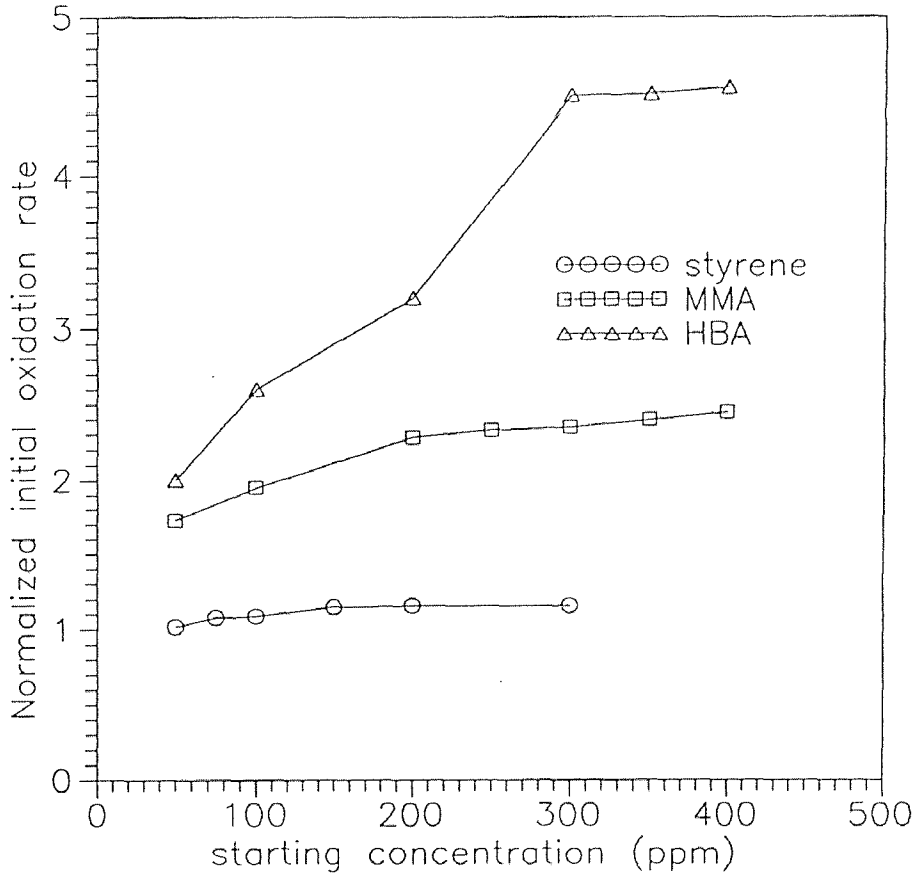

Figure 17. Normalized Oxidation Rate of Monomers at Different Starting Concentrations, Normalized initial oxidation rate = initial oxidation rate/baseline oxidation rate. A plateau is reached as expected, and no substrate inhibition is observed.

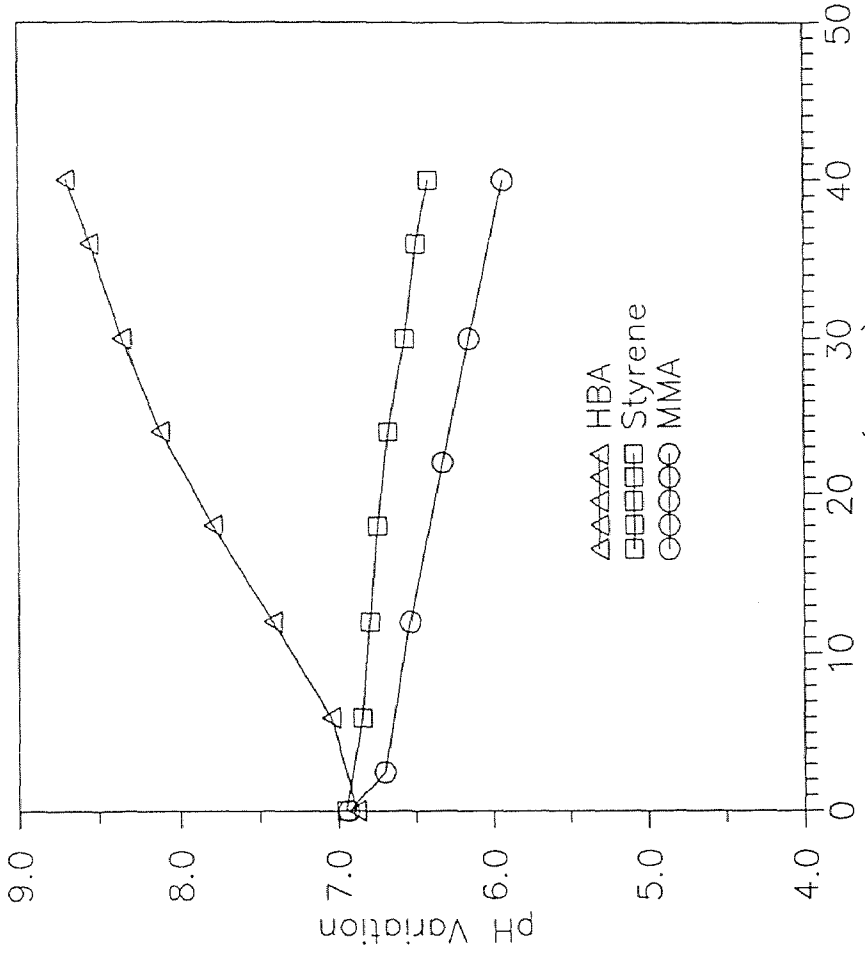

Figure 18. Variation of pH with Substrate Injection at 75 ppm.

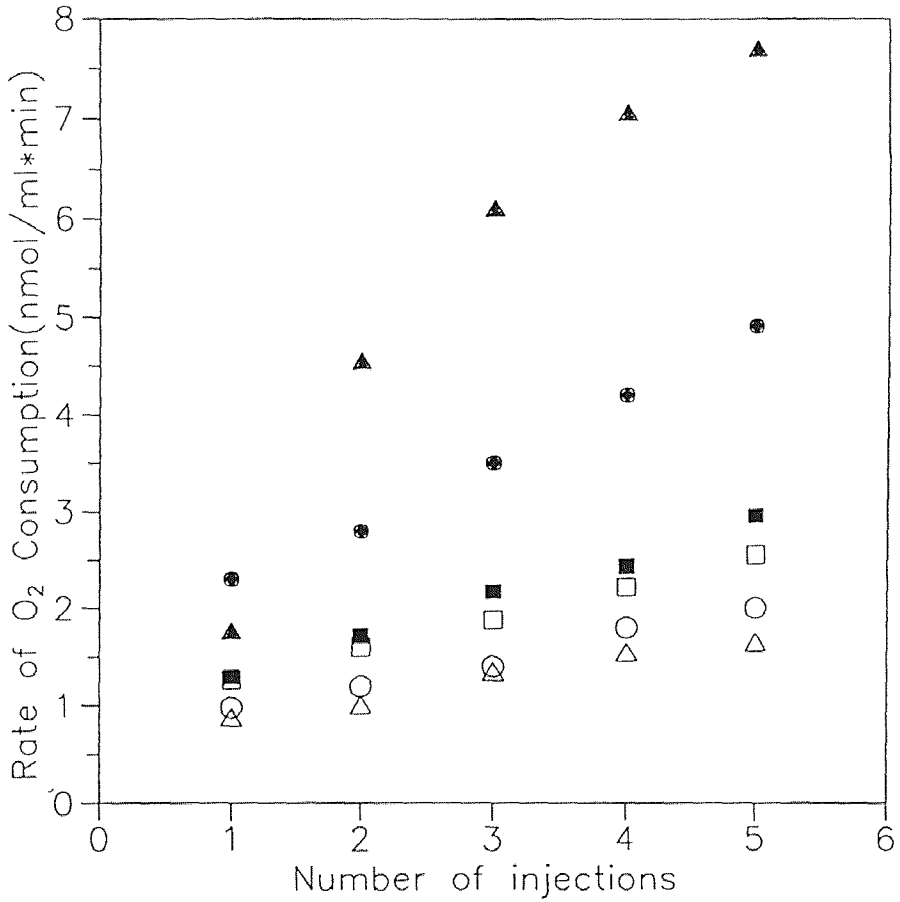

Figure 19. Substrate Dependent Oxygen Consumption with Repeated Injections of 75 ppm.

△△△△△ baseline for HB sodium salt
▲▲▲▲▲ substrate dependent O_2 consumption for HB sodium salt
□□□□□ baseline for styrene
■■■■■ substrate dependent O_2 consumption for styrene
○○○○○ baseline for MMA
●●●●● substrate dependent O_2 consumption for MMA

reflected by these rates is analogous to the observed trend in oxygen consumption rates and pH.

Table 4 summarizes the response as measured in terms of oxygen uptake when the microbes are challenged with monomers during five different tests. It is observed that the response from baseline oxygen uptake is highest for HBA followed by MMA and styrene. The results indicate the natural relative degradability of these monomers in this environment.

It is clearly seen that styrene, which is a benzene derivative, is relatively difficult to degrade because the degradation mechanism includes a formidable ring opening step. MMA is branched chain compound and HBA is straight chain compounds, and they can be biodegraded relatively easily. A comparatively high biodegradation rate for HBA is understandable because the monomer does not have a double bond in its chemical structure and is already partially oxidized.

5.3 Studies with Ethylene Glycol and Tetraethylene Glycol

Figure 20 shows ethylene glycol disappearance as a function of time for several substrate concentrations. No ethylene glycol was lost in the abiotic control for this figure.

Figure 21 and 22 show similar oxygen and pH profiles for ethylene glycol and its tetramer. Figure 21 additionally indicates complete disappearance of ethylene glycol before the oxidation pattern is complete. It shows high oxygen consumption even after EG concentration has reached zero. The presence of intermediates is the reason for this observation.

Figure 23 and the resulting calculations in Figures 24 and 25 show that tetraethylene glycol is mineralized more when compared to ethylene glycol. Corrected oxidation rates (Figure 26) for ethylene glycol are higher at all concentrations than they are for its tetramer. On a total carbon basis, however, the tetramer is oxidized at a higher rate than its monomer.

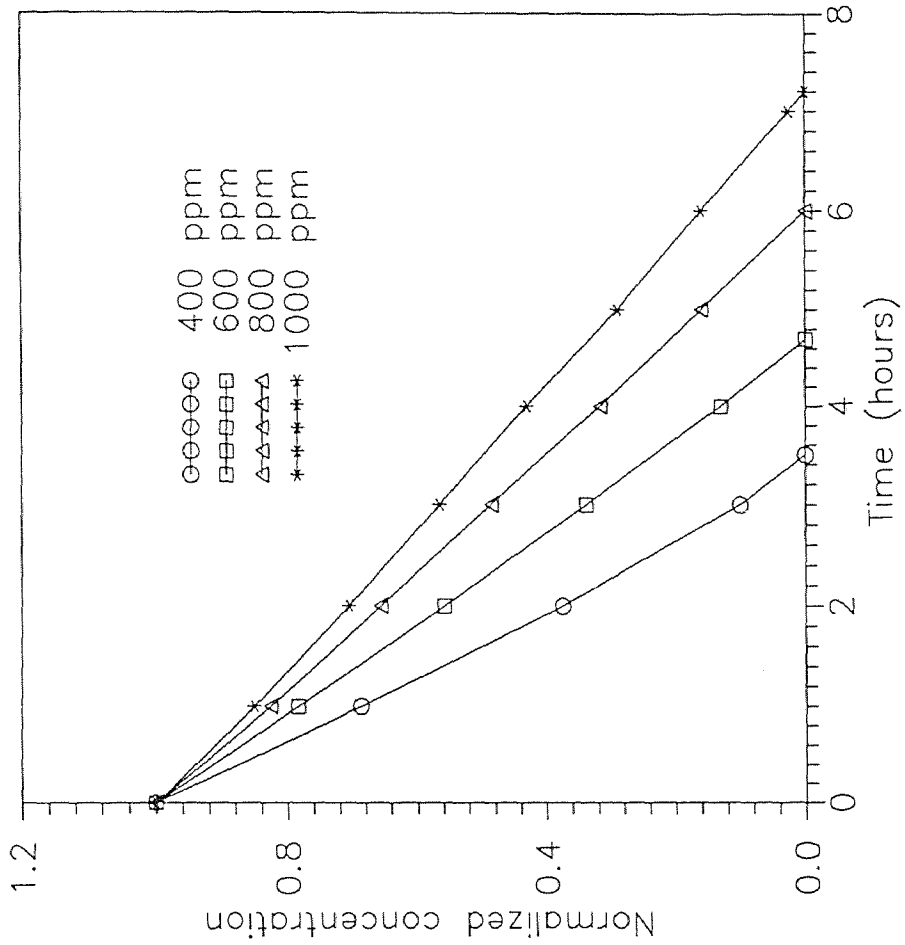

Figure 20. Biodegradation of Ethylene Glycol at Different Starting Concentrations.

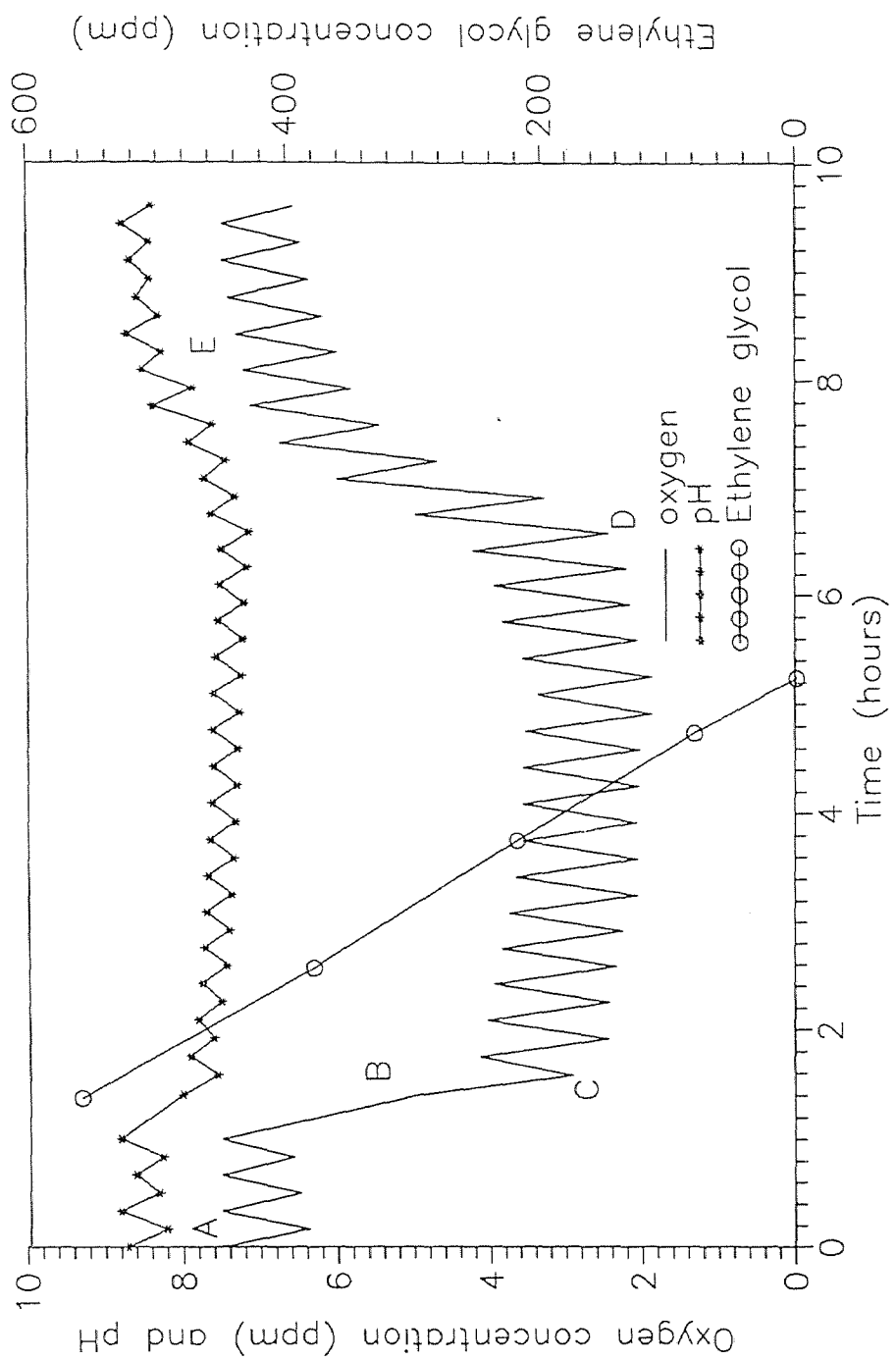

Figure 21. Biodegradation of Ethylene Glycol with Time Based Addition of DO Supply (Air). AB: baseline, B: injection, BC: initiation, CD: reaction, DE: completion.

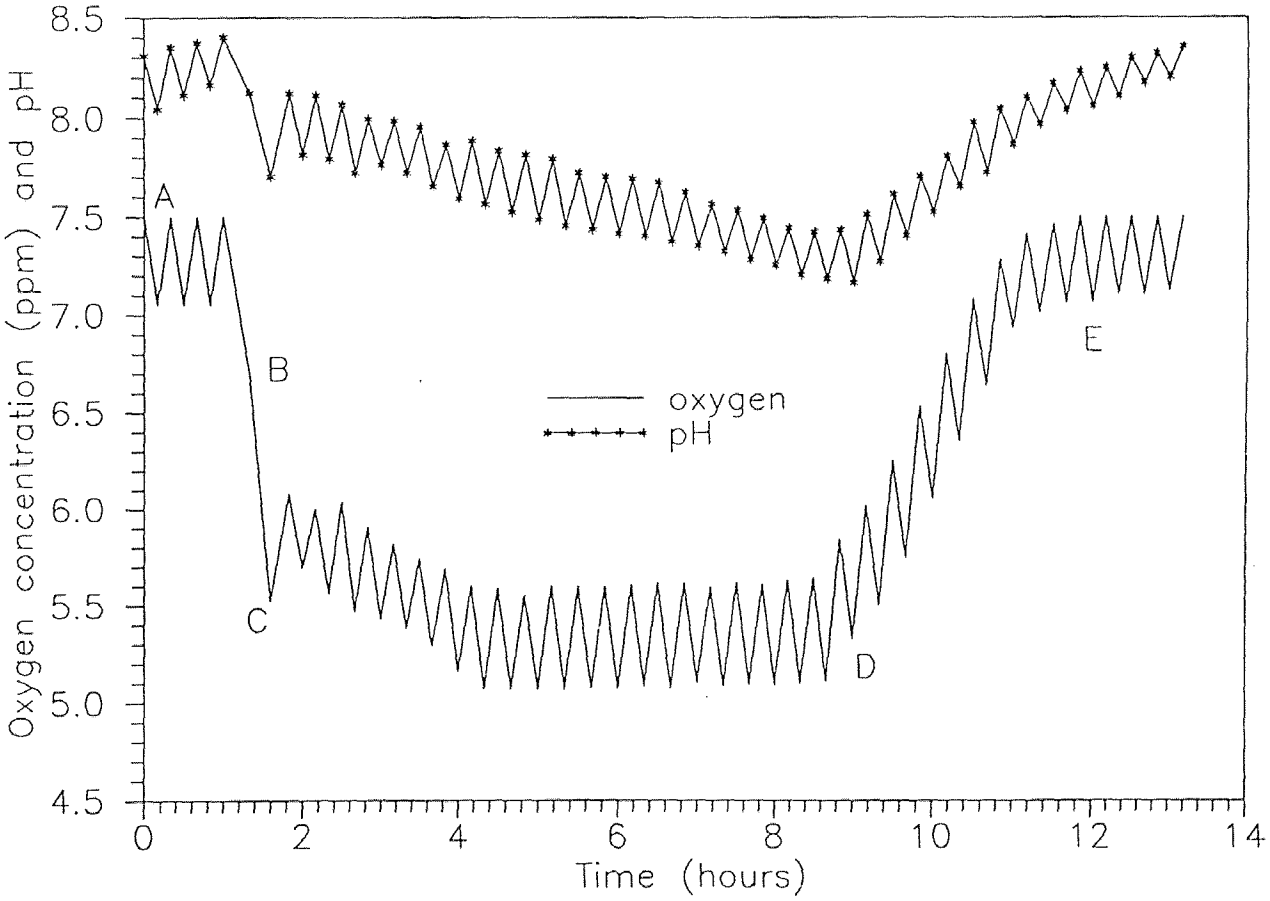

Figure 22. Biodegradation of Tetraethylene Glycol with Time Based Addition of DO Supply (Air). AB: baseline, B: injection, BC: initiation, CD: reaction, DE: completion.

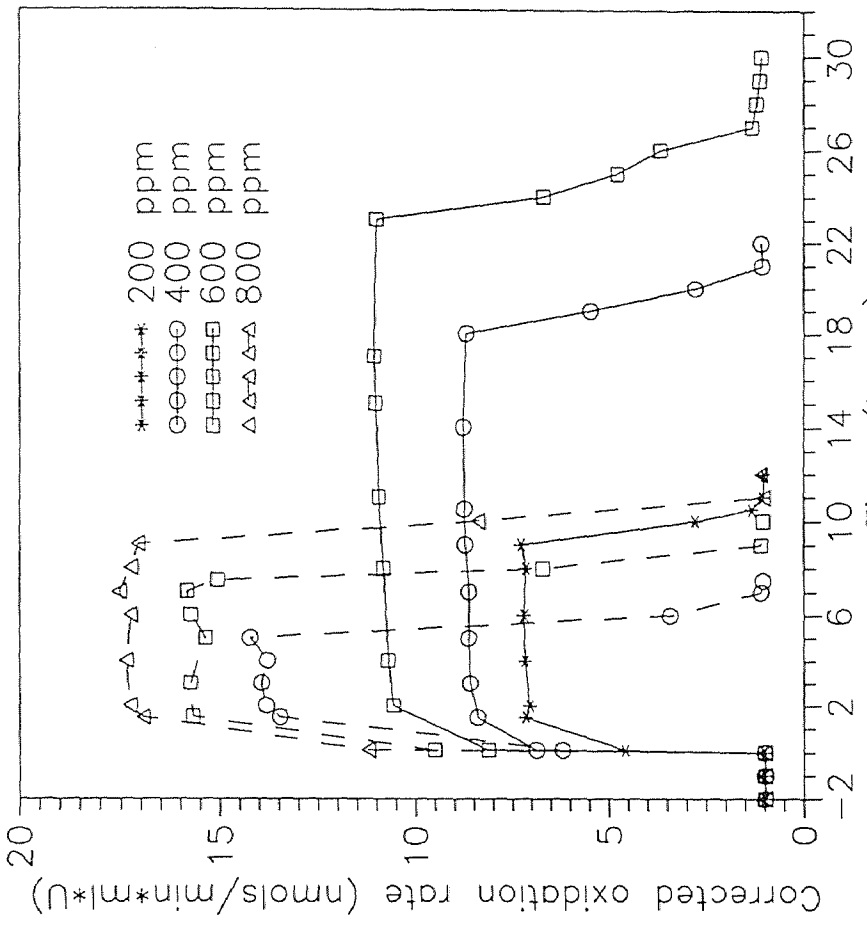

Figure 23. Corrected Oxidation Rate of Ethylene Glycol (Dashed Line) and Tetraethylene Glycol (Solid Line) at Different Starting Concentrations. Corrected oxidation rate = oxidation rate/U. U is defined as a unit activity giving a baseline respiration rate of 1.0 nmols/ml*min.

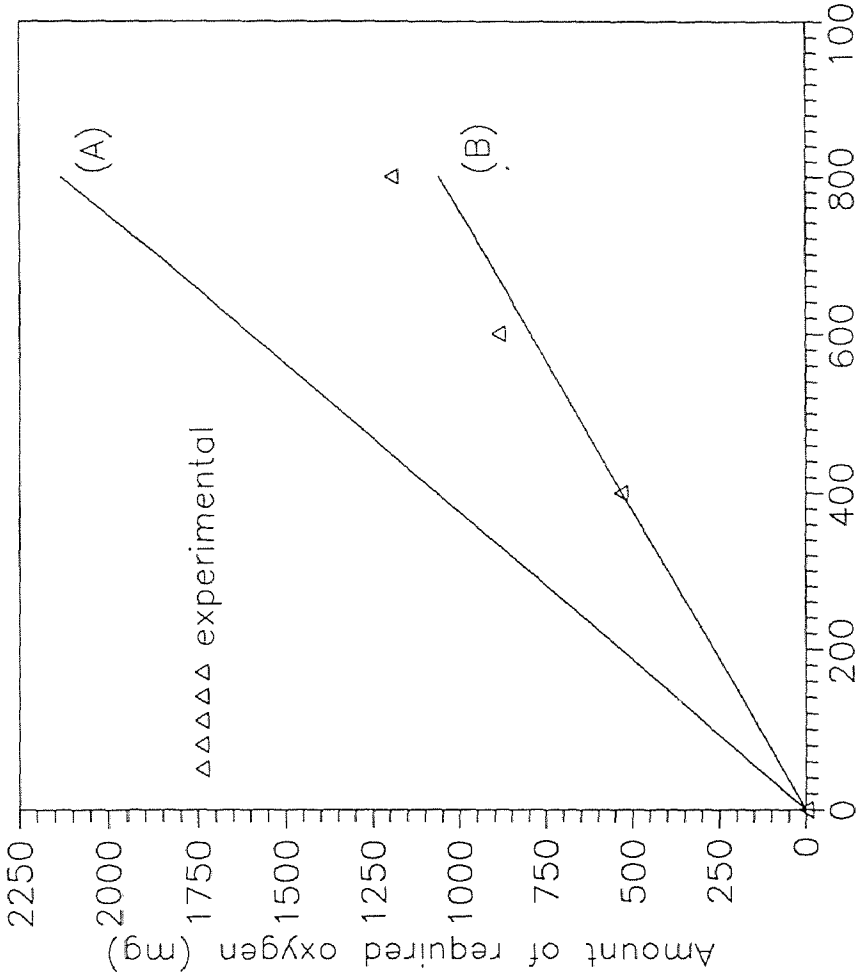

Figure 24. Comparison of the Required Oxygen Amount in Ethylene Glycol Biodegradation with 2 liter reaction volume. Line (A): respiration; Line (B): with biomass growth

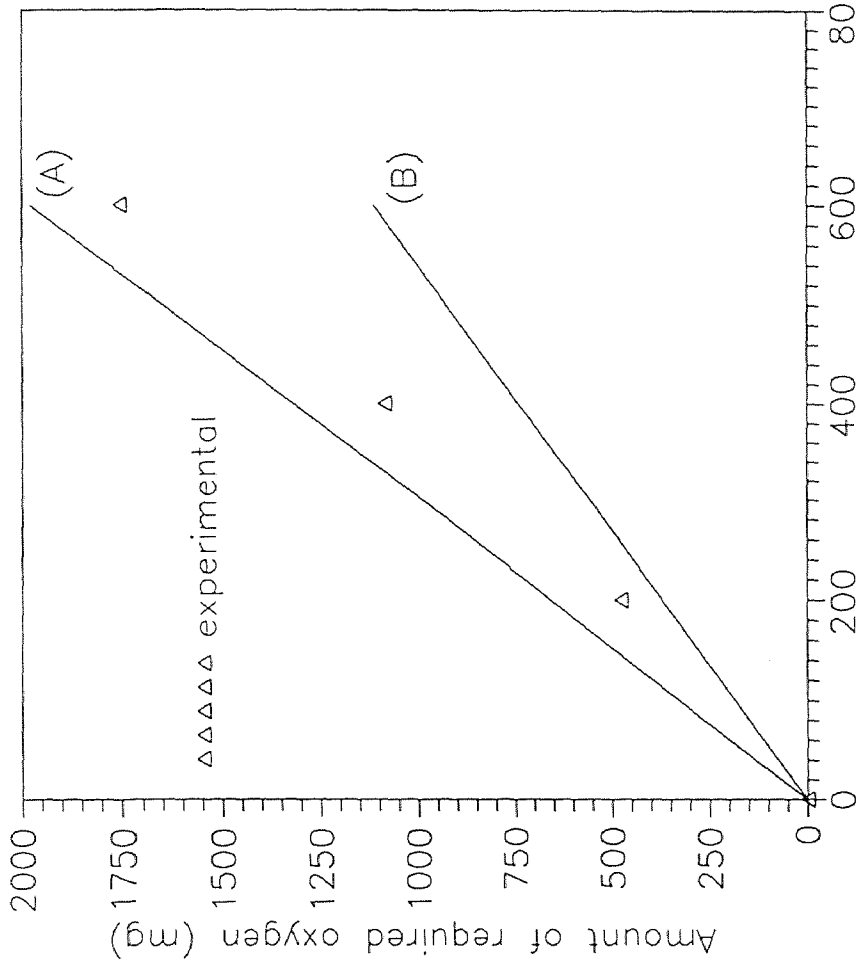

Figure 25. Comparison of the Required Oxygen Amount in Tetraethylene Glycol Biodegradation with 2 liter reaction volume. Line (A): respiration; Line (B): with biomass growth.

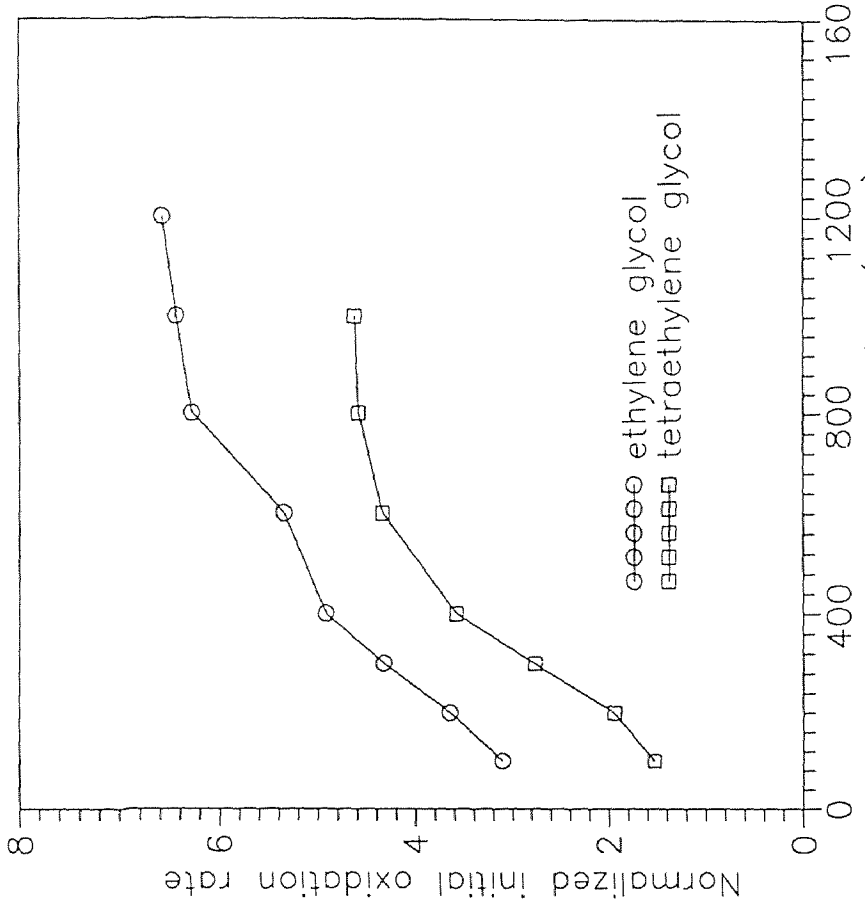

Figure 26. Normalized Oxidation Rate of Ethylene Glycol and Its Tetramer at Different Starting Concentrations, Normalized initial oxidation rate = initial oxidation rate/baseline oxidation rate. A plateau is reached as expected, and no substrate inhibition is observed.

By GC analysis of the ethylene glycol oxidation reaction medium, it was observed that three new peaks were formed after 30 minutes of reaction time which were not present initially. The area of these peaks increased for some time, after which they started decreasing and eventually disappeared. Appendix B shows the raw GC data.

TOC and TIC analyses were done to ascertain that all the available organic carbon at the start was converted to inorganic carbon by the end, when the intermediates and ethylene glycol could no longer be detected on GC.

Figure 27 shows the results of this analysis. TOC concentration decreases slowly during the first 2.5 hrs. of the reaction. This phase coincides with disappearance of ethylene glycol and build up of intermediates A, B, and C from GC analysis. During this time concentration of TIC also increase a little at a gradual rate.

After 3 hours of reaction time the dynamics change substantially and the decrease in TOC and increase in TIC are much more rapid. This phase describes the degradation of intermediates B and C. At the end of 7.5 hrs 95 % of the initial organic carbon was converted to inorganic carbon, mainly CO_2.

Figure 28 shows the result of TIC and TOC changes during biodegradation of tetraethylene glycol. The graph indicates that the biodegradation trend of tetraethylene glycol is the same as that seen for ethylene glycol.

Table 2 summarizes the relative bio-oxidation responses of ethylene glycol, tetraethylene glycol, and several other selected substrates.

Figure 29 summarizes the fate of ethylene glycol and the intermediates in a typical experiment. At time zero when ethylene glycol is injected there are no intermediates. As the reaction proceeds three intermediates were detected and one of them was identified as formaldehyde (C in Figure 29).

Intermediate A has a very short half life compared to B and C. Its concentration starts decreasing even before ethylene glycol has been completely degraded. In fact both intermediates B and C reach their maximum concentration (which makes sense since no

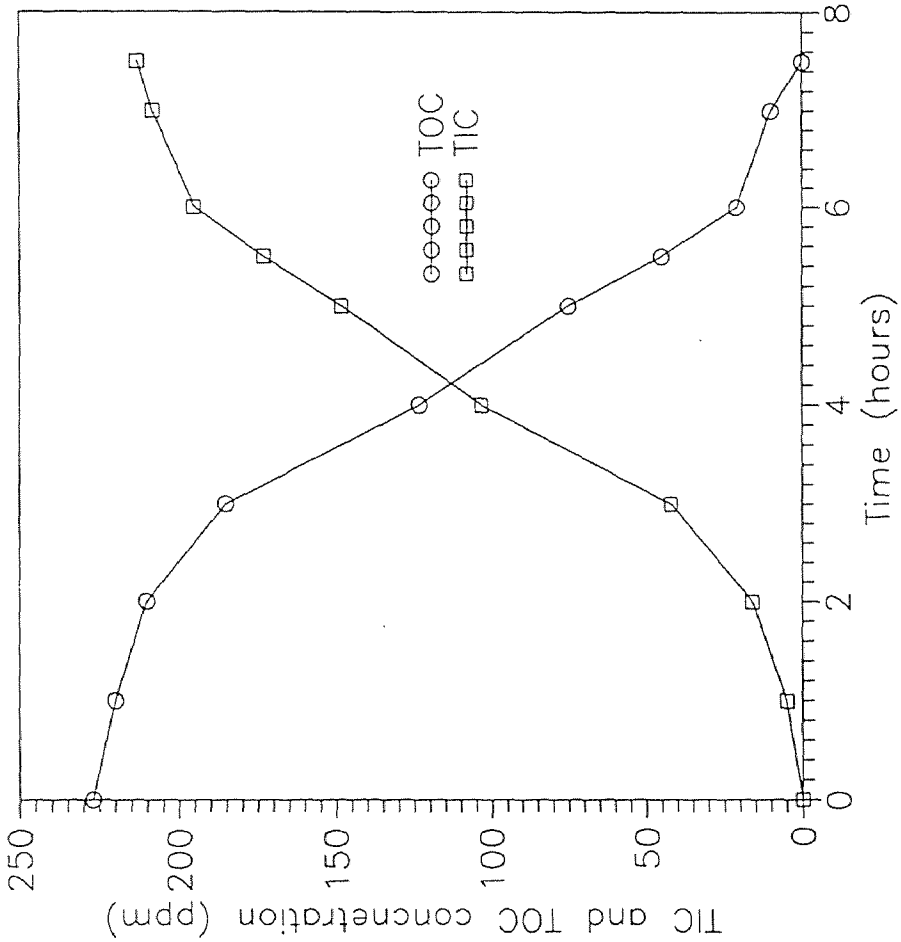

Figure 27. TIC and TOC in Biodegradation of Ethylene Glycol (600 ppm)

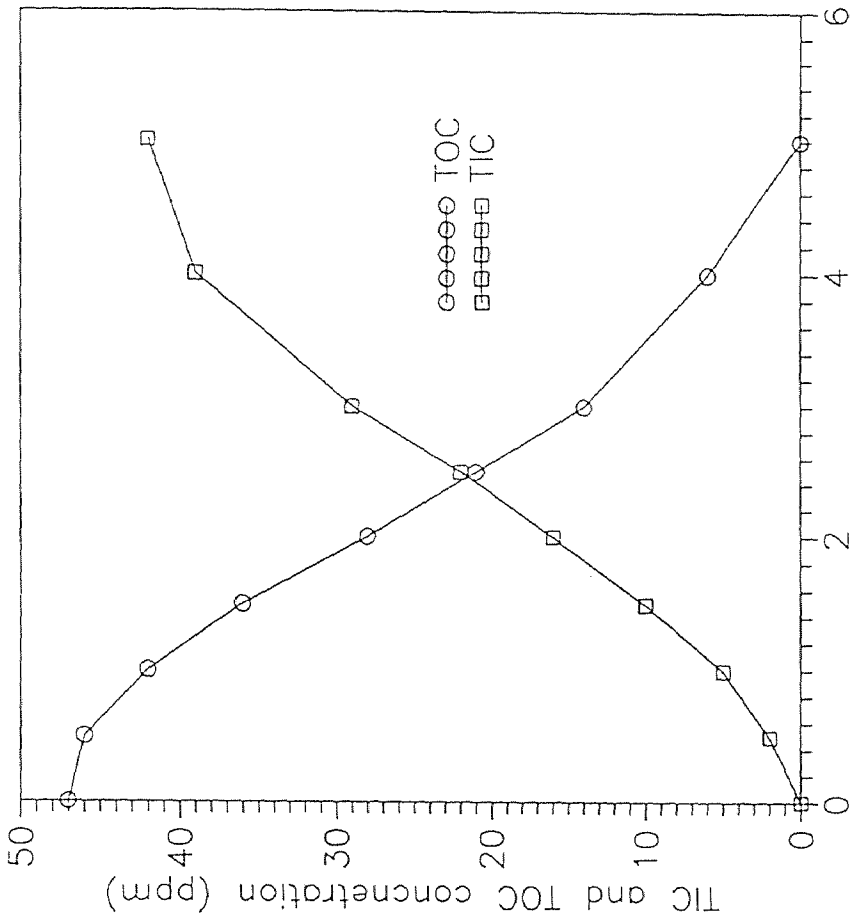

Figure 28. TIC and TOC in Biodegradation of Tetraethylene Glycol (100 ppm)

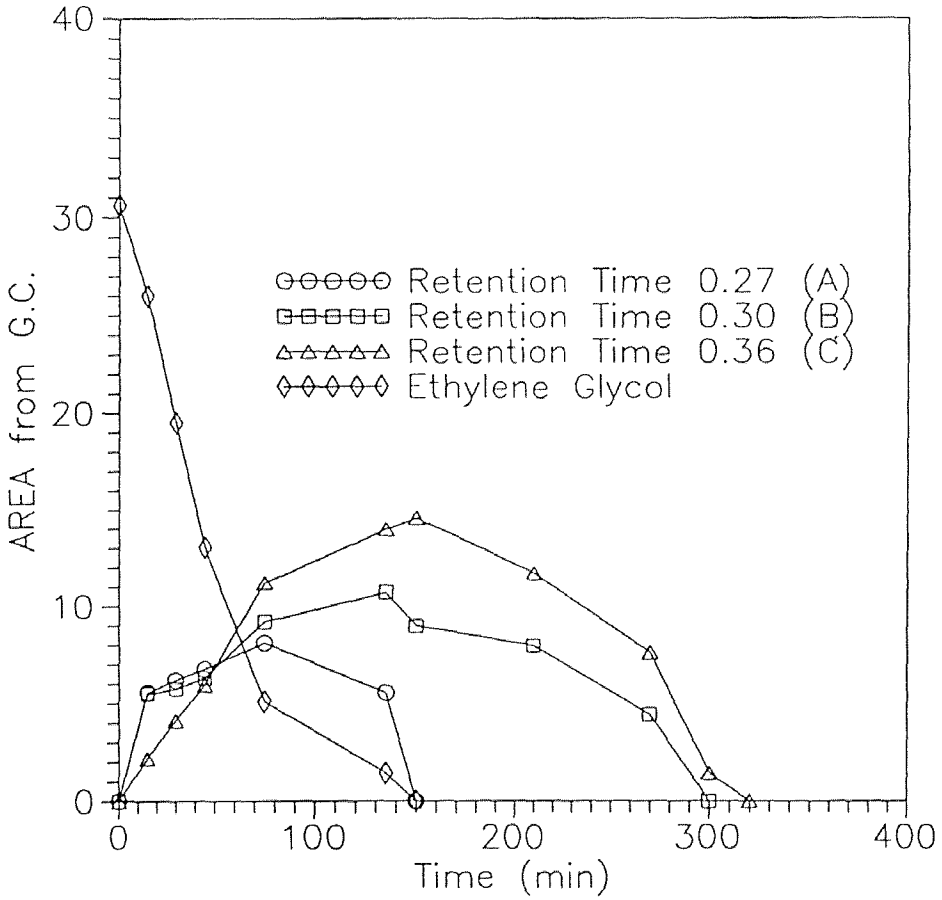

Figure 29. Reaction of Ethylene Glycol(400 ppm) witn Biocatalyst. Y-axis is just area from G.C. because intermediates are not identified so that the exact concentration of intermediates could not be found.

more ethylene glycol is available to form the intermediates) by the time the ethylene glycol concentration reaches zero. Both intermediates B and C are fairly stable compounds. After ethylene glycol is completely degraded (150 minutes), it takes another 150 minutes for intermediate B to completely degrade while C (identified as formaldehyde) is completely degraded 40 minutes later.

5.4 Phenol Degradation under the Influence of Magnetic Fields

The effect of 0.49 tesla unipolar north and south magnetic fields on phenol disappearance is shown in figure 30 for several concentrations. South polar irradiation intensified degradation at all concentrations, and the north pole field inhibited degradation.

Figure 31 summarizes the data in terms of corrected oxidation rates, and the conclusions are the same as for Figure 30.

Results obtained under the influence of north pole, south pole and during the control experiments are given in Table 5. It can be seen that the highest average rate of phenol biodegradation and oxygen consumption occurred when the south pole was attached to the bioreactor.

When the magnetic south pole was applied, the biological oxidation activity (measured as dissolved oxygen consumption rate) increased by more than a factor of two as compared to the control experiment without magnetic field. Figure 32 shows the effect of magnetic fields on the rate of dissolved oxygen consumption. It can be seen that the rate increases markedly after 4 days under the influence of the south pole as compared to the control and the north pole.

One of the measures of biodegradation is the increase in activity (measured as rate of dissolved oxygen consumption) of the microbes in the presence of a substrate such as phenol. An increase in dissolved oxygen consumption indicates that it is being utilized by the microorganisms to break down phenol into its metabolic products which ultimately are CO_2 and water.

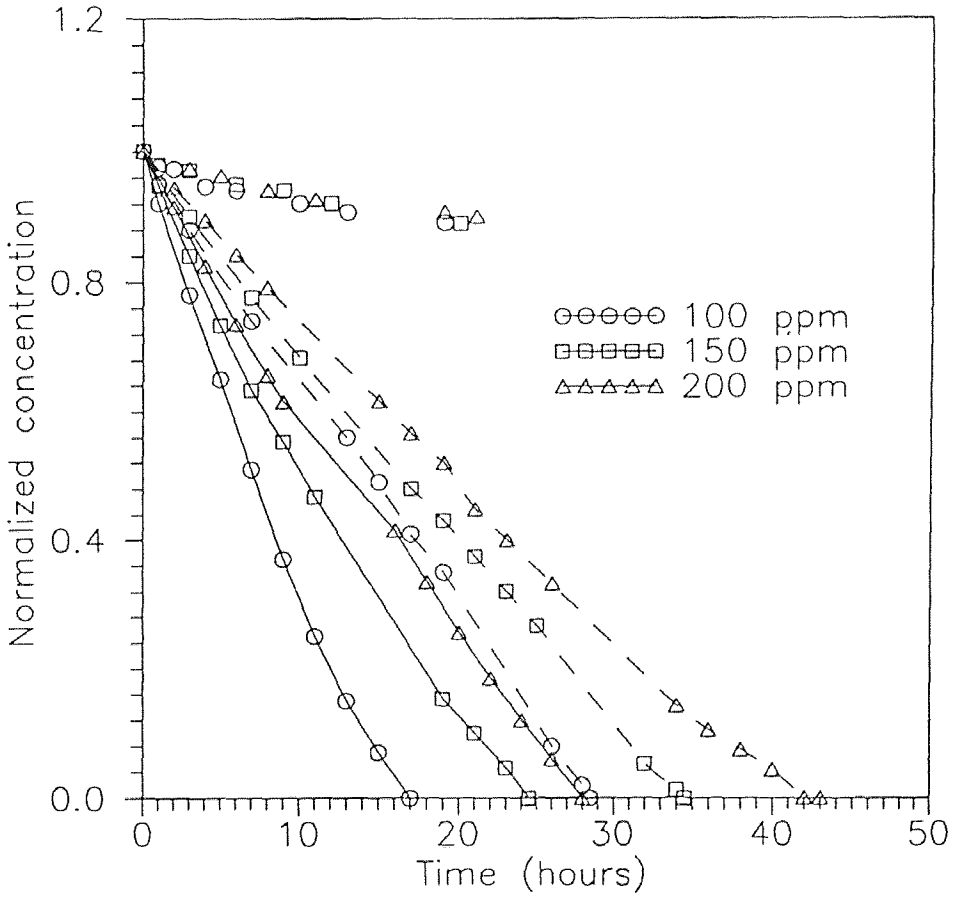

Figure 30. Effect of a 0.49 Tesla Magnetic Field on Phenol Biodegradation with Different Starting Concentrations. Solid line: south pole field; no line: north pole field; dashed line: control (without magnetic field).

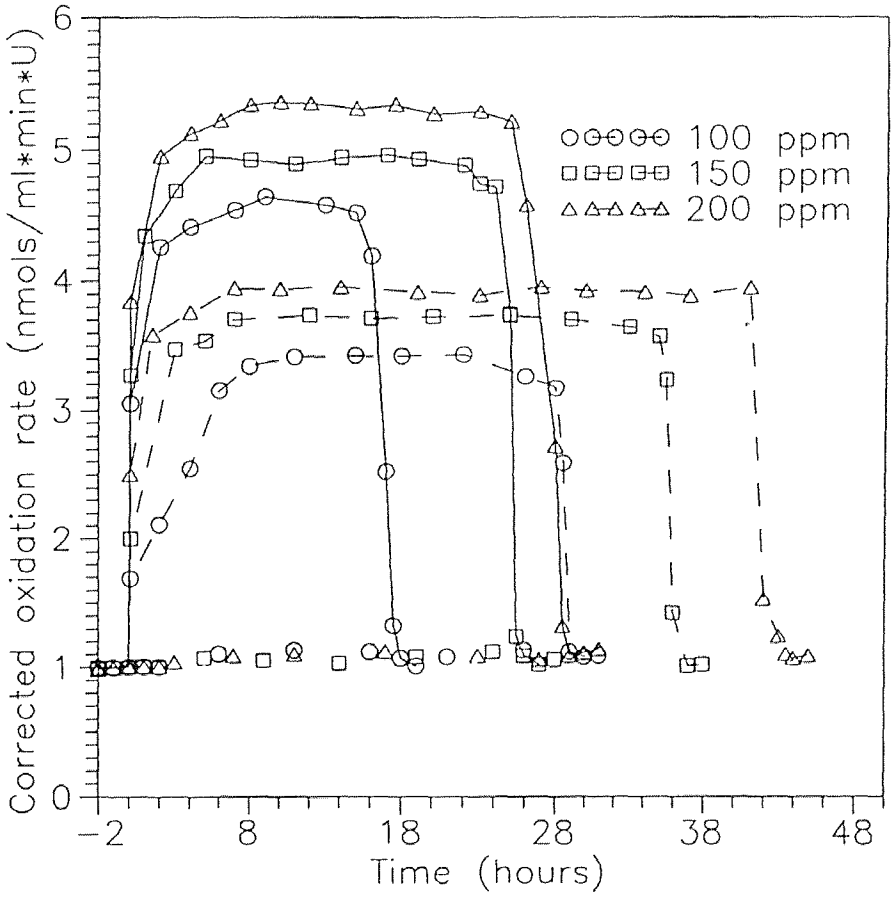

Figure 31. Corrected Oxidation Rate of Phenol Biodegradation at Different Starting Concentrations under 0.49 Tesla Magnetic Field. Corrected oxidation rate = oxidation rate/U. U is defined as a unit activity giving a baseline respiration rate of 1.0 nmols/ml*min. No line:north pole field; dashed line: control (without magnetic field); solid line: south pole field.

Table 5. Effect of Magnetic North and South Pole Fields on Phenol Biodegradation in Batch Recirculation Bioreactor. Values given represent mean ± standard deviation. The intervals of confidence are indicated in brackets.The interval of confidence is a probability that the population parameter falls within the boundary of the interval. N.D, not detectable. Control means without any magnetic field.

Parameters	Control	South pole	North pole
Rate of O_2 consumption (nmol/ml*min)	0.615±0.053 (92.5 %)	1.546± 0.165 (88 %)	0.365 ± 0.045 (86.5 %)
Secreted extracellular enzyme concentration (μg/ml)	170.5± 0.7 (99 %)	2357 ± 46.2 (97.5 %)	N.D
Rate of phenol biodegradation (ppm/hr)	3.113 ± 0.02 (99 %)	4.437 ± 0.253 (95 %)	0.476±0.043 (90 %)

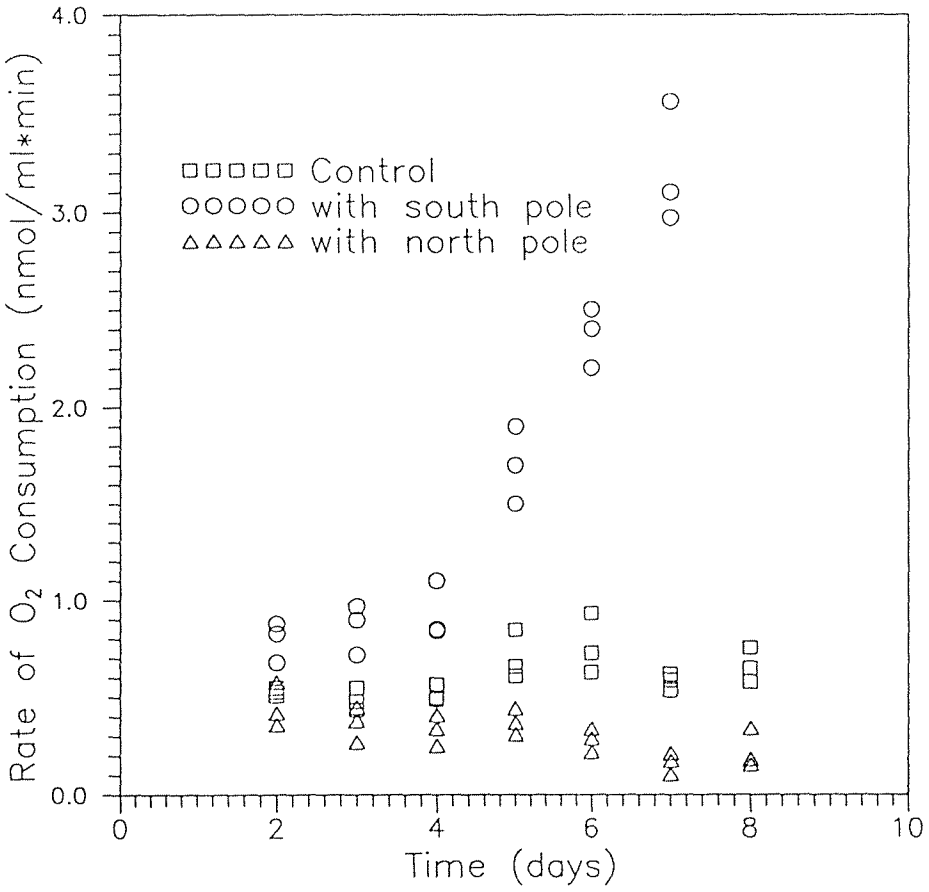

Figure 32. The Effect of Magnetic South and North Pole Field on the Rate of O_2 Consumption during Phenol Biodegradation in batch recirculation mode with immobilized activated sludge. Control means without magnet. Three independent runs with different biomass batches were utilized.

The phenol consumption rate was faster by nearly 30 % in the experiment with the south pole as compared to the control. Figure 33 indicates that the phenol concentration decreased rapidly under the influence of the south pole in comparison with the north pole and the control. The observed trend compares closely with that for the rate of dissolved oxygen consumption and increase in extracellular protein concentration.

Significant production of extracellular protein verified that biological activity was increased when a magnetic south pole was applied to the system as compared to the control as shown in Figure 34. Microorganisms release enzymes extracellularly which in turn attack the substrate. A higher amount of proteins in the reaction medium may serve as a measure of biodegradation.

The poles were reversed several times. Initially no magnetic field was applied, then the south pole was applied three times with the north pole twice alternatively over the duration of the experiment. The north pole was consistently inhibitory and the south pole activating as seen from the dissolved oxygen consumption rates in Figure 35.

Figures 36, 37 and 38 summarize the data obtained from analysis of phenol, DO and extracellular enzyme concentration, respectively, during biodegradation experiments.

Curve "A" represents an experiment conducted with bacteria which were not pre-acclimated with the south pole magnetic field, and were not exposed to magnetic field during the course of the experiment. This is the control.

Curve "B" represents magnetically pre-acclimated bacteria which were used in an experiment conducted in the absence of any magnetic field.

Curve "C" and curve "D" are experiments conducted with magnetically pre-acclimated bacteria in the presence of south pole magnetic field, curve "C" with 0.35 tesla and curve "D" with 0.15 tesla.

Biodegradation rates in all cases were gradually increased as the system stabilized after 2 or 3 days. The degradation rates for phenol were in the range of 2.5 to 3.5 ppm/hr with microbes not acclimated and not exposed to magnetic fields (A). With magnetically

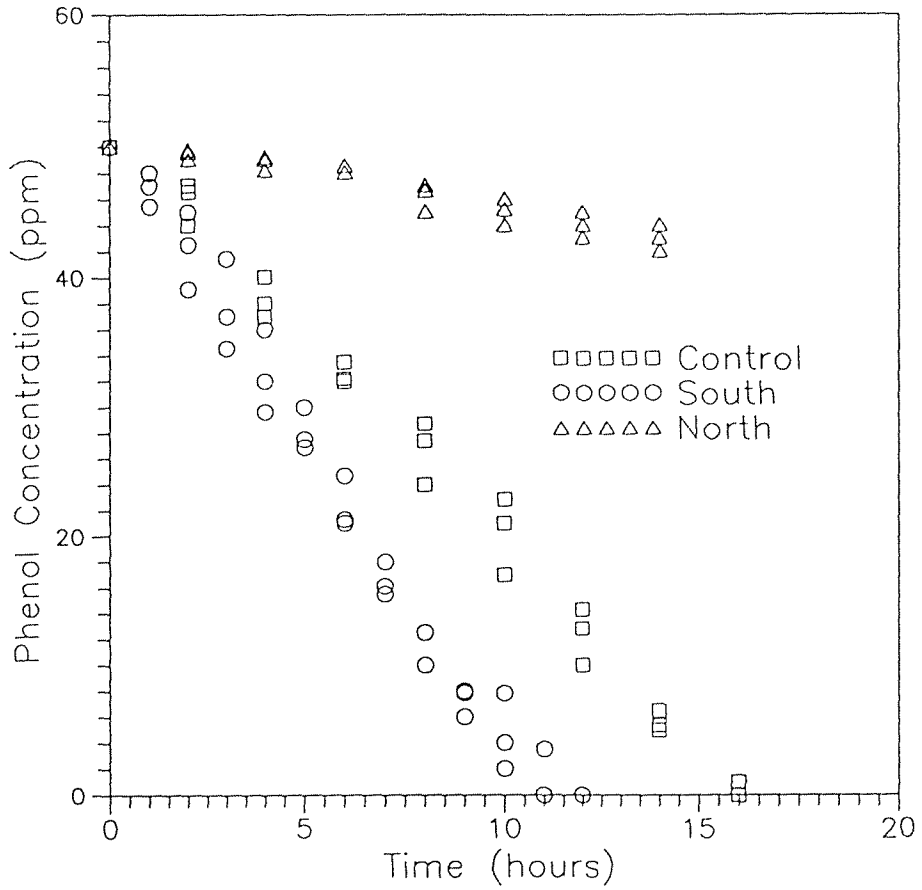

Figure 33. The Effect of Magnetic South and North Pole Field on the Rate of Biodegradation when phenol was used as sole carbon source. Control means without magnet. Three independent runs with different biomass batches were utilized.

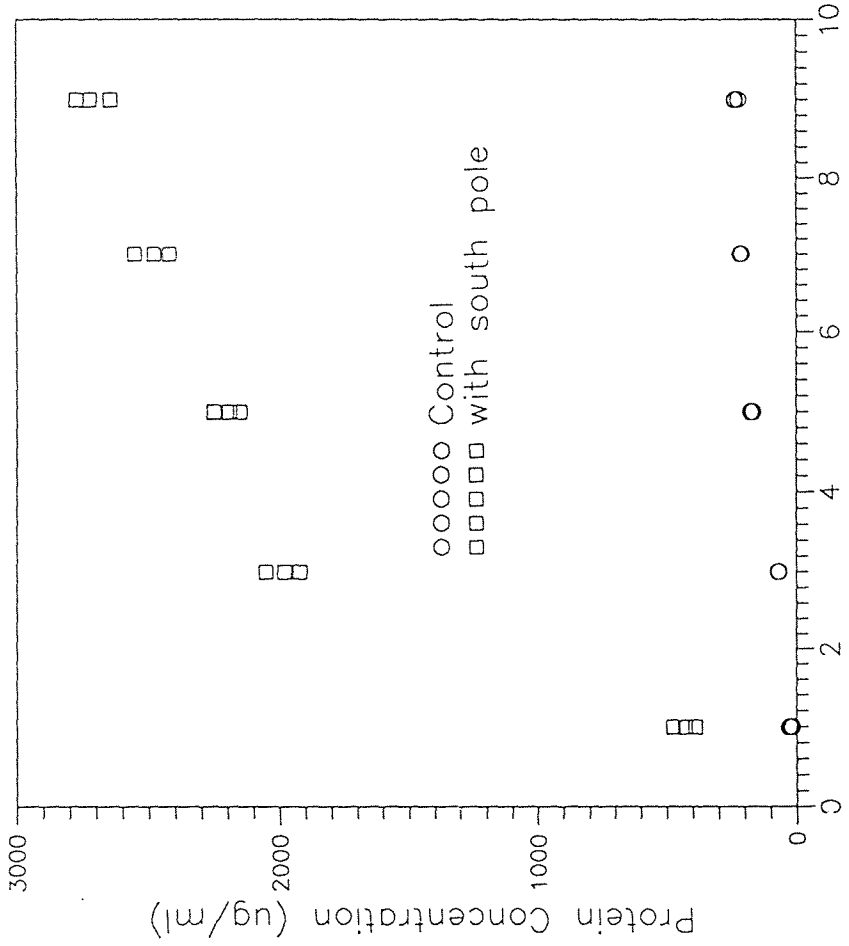

Figure 34. The Effect of Magnetic South Pole Field on the Protein Concentration. (control means without magnet) Protein was not detected in reactor with north pole. Three independent runs with different biomass batches were utilized.

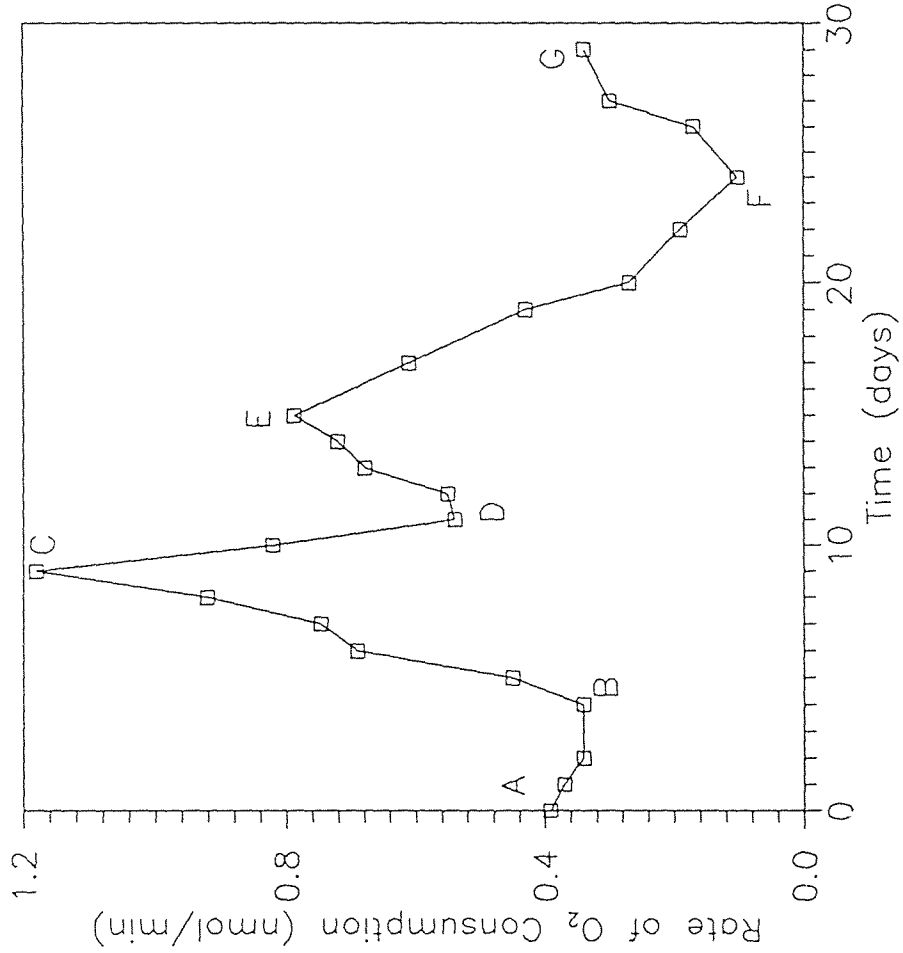

Figure 35. The Effect of Alternating Magnetic Field on the Rate of O_2 Consumption. AB control, BC with south pole, CD with north pole, DE with south pole, EF with north pole, FG with south pole.

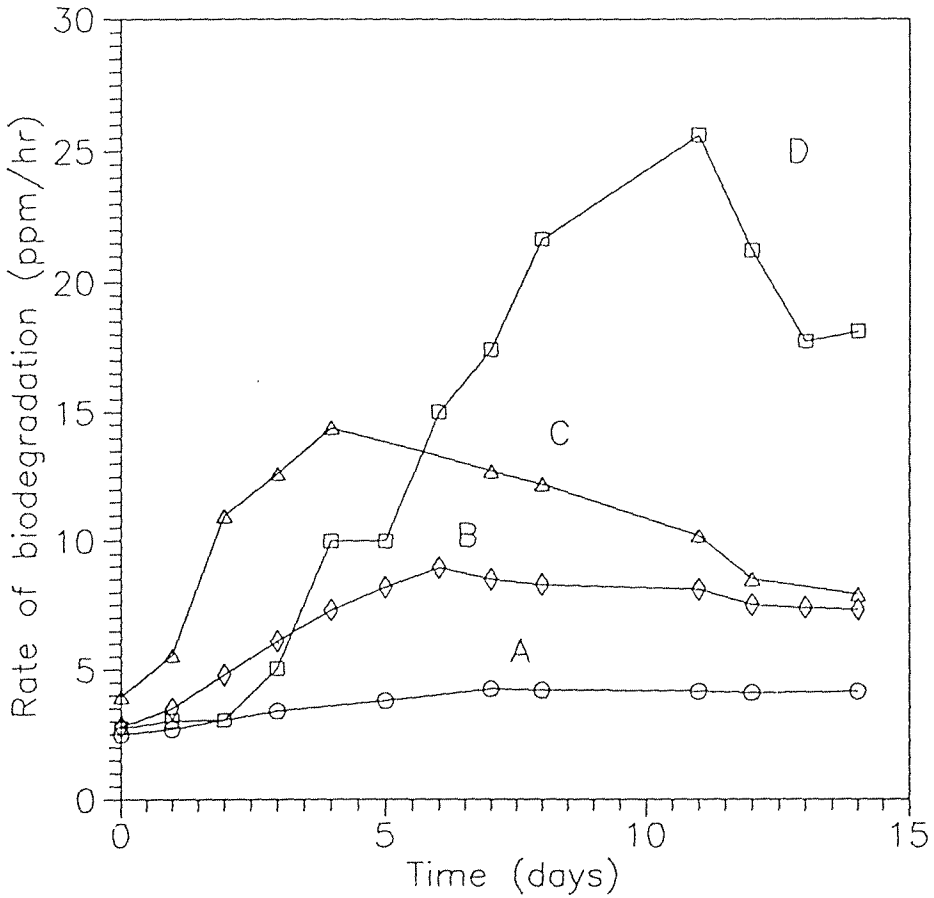

Figure 36. Effect on Rate of Phenol Biodegradation at Initial Concentrations of 100 ppm.
A: non acclimated free cells, no magnet during run
B: acclimated free cells, no magnet during run
C: acclimated free cells, 0.35 tesla south pole irradiation during run
D: acclimated free cells, 0.15 tesla south pole irradiation during run

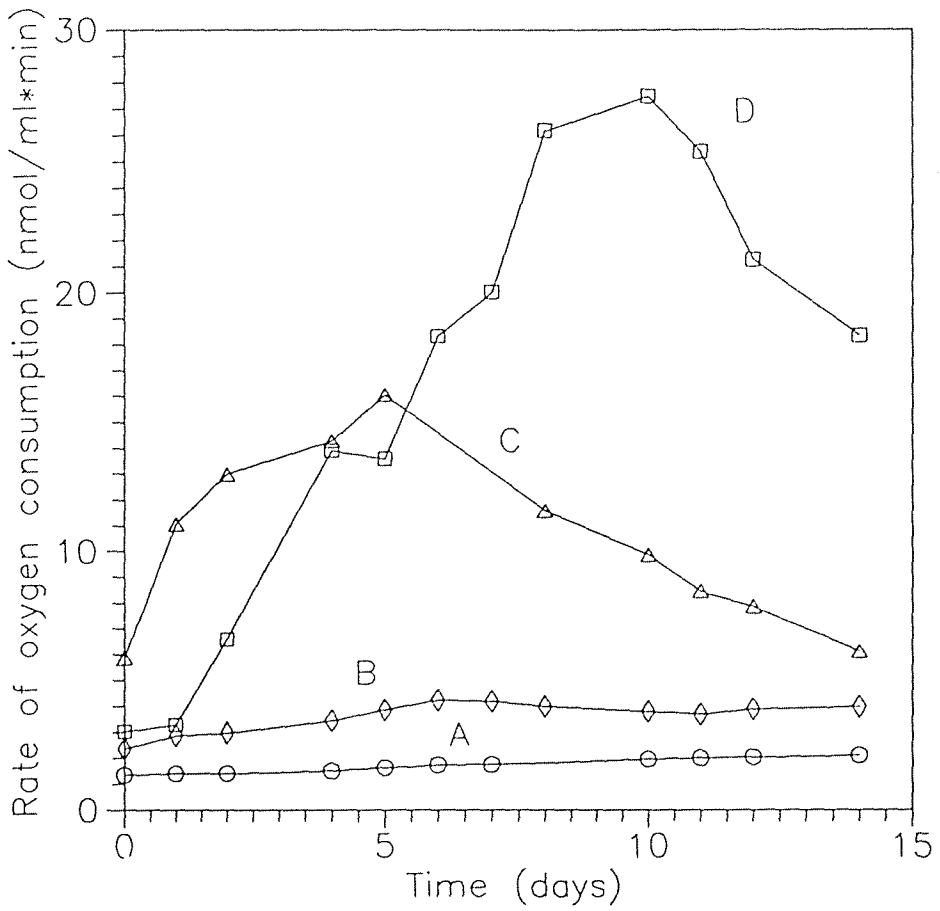

Figure 37. Effect on Rate of Oxygen Consumption with 100 ppm Phenol Substrate. A: non acclimated free cells, no magnet during run
B: acclimated free cells, no magnet during run
C: acclimated free cells, 0.35 tesla south pole irradiation during run
D: acclimated free cells, 0.15 tesla south pole irradiation during run

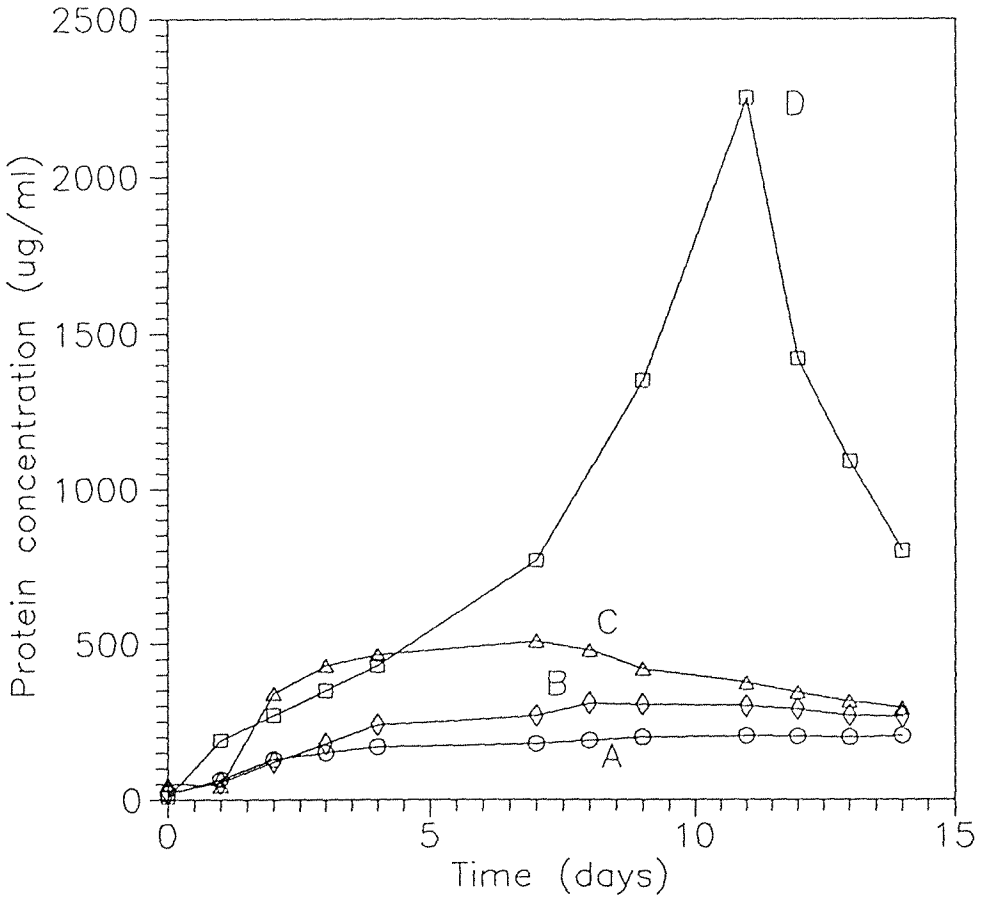

Figure 38. Effect on Protein Concentration with 100 ppm Initial Phenol Concentrations. A: non acclimated free cells, no magnet during run
B: acclimated free cells, no magnet during run
C: acclimated free cells, 0.35 tesla south pole irradiation during run
D: acclimated free cells, 0.15 tesla south pole irradiation during run

pre-acclimated bacteria without exposure to magnetic field during the run the rates were in the range of from 2.5 ppm to 8.0 ppm/hr. This suggests that the pre-acclimation step enhanced the maximum rate by about 2 times.

Further enhancement of oxidation rates was realized when magnetically pre-acclimated bacteria were used to degrade phenol in the presence of further magnetic south pole irradiation.

With a field strength of 0.35 tesla (curve "C"). The maximum rates ranged from 2.5 to 14.5 ppm/hr with an enhancement of 4 times over the control experiment. With a field strength of 0.15 tesla (curve "D") the rates ranged from 2.5 to 26 ppm/hr with an enhancement of 7.5 times the rates observed in the control experiment.

Figure 37 shows results from the analysis of oxygen consumption rates. The curves A, B, C and D follow the same trend as was seen in the analysis of phenol consumption.

Oxygen consumption rates of microbes not pre-acclimated with the magnetic field, and without exposure to magnetic field during biodegradation experiments are the lowest in the range of 1.5 to 2.0 nmoles/(min-ml) (curve "A"). Oxygen uptake rate (OUR) for microbes pre-acclimated with south pole magnetic field are a little higher than the controls. The OUR ranged from 2.5 to 4.5 nmoles/(min-ml) (curve "B"). The OUR for pre-acclimated microbes with exposure to magnetic field during biodegradation are substantially higher.

Curve "C" shows OUR in the presence of 0.35 tesla of magnetic field. The rates ranges from 3 to 16 nmoles/(min-ml), a maximum enhancement of 8 times over the control. Curve "D" shows OUR in the presence of 0.15 tesla of magnetic field. The rate range from 6 to 27 nmoles/(min-ml), a maximum enhancement of 13.5 times over the control experiment.

Figure 38 shows results from analysis of extracellular enzymes (measured as protein concentration by standard Lowry test). The observed trend follows the pattern seen in the analysis of OUR and phenol concentration. With essentially no extracellular

enzymes present at the start, their concentration increased as the microbes were challenged with phenol.

Maximum concentration of total extracellular protein observed in the control was 200 μg/ml. In the case of pre-acclimated microbes the maximum concentration was 350 μg/ml. In the case where pre-acclimated microbes were exposed to the magnetic field during biodegradation the maximum extracellular enzyme concentration was 550 μg/ml with 0.35 tesla field strength and was 2300 μg/ml with 0.15 tesla field strength, an increase of one order of magnitude from the control experiment.

Results from the analysis of phenol, OUR and extracellular enzyme concentration show that south pole magnetic field increases biological activity for phenol among microorganisms from activated sludge. This increase in activity can be obtained by pre-acclimating the microbes for a short time in the magnetic field, and also by continuous exposure of the microbes to the field during biodegradation experiments.

Two interesting observations can be made from this analysis. First, biological activity in the control and in the pre-acclimated microbes not later exposed to the magnetic field increases gradually as the system stabilizes, and then the activity levels off. On the other hand when the pre-acclimated microbes were exposed to the magnetic south pole field (0.15 and 0.35 tesla) the biological activity increased significantly and reached a maximum (10 days) after which it started decreasing. This could be due to inhibition from extended exposure to the magnetic field. No phenol was biodegraded during these experiments. The rates were slow, but phenol concentration was detected in all the cases to less than 1 ppm at the end of the run.

Secondly, the enhancement of biological activity is dependent on the strength of the magnetic field. Biological activity was more enhanced in the long run in the presence of 0.15 tesla than it was in the presence of 0.35 tesla. This means that there exists an optimum value of field strength.

Figure 39, derived from Figure 31, shows that phenol oxidation without magnetic field exposure and with south polar exposure follows a pattern between respiration and biomass growth. This implies that south pole magnetic field did not change the mechanism or the reaction pathway because the total amount of oxygen consumed remained the same. Only the rate increased.

Figures 40 and 41 show that for both phenol disappearance and oxygen consumption, the magnetic effects of north and south poles are consistently inhibitory and accelerating, respectively, over a variety of concentration ranges from 50 to 250 ppm.

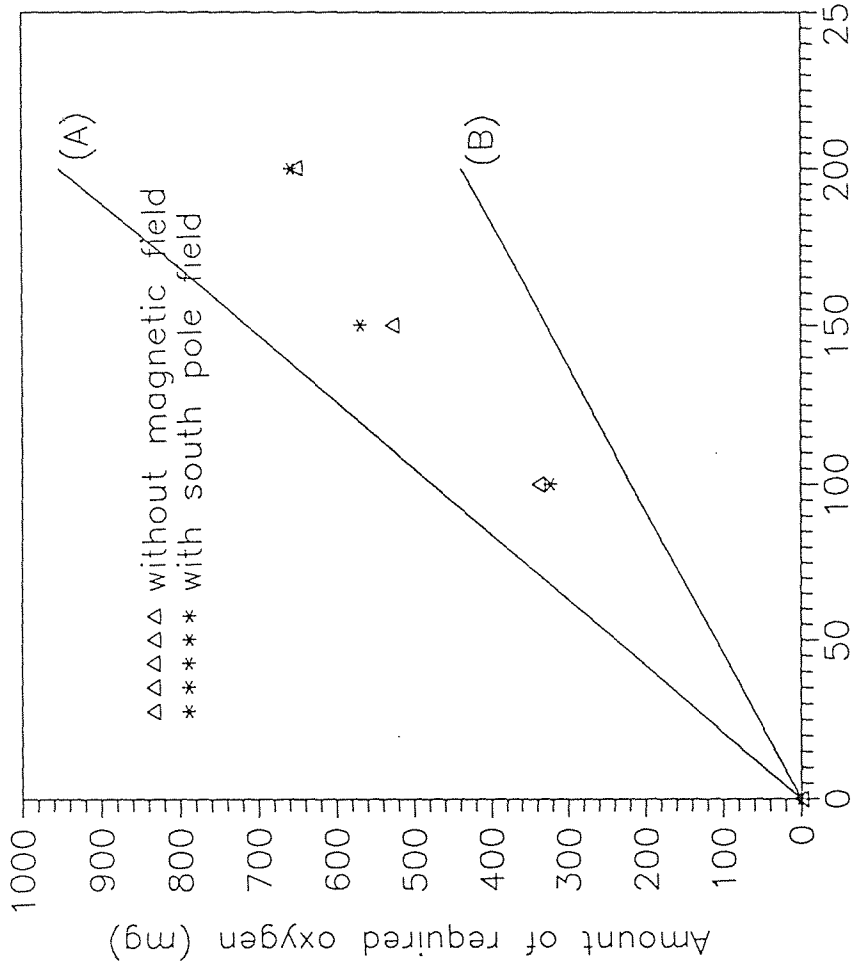

Figure 39. Comparison of the Required Oxygen Amount in Phenol Biodegradation under Magnetic Field with 2 liter reaction volume. Line (A): respiration; Line (B): with biomass growth.

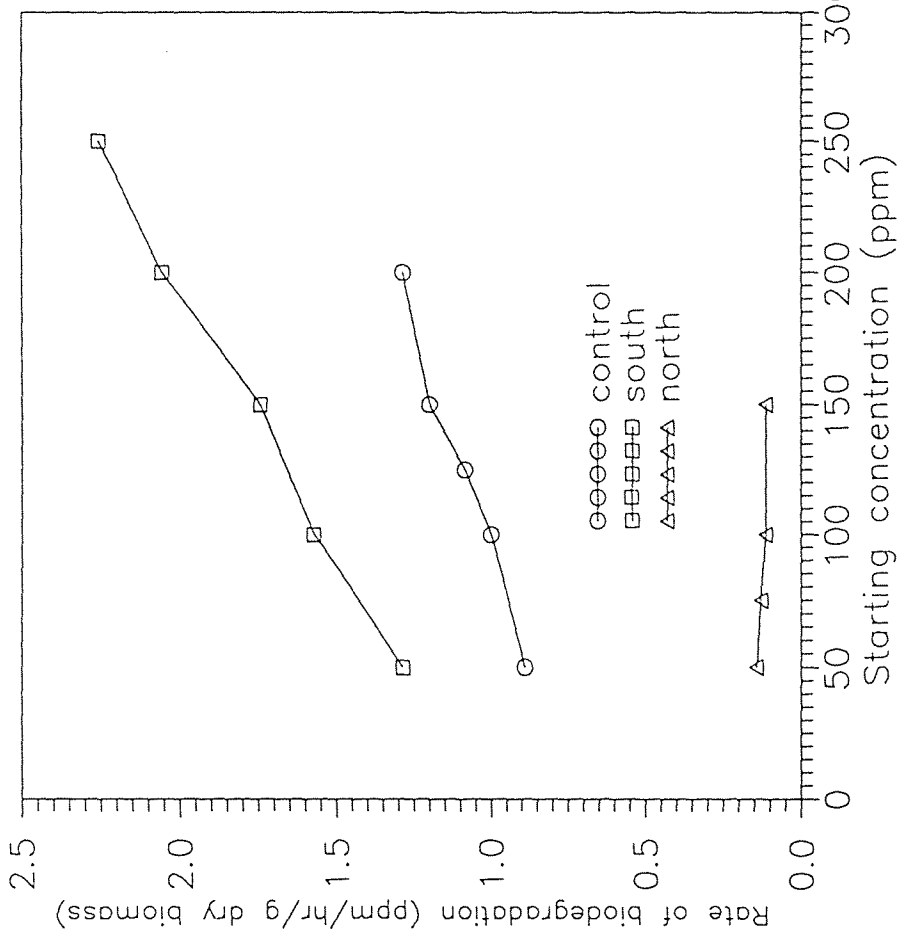

Figure 40. Rate of Phenol Disappearance at Different Starting Concentrations under 0.49 Tesla Magnetic Field.

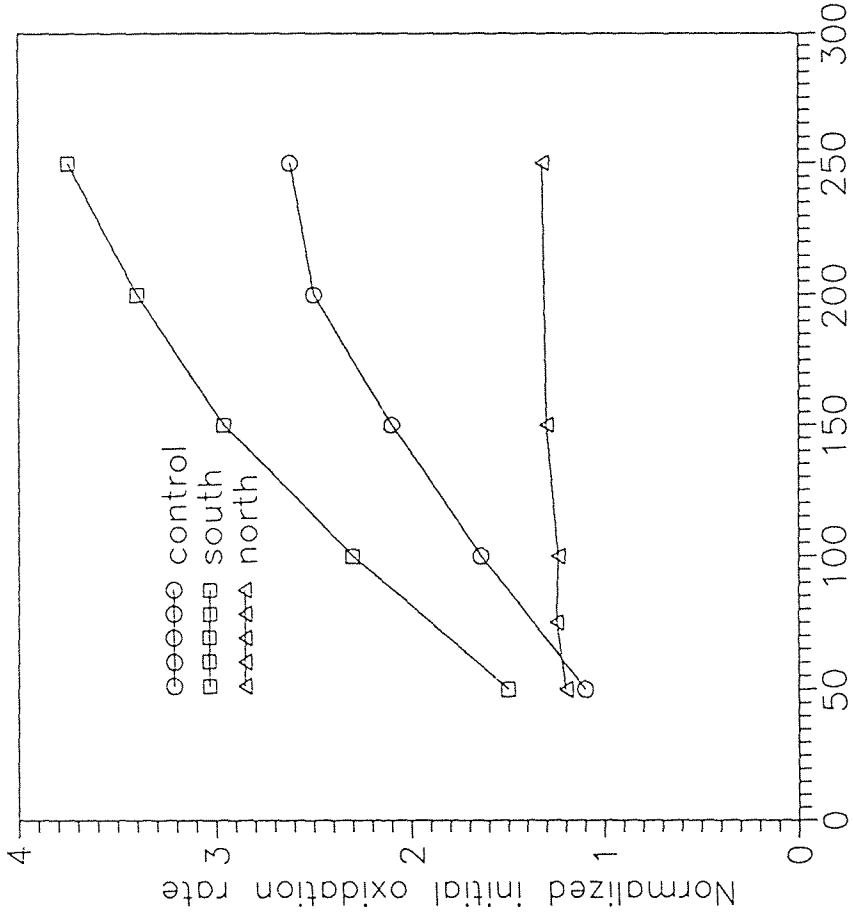

Figure 41. Initial Bio-oxidation Response of Phenol at Different Starting Concentrations. Normalized initial oxidation rate = initial oxidation rate/baseline oxidation rate.

CHAPTER 6

KINETIC STUDIES AND MODELLING

6.1 Assumptions for the Model

Monod kinetics are used to describe the reaction because of applicability and widespread use in the literature. A Monod model, non-inhibitory for substrate concentration, is selected. The following assumptions are made in the development of the model.

1. The liquid phase is homogeneous due to the high recirculation rate.
2. Temperature is constant.
3. Dissolved oxygen is never limiting the process.
4. Reaction occurs in the liquid phase as well as in the beads.
5. Although biomass growth occurs only in the beads, the rate of its production can be based on the entire reactor volume by defining an apparent biomass concentration (b). The value of b represents the amount of biomass in the beads divided by the volume of reactor contents.

6.2 Governing Equation for the System

Based on the above assumption, the system can be described by the following two equations [86] for substrate utilization and biomass growth.

$$-\frac{dS}{dt} = \frac{k_m' S}{K+S}\left(\frac{b}{Y}\right), \text{ and} \tag{6.1}$$

$$\frac{db}{dt} = \frac{k_m' S}{K+S} b \tag{6.2}$$

Initial conditions are

$S = S_O$ at $t = 0$
$b = b_O$ at $t = 0$ in the system,

where S = Substrate concentration (ppm),

k_m' = Maximum substrate utilization (hr^{-1}),

K = Half velocity coefficient (ppm),

t = Time (hr),

b = Biomass concentration (mg/l), and

Y = Yield coefficient (mg biomass/ mg substrate).

The two combined ordinary differential equations were solved to determine the theoretical substrate and biomass profiles during a typical experiment using a computer program IVPRK (based on fifth order Runge-Kutta-Verner method) of the IMSL package shown in Appendix C.

6.3 Evaluation of k_m' and K

The kinetic parameters describing the maximum substrate utilization rate (k_m') and half velocity coefficient (K) for HBA, MMA, EG, and phenol were determined from batch experiments. The substrates were added separately in a shaker flask containing 100 ml reaction medium and a biomass concentration of 1.75 g dry biomass/liter.

These flasks were mounted on a shaker-incubator (Lab-line, Model 3528, reciprocating type) at room temperature (25 to 27 ^oC), and shaken at 120 rpm.

Substrate concentrations were measured periodically as discussed before. The Monod constants k_m' and K for each compound were determined by substituting the measured substrate concentrations at their respective times in the above equation (6.1). The equation was solved using finite difference method for the constants. The computer

program used to solve this equation is available in the RNLIN of the IMSL package shown in Appendix D.

The same analogy could not be applied to styrene which was also studied because during styrene biodegradation considerable amounts of styrene was found to be adsorbed on the calcium alginate gel. The resulting kinetic model therefore does not follow the simple Monod equation. In addition the concentration of tetraethylene glycol (TEG) was not determined by an analytical method because of the difficulty of analysis of such a large molecule and because it was intended to see if a biodegradation reaction could be monitored by measuring DO and pH alone. Hence kinetic analysis of TEG biodegradation was not performed.

Table 6 shows the values of $k_m^{'}$ and K evaluated by the shaker flask experiments based on equation (6.1). The $k_m^{'}$ values tabulated in Table 6 show the following trend: EG> HBA> MMA> phenol. Since the value of $k_m^{'}$ is a direct indication of the maximum rate of biodegradation. We can say that EG is most easy to degrade followed by HBA, MMA and phenol.

These results also make sense from the chemical structure point of view of these substrates. It is natural to assume that EG which is a simple straight chain molecule is more easy to degrade than HBA which is also a simple straight chain molecule but has a high molecular weight. Also simple straight chain molecules (EG, HBA) are more easy to degrade than a branched chain molecule with a double bond like MMA. Finally there are ring compounds like phenol which are more complex than simple branched chain compounds and hence more difficult to degrade.

6.4 Determination of Yield Coefficient (Y)

Figure 11 shows the oxygen requirements for the two extreme (theoretical) cases of yield coefficients. One is for no biomass growth (line A) for which Y is zero and the second is for biomass growth (line B) for which Y is 0.6. Also shown in the figure are oxygen

Table 6. Kinetic Coefficient in Model, k_m' : Maximum substrate utilization, K : Half velocity coefficient. The values of K_m' and K are calculated by computer program as shown in Appendix D.

Compound	k_m' (hr^{-1})	K (ppm)
MMA	4.244×10^{-3}	7.624
HBA	3.786×10^{-3}	8.352
Ethylene glycol	4.094×10^{-2}	11.842
Phenol without magnetic field	9.368×10^{-4}	2.98
Phenol with magnetic field	1.251×10^{-3}	6.54

requirement data points obtained from experimentation. The yield coefficient lies between zero and 0.6 (mg biomass/mg substrate). This was determined by linear interpolation of the slopes and the Y values of the theoretical data. Linear interpolation was used under the assumption that the substrate concentration range studied was not high for any inhibition effect. The Y_{exp} thus obtained are tabulated in Table 3.

6.5 Comparison Theoretical and Experimental data

Figures 42-46 show the comparison between the experimental data and the theoretical profiles using Monod kinetics for substrate degradation, and the theoretical profile for biomass growth.

In all the cases it is seen that the theoretical profile matches relatively closely to the experimental data suggesting that the equation used and the assumptions made adequately describe the system. However, as shown in Table 7, the model does predict biomass growth. Actual biomass growth is very slight since fixed nitrogen is not fed to the system.

Table 7. Predicted Biomass Increase with Different Substrate Concentrations. Initial biomass concentration was 1750 mg/l. Actual biomass growth is very slight since fixed nitrogen is not fed to the system.

Compound	Injected Concentration (ppm)	Predicted biomass increase (mg)	Predicted % increase in biomass (%)
MMA	100	53.7	3.06
	150	80.55	4.60
HBA	100	33.58	1.91
	200	67.17	3.83
Ethylene Glycol	600	313.25	17.9
	800	417.67	23.87
Phenol without magnetic field	150	50.59	2.89
	200	67.46	3.85
Phenol with magnetic south pole field	150	46.83	2.67
	200	62.44	3.56

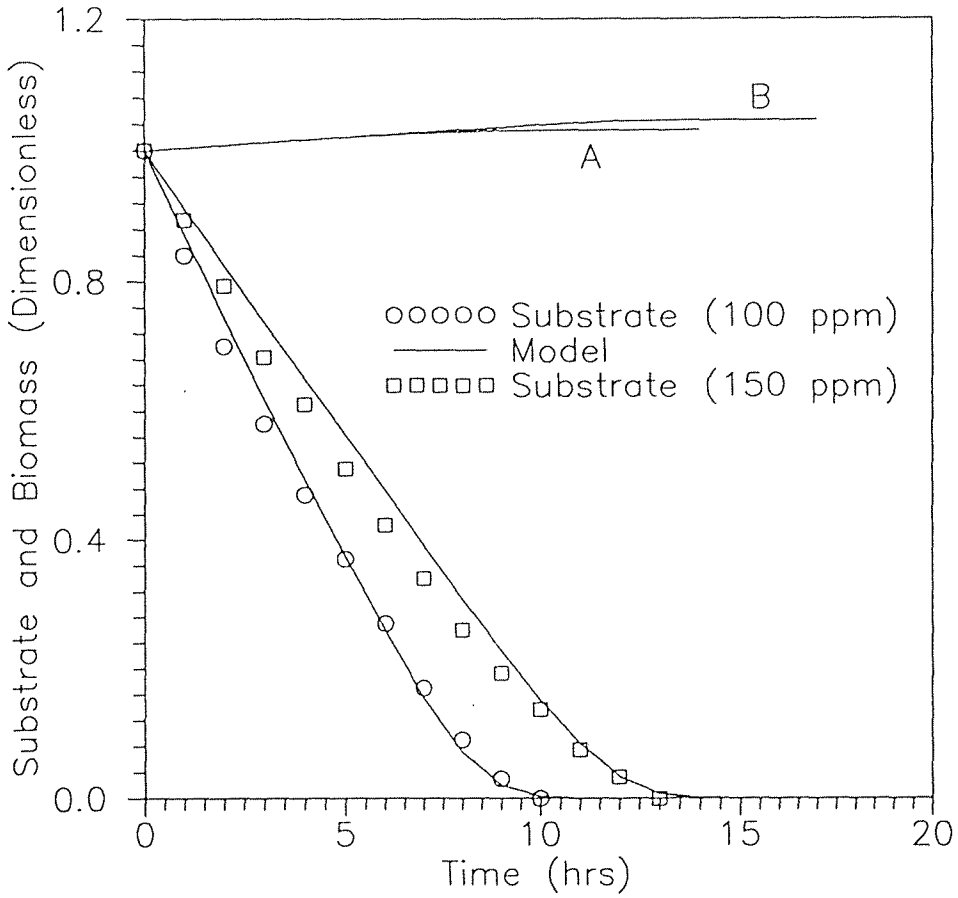

Figure 42. Change in Substrate and Biomass Concentration in MMA Biodegradation with 100 ppm and 150 ppm of starting concentration and 1750 mg/l biomass concentration. Line A and B show how much biomass increase with MMA injections theoretically.

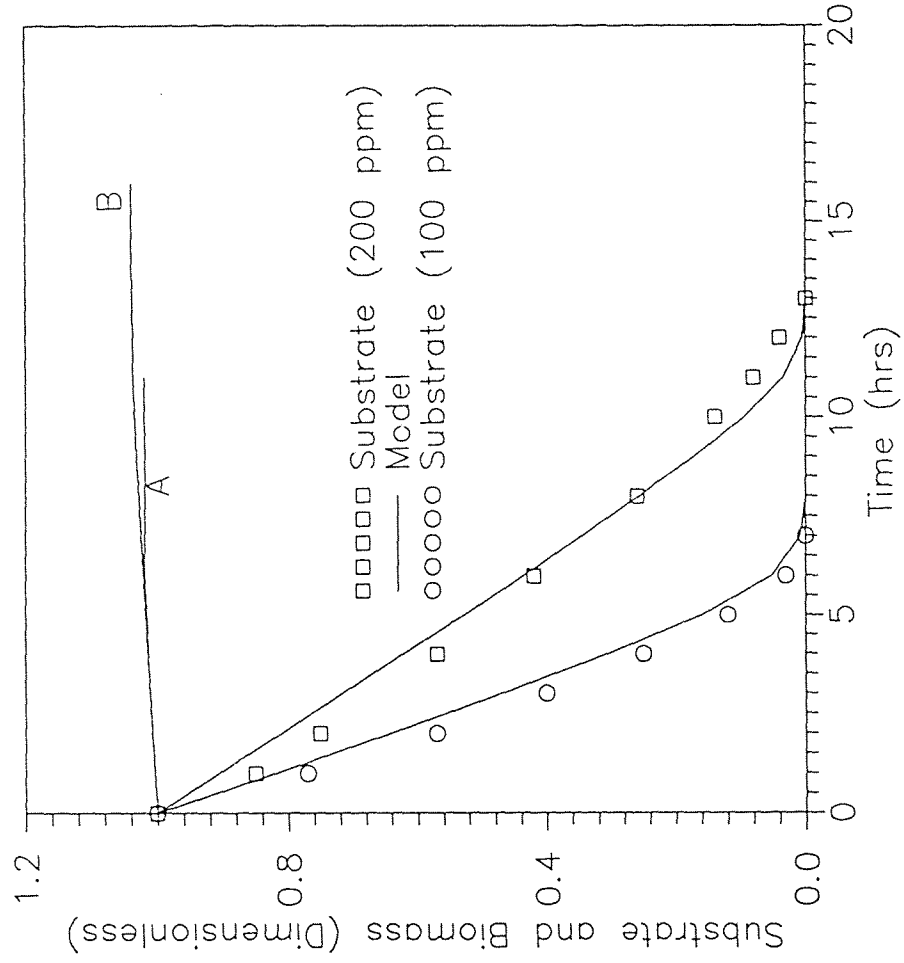

Figure 43. Change in Substrate and Biomass Concentration in HBA Biodegradation with 100 ppm and 200 ppm of starting concentration and 1750 mg/l biomass concentration. Line A and B show how much biomass increases with HBA injections theoretically.

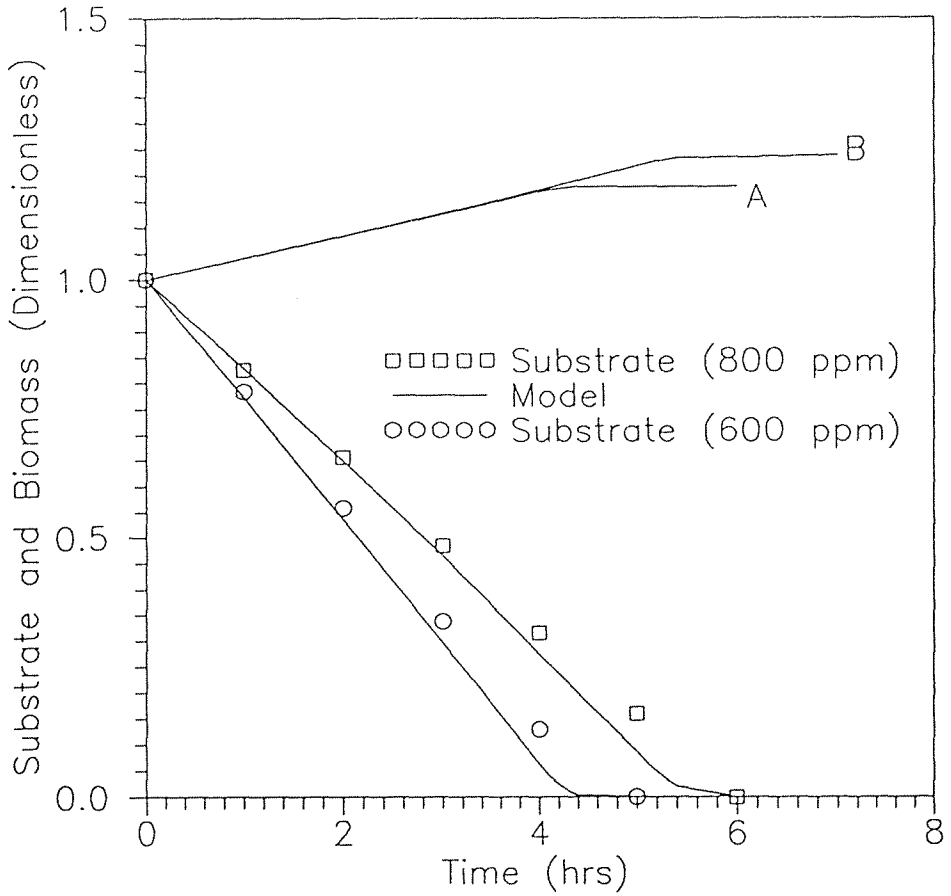

Figure 44. Change in Substrate and Biomass Concentration in Ethylene Glycol with 600 ppm and 800 ppm of starting concentration and 1750 mg/l biomass concentration. Line A and B show how much biomass increases with ethylene glycol injections theoretically.

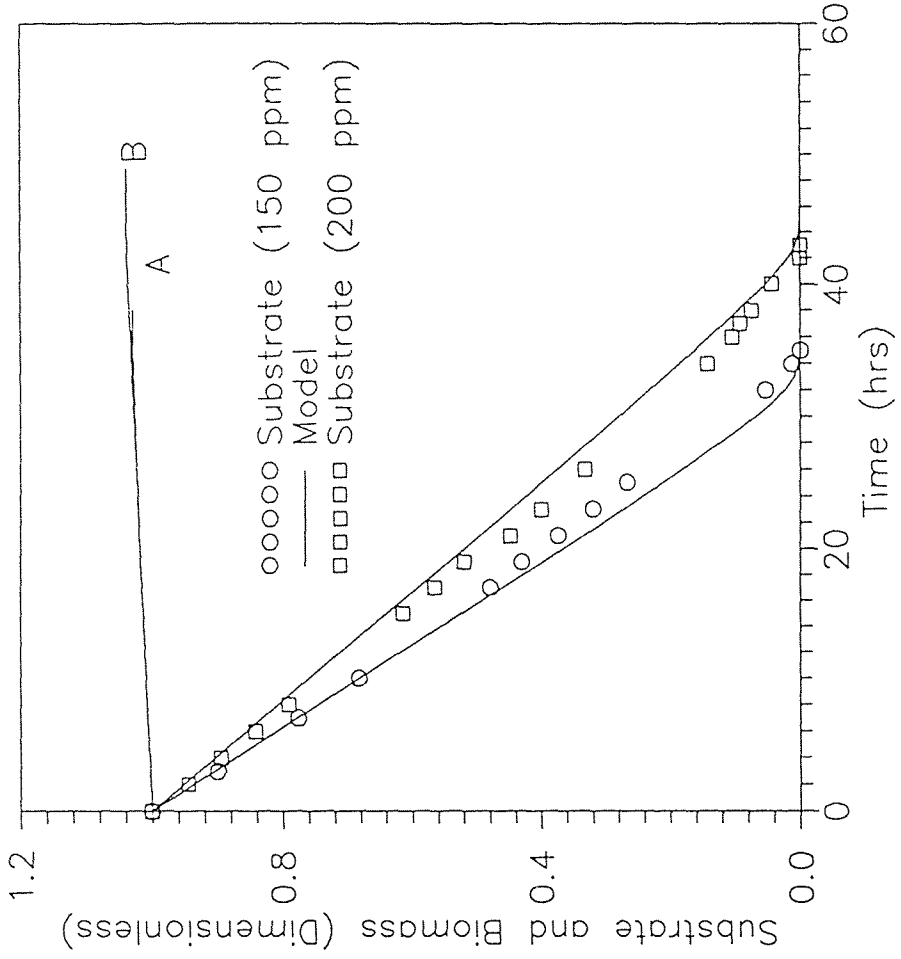

Figure 45. Change in Substrate and Biomass Concentration in Phenol Biodegradation with 150 ppm and 200 ppm of starting concentration and 1750 mg/l biomass concentration. Line A and B show how much biomass increases with phenol injections theoretically without magnetic field.

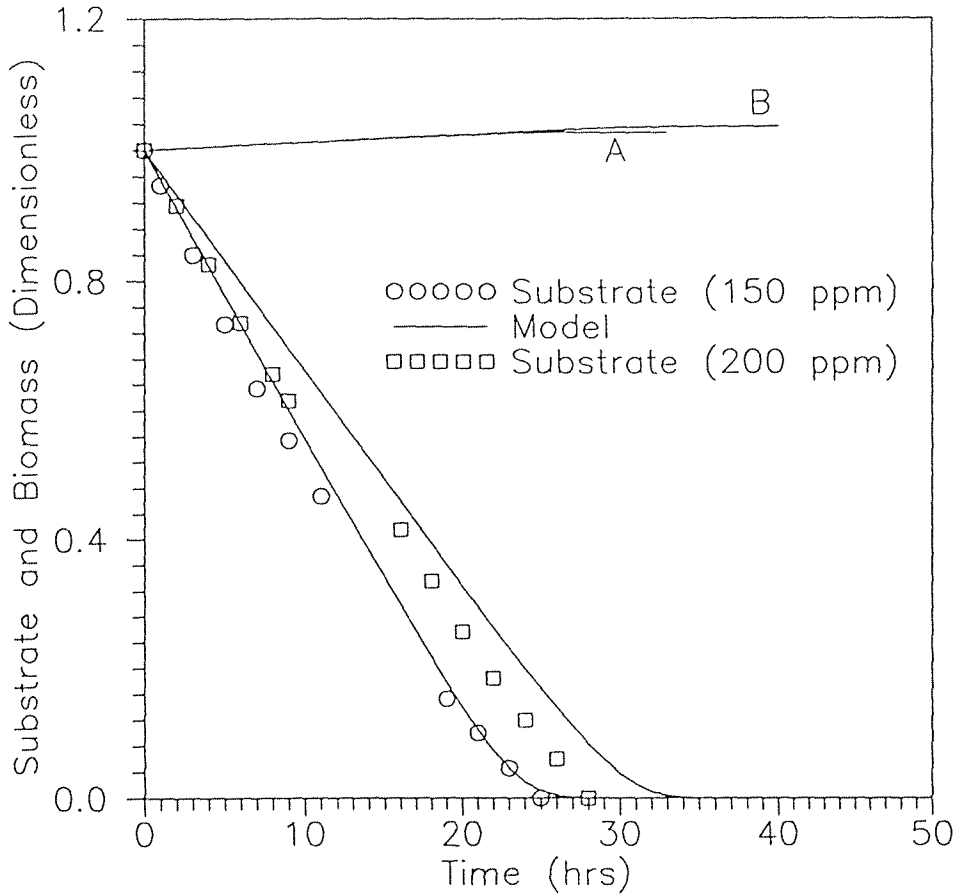

Figure 46. Change in Substrate and Biomass Concentration in Phenol Biodegradation under South Pole Magnetic Field with 150 ppm and 200 ppm of starting concentration 1750 mg/l biomass concentration. Line A and B show how much biomass increases with phenol injections under magnetic south. field (0.49 tesla).

CHAPTER 7

CONCLUSIONS AND RECOMMENDATIONS

The figures in Appendix A illustrate the typical patterns of dissolved oxygen (DO) concentration in the experimental apparatus used in this work upon injection of substrate.

With verification of mineralization, this bio-oxidation pattern is a potential tool that not only gives a good estimate of the oxygen demand of a given organic substrate but also does so in significantly less time than that required in the standard 5 day biochemical oxygen demand (BOD_5) test. It has been established with phenol that complete mineralization occurs on the basis of O_2 consumption measurements. With styrene, MMA, and HBA, mineralization has likely occurred upon return to baseline conditions. TOC results with ethylene glycol and tetraethylene glycol also indicate complete mineralization.

Further work verifying complete mineralization of each sample studied is recommended if the bioreactor is to be used as an instrument for quantification of substrate amounts.

In relative terms, it may be said that HBA has a degradability number of 100, styrene of 22, and MMA of 62. The higher the number, the higher the chance to degrade the substance. Rates of biodegradation for the remaining compounds are presented in Table 2.

An inhibitory effect is observed on phenol degradation by microorganisms exposed to the magnetic north field. An enhancing effect by the magnetic south pole is observed.

Acclimation of free cells to the south pole magnetic field prior to immobilization increases bio-oxidation and phenol destruction by about 100 %. Optimization studies with respect to field strength and time are needed since higher magnetic irradiation apparently decreases the rate of biodegradation, as does longer exposure. Maximum observed

enhancement with twice irradiated cells was 750 % higher than the control run with no magnetic field.

In the partial oxidation study, only one intermediate product has been identified in the biodegradation of ethylene glycol. It would be useful to find the two remaining and possibly other intermediates, and to further update kinetic studies. partial biological oxidation may yield useful products, and may have the potential of being an important technology, such as chemical partial oxidation.

In the study, the effect of substrate structure has been proposed. But other factors such as linkage (monomer to monomer) and origin (biological or synthetic), etc., should be further investigated. More study is needed to verify magnetic effects and to determine the optimal strengths of magnetic fields for activation as well as inhibition.

The model may be improved by setting up four partial differential equations, each describing the bead and the whole system which include substrate and oxygen. Also formation of partially oxidized intermediates needs to be addressed. The formation of gaseous products of partial oxidation such as CO and H_2 needs to be investigated. Any biomass accumulation needs to be more accurately measured experimentally.

APPENDIX A

Typical Bio-oxidation Pattern in the Biodegradation of Various of Organic Compounds

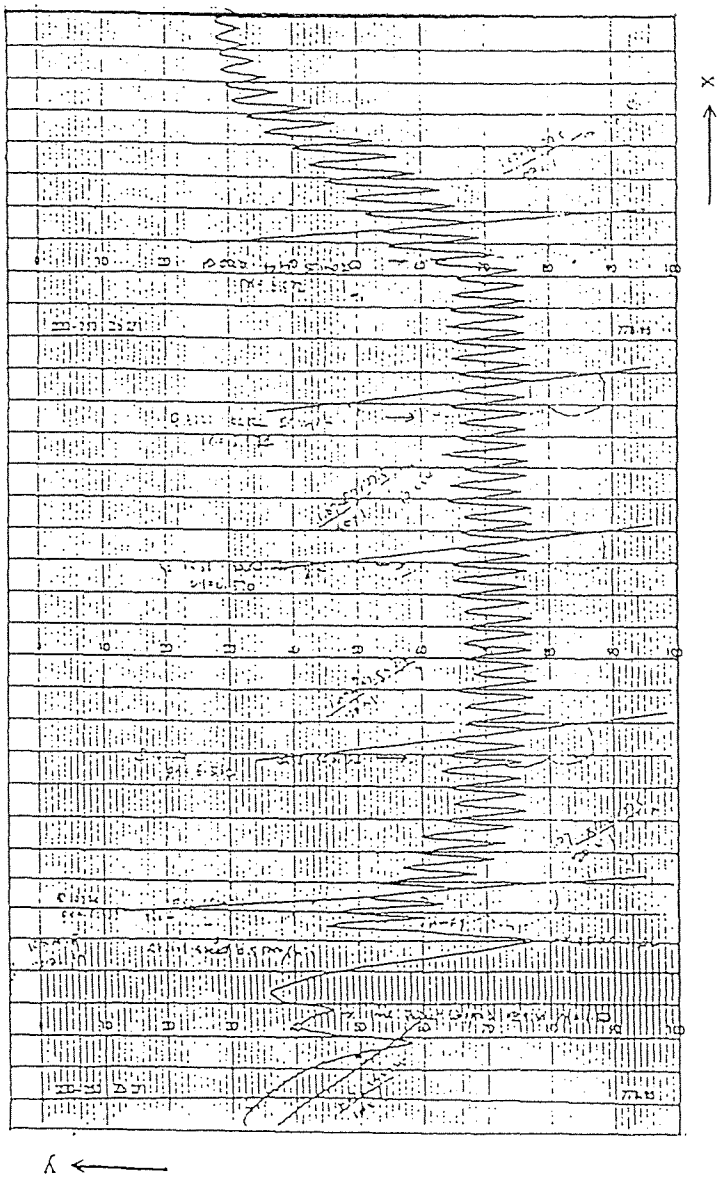

A1 : The Bio-oxidation Pattern in Biodegradation of Acetonitrile
x : Time (hours); y : DO (nmonl)

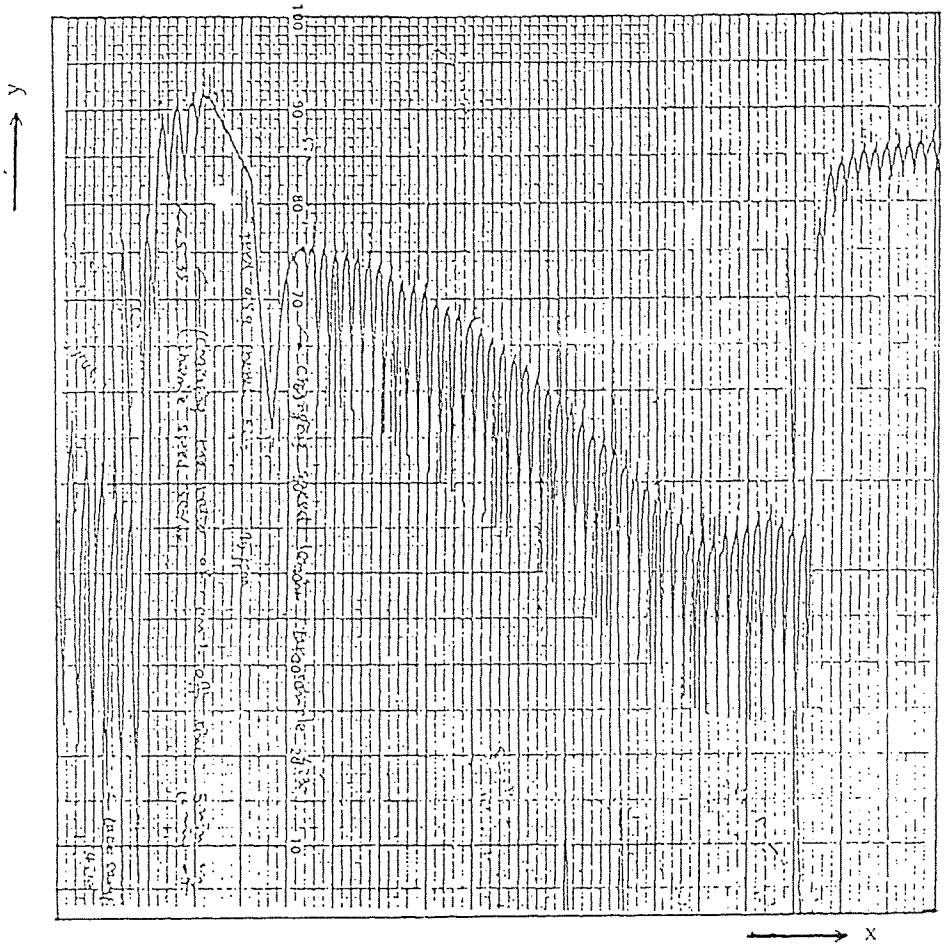

A2 : The Bio-oxidation Pattern in Biodegradation of Phenol
x : Time (hours); y : DO (nmonl)

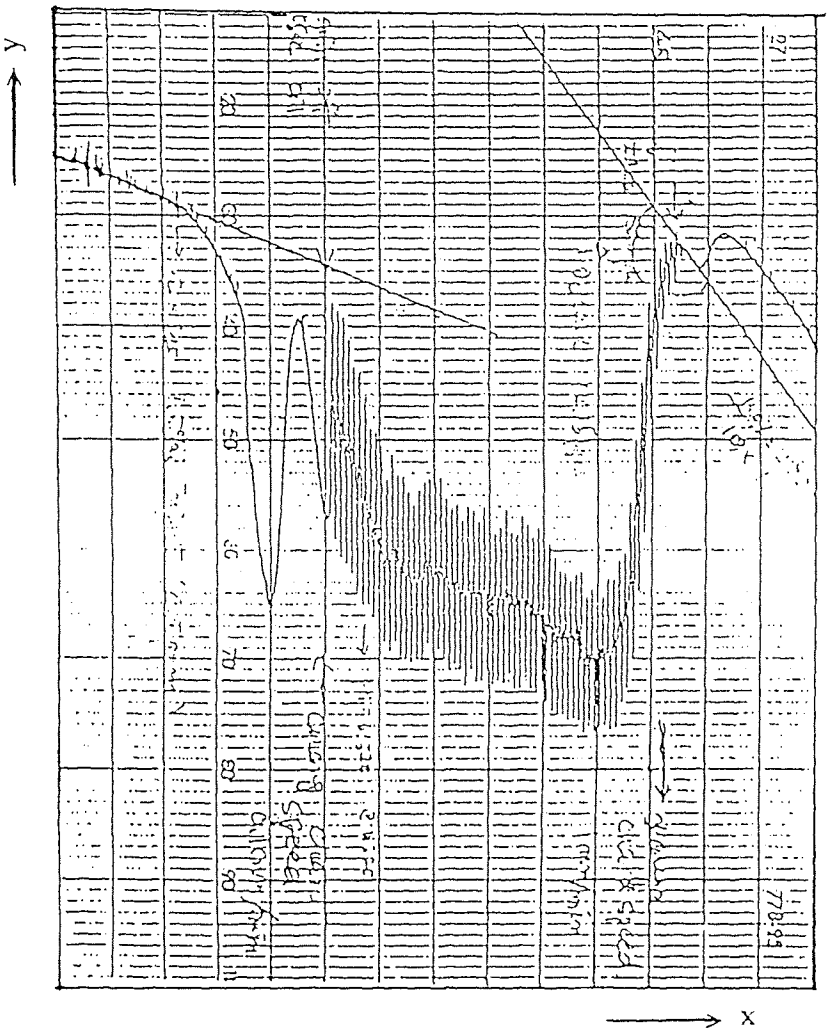

A3 : The Bio-oxidation Pattern in Biodegradation of Tetrahydrofuran
x : Time (hours); y : DO (nmonl)

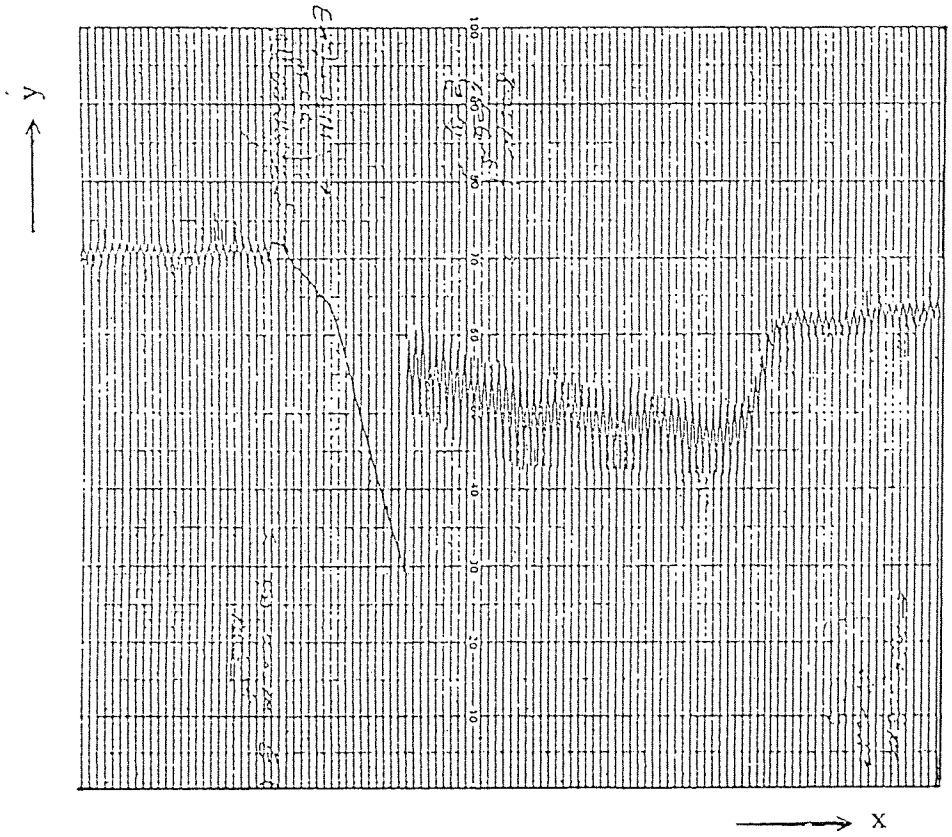

A4 : The Bio-oxidation Pattern in Biodegradation of Ethanol
x : Time (hours); y : DO (nmonl)

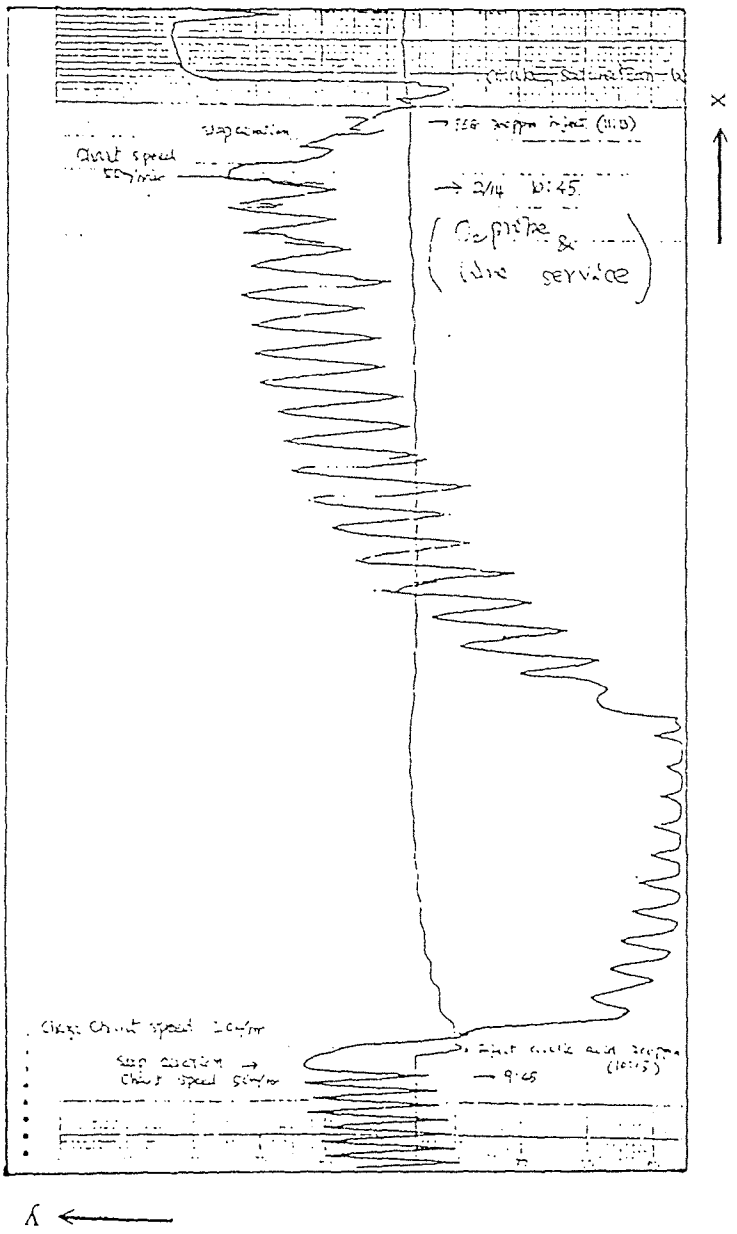

A5 : The Bio-oxidation Pattern in Biodegradation of Acetic Acid
x : Time (hours); y : DO (mmol)

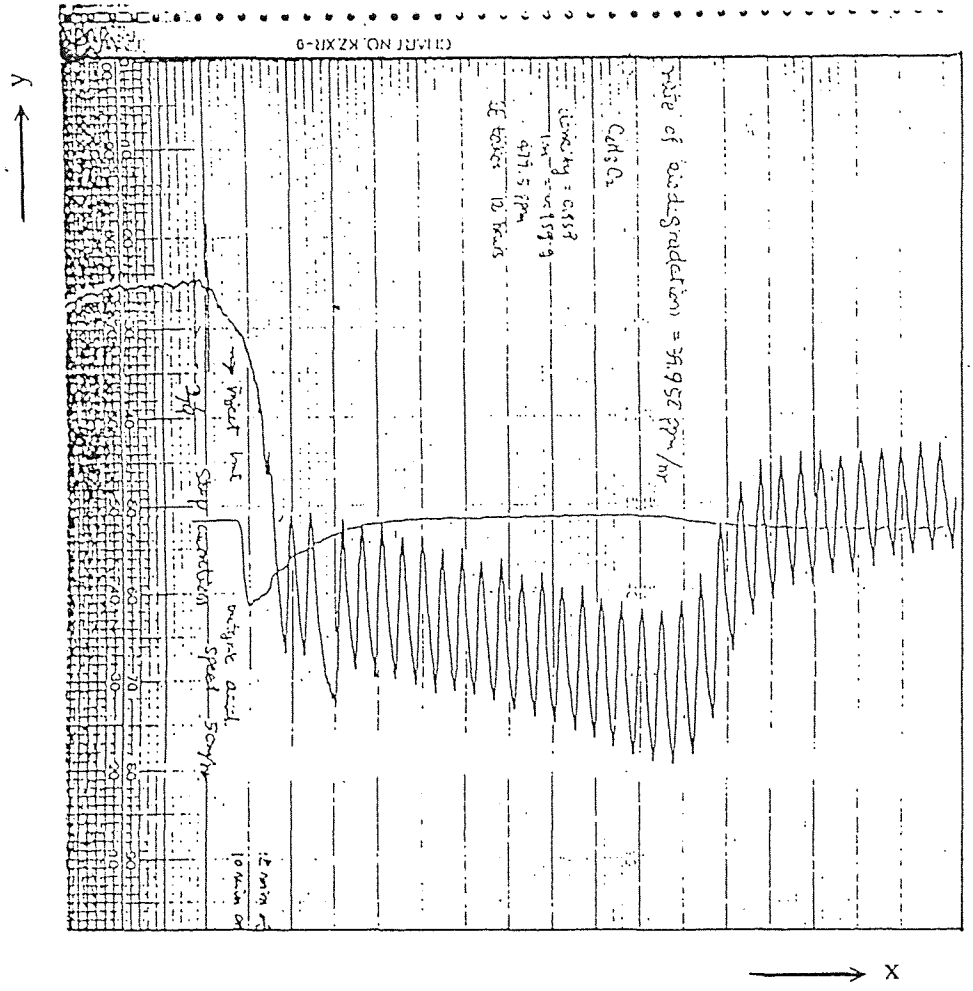

A6 : The Bio-oxidation Pattern in Biodegradation of Butyric Acid
x : Time (hours); y : DO (nmonl)

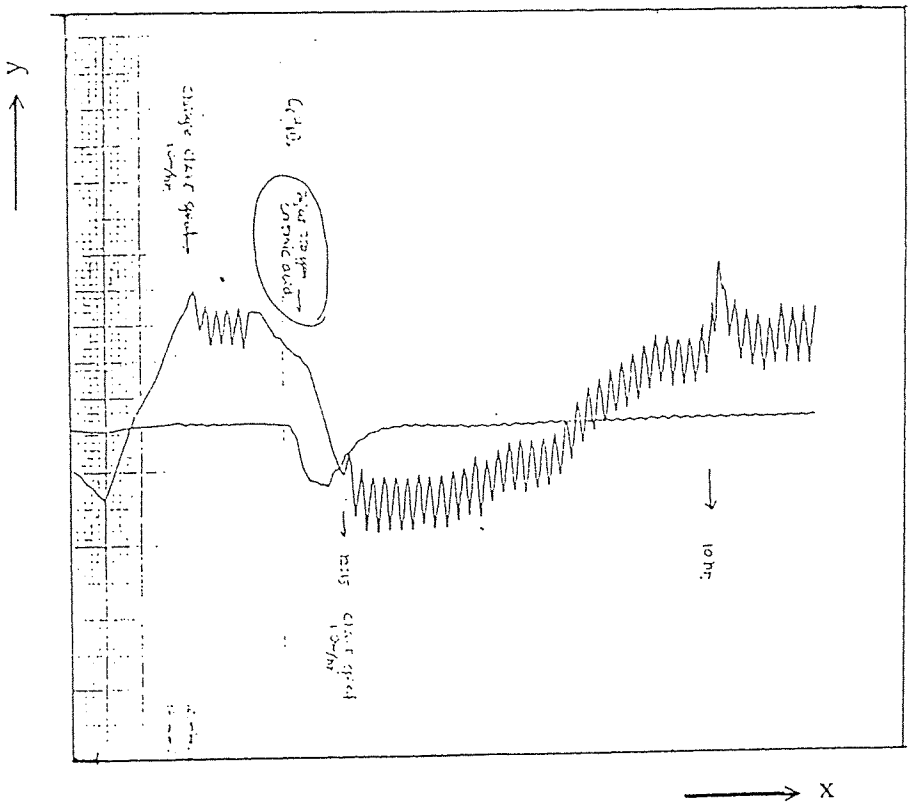

A7 : The Bio-oxidation Pattern in Biodegradation of Crotonic Acid
x : Time (hours); y : DO (nmonl)

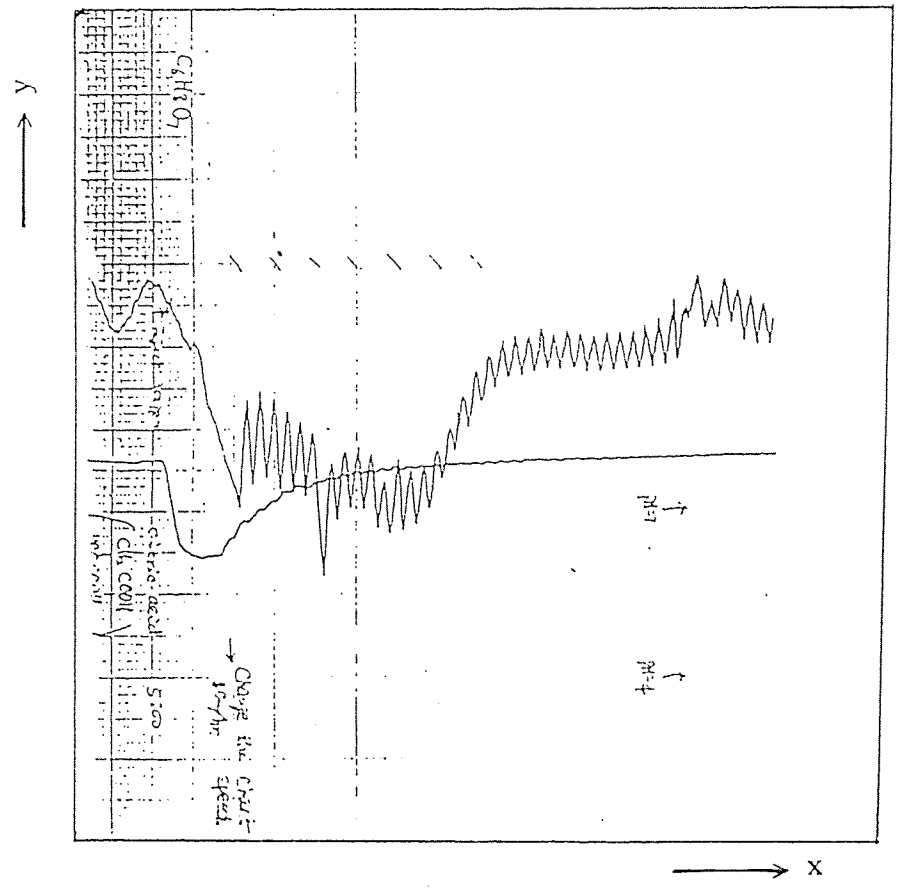

A8 : The Bio-oxidation Pattern in Biodegradation of Citric Acid
x : Time (hours); y : DO (nmonl)

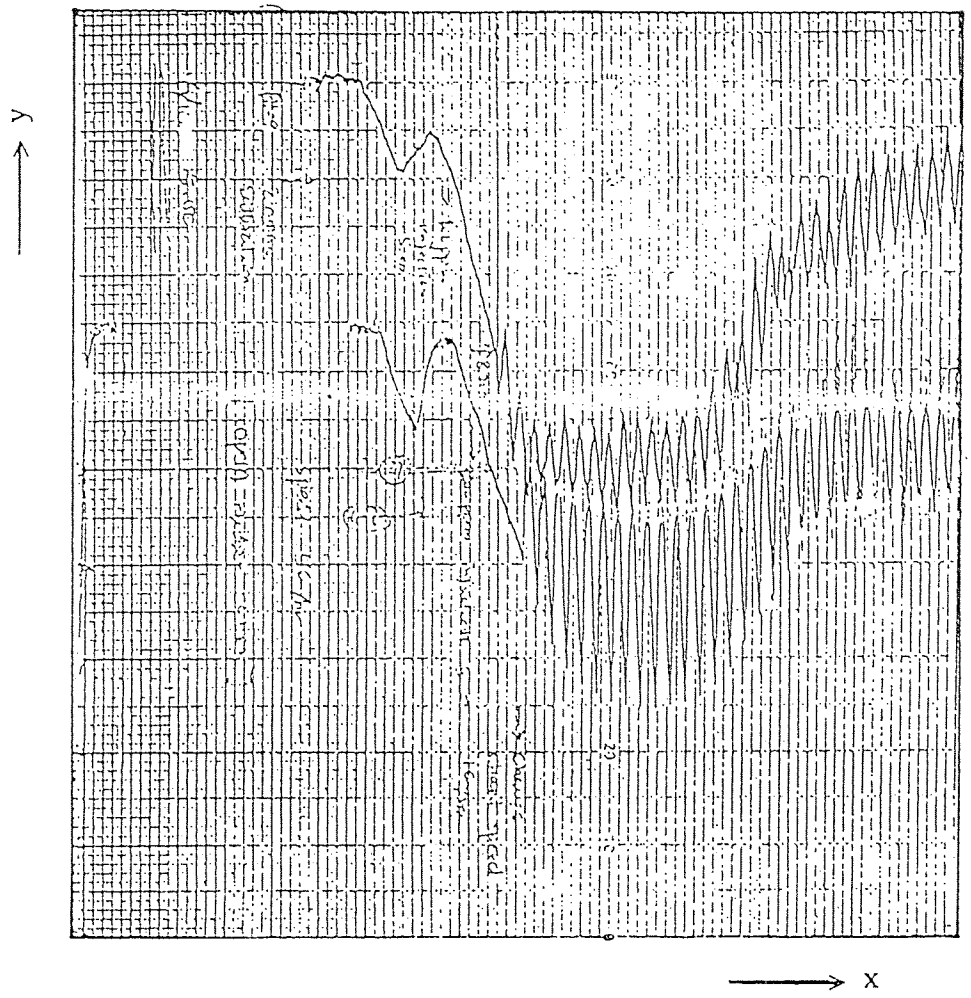

A9 : The Bio-oxidation pH Pattern in Biodegradation of Hydroxybutyric Acid
x : Time (hours); y : DO (nmonl) and pH

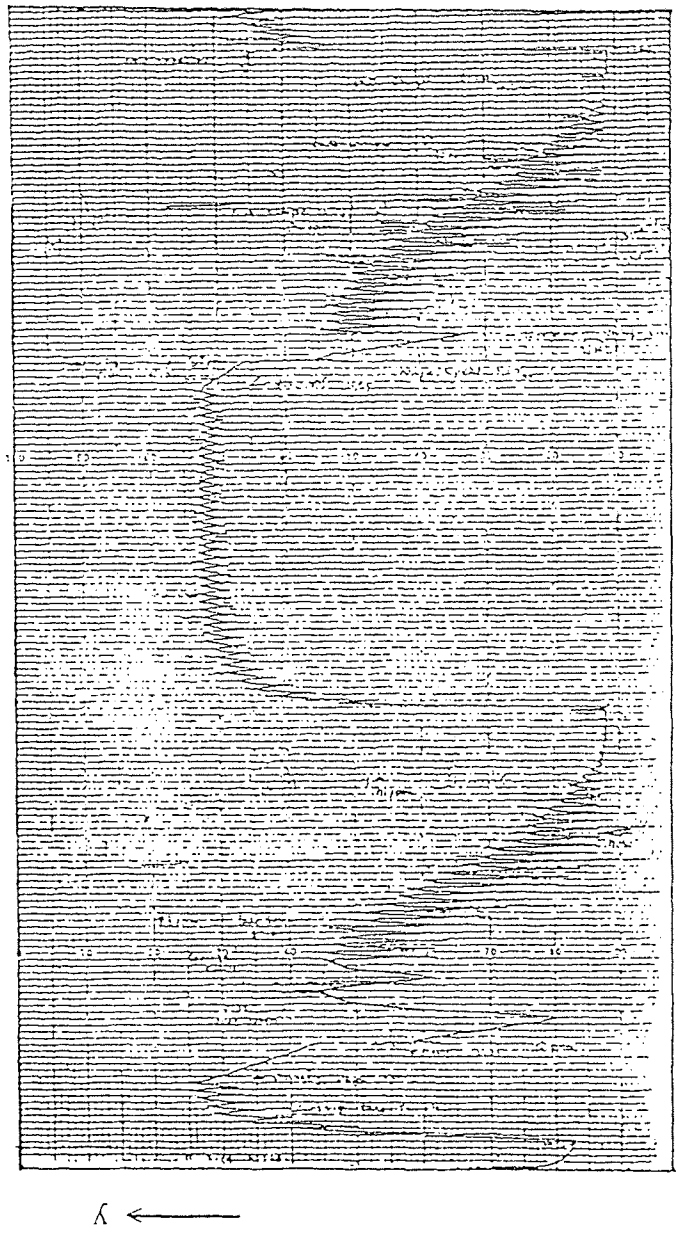

A10 : The Bio-oxidation Pattern in Biodegradation of Phenol with Magnetic Field
x : Time (hours), y : DO (nmonl)

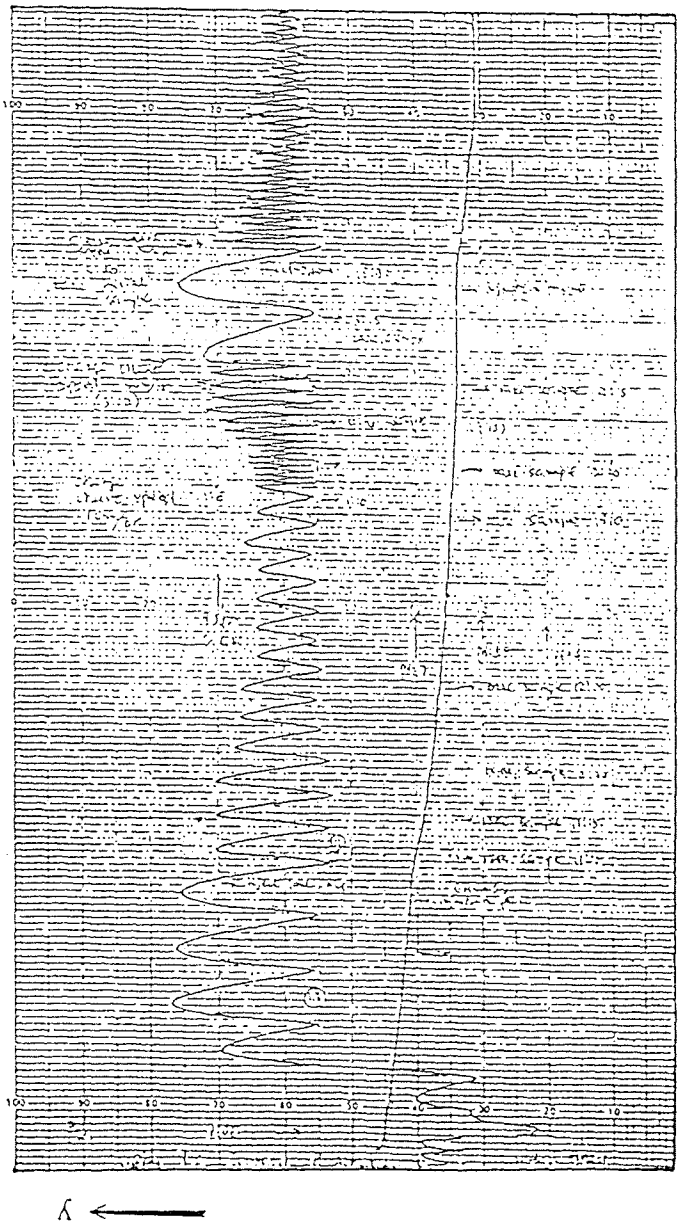

A11 : The Bio-oxidation Pattern in Biodegradation of MMA with H_2O_2
x : Time (hours); y : DO (nmonl)

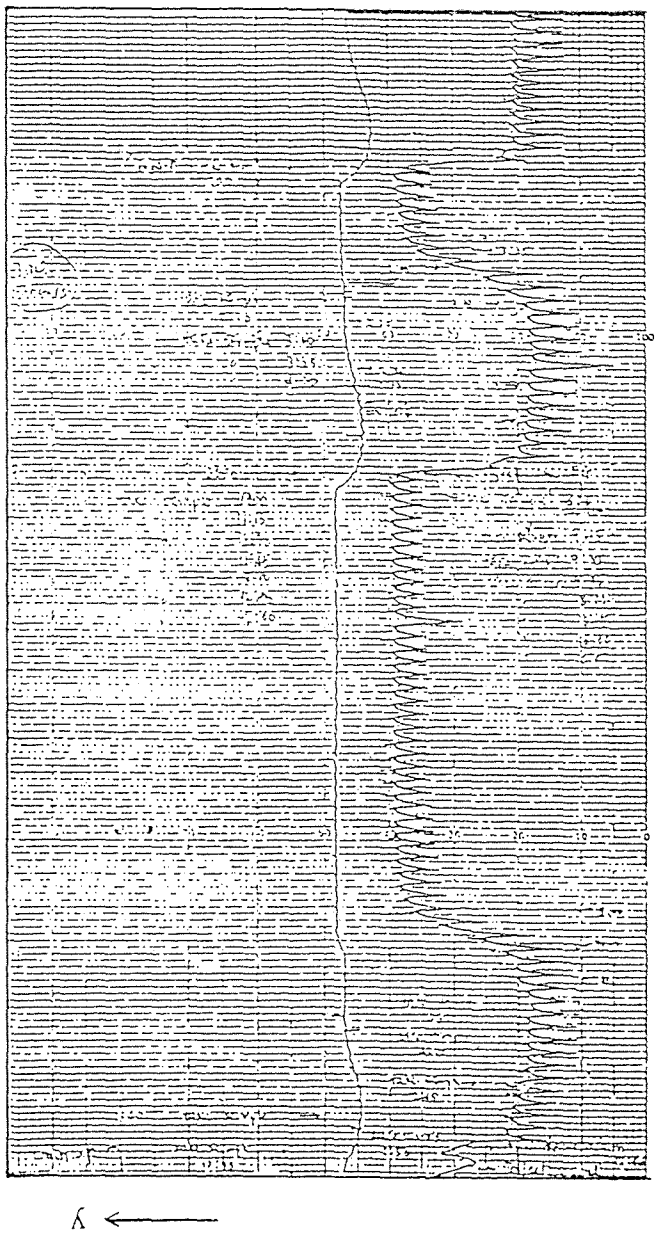

A12 : The Bio-oxidation Pattern in Biodegradation of Ethylene Glycol
x : Time (hours); y : DO (nmonl)

APPENDIX B

G.C. Peak in the Biodegradation of Ethylene Glycol

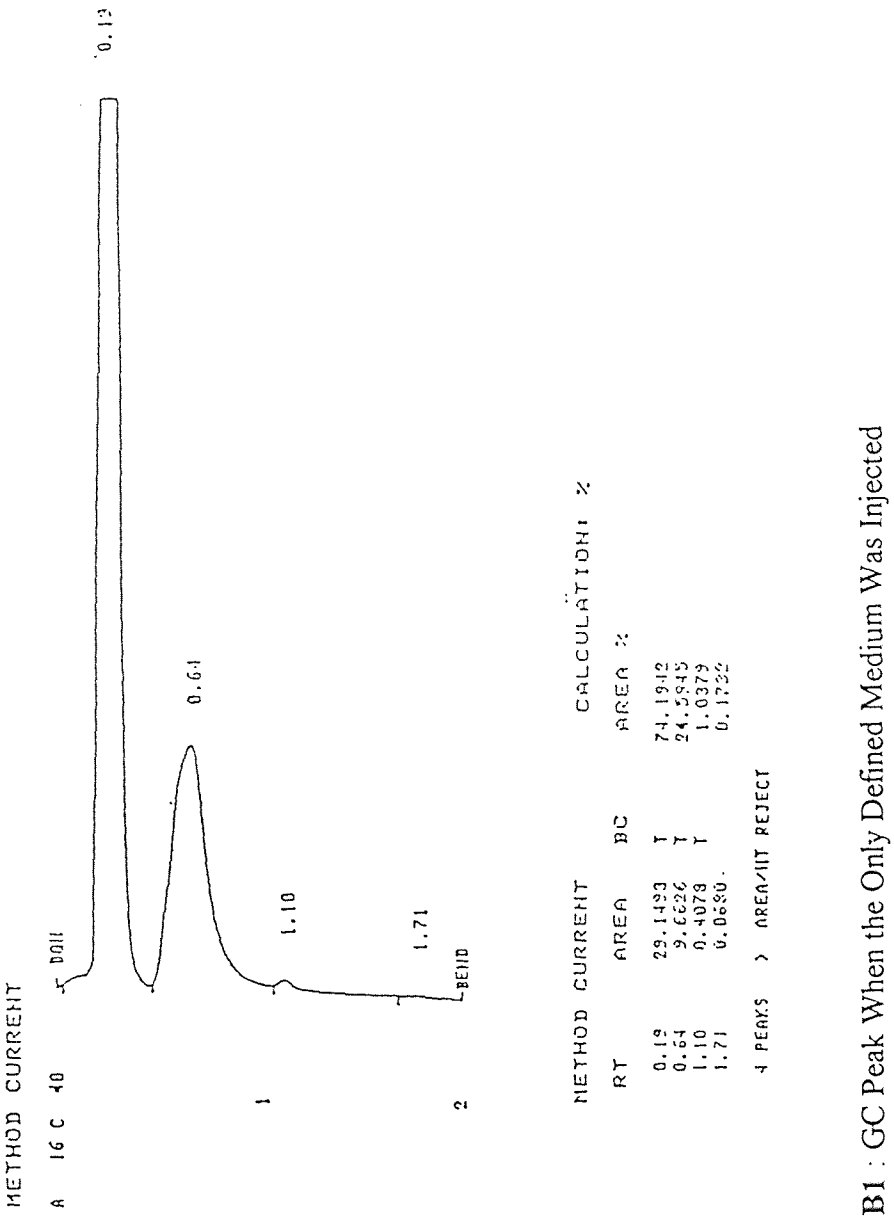

B1 : GC Peak When the Only Defined Medium Was Injected

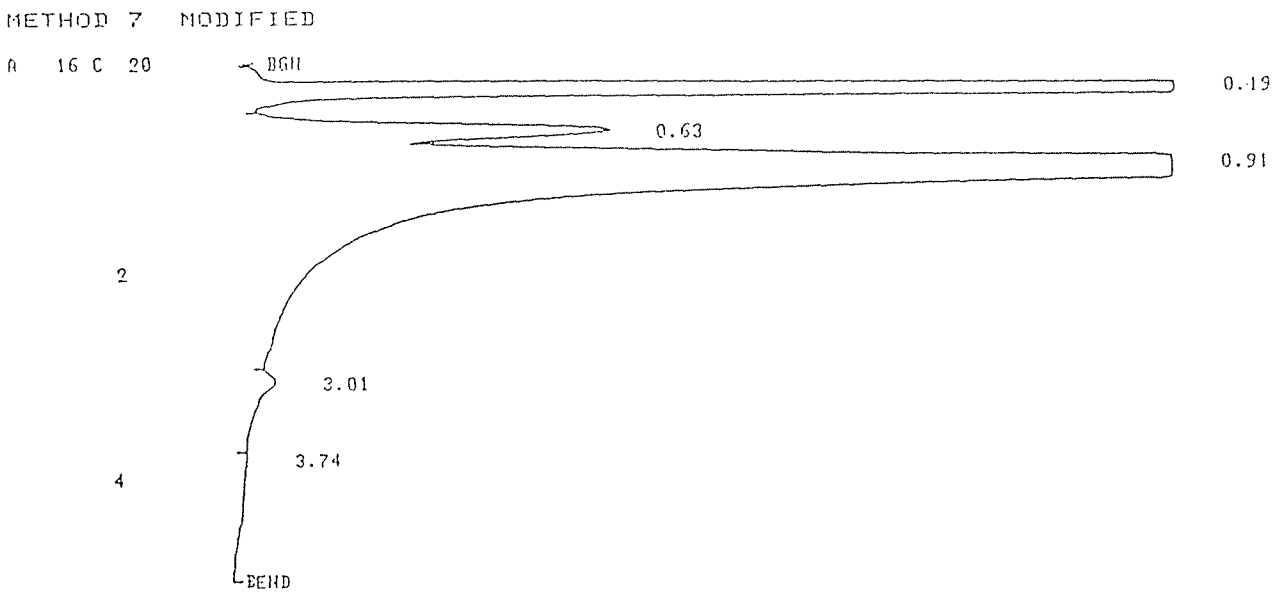

METHOD 7 MODIFIED CALCULATION: %

RT	AREA	BC	AREA %
0.19	43.5383	T	18.3933
0.63	10.7123	T	4.5257
0.91	177.7198	T	75.0823
3.01	3.1265	T	1.3208
3.74	1.6027		0.6771

5 PEAKS > AREA/HT REJECT

B2 : GC Peak When the Only Defined Medium with Ethylene Glycol Was Injected without Biomass.

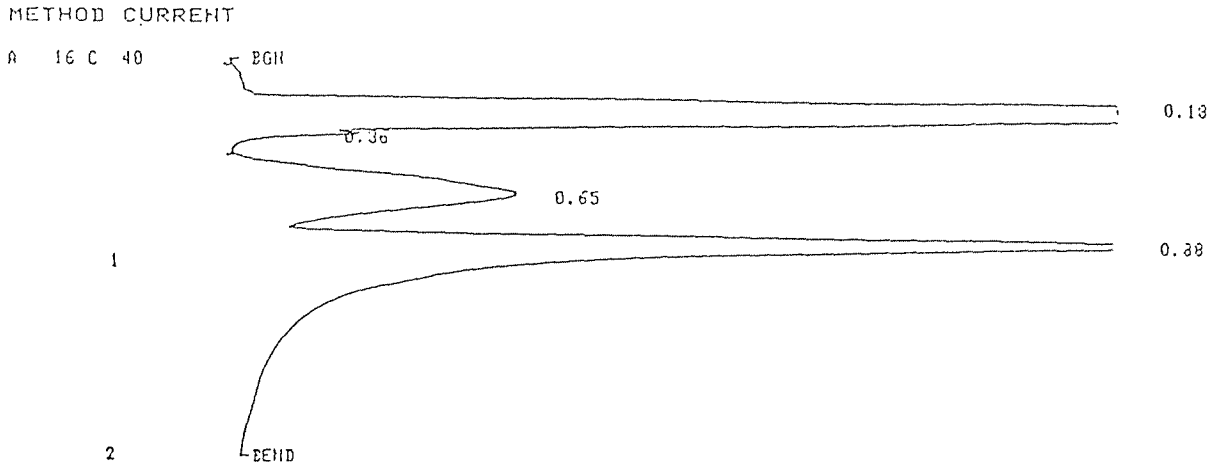

METHOD CURRENT CALCULATION: %

RT	AREA	BC	AREA %
0.13	30.9091	T	43.3090
0.36	0.7909	V	1.1083
0.65	10.8142	T	15.1526
0.88	28.8544		40.4300

4 PEAKS > AREA/HT REJECT

B3 : GC Peak at 10 Minutes After Injection of Ethylene Glycol.

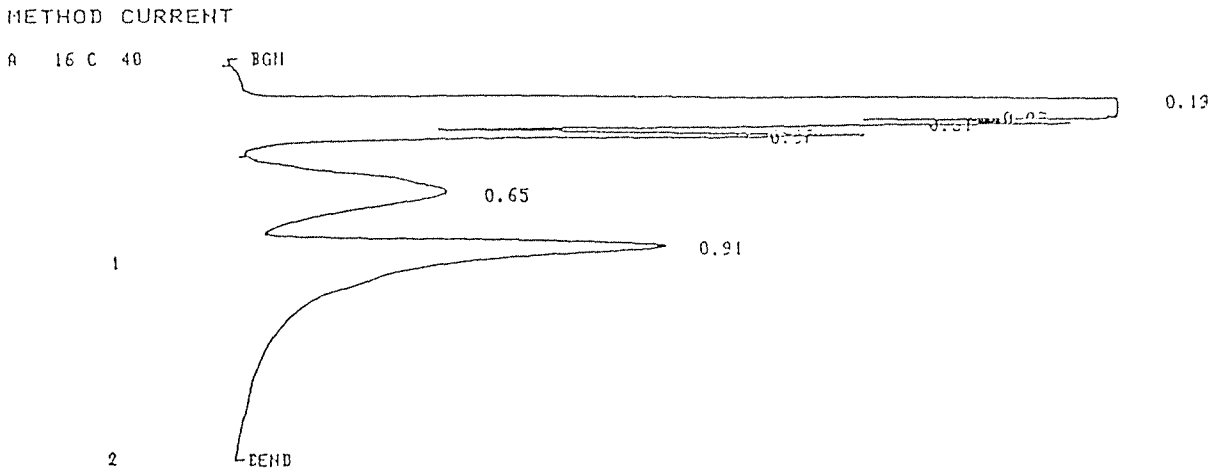

METHOD CURRENT CALCULATION: %

RT	AREA	BC	AREA %
0.19	21.3961	T	34.4763
0.27	6.2155	T	10.0152
0.31	5.7541	T	9.2718
0.37	4.1398	T	6.6706
0.65	8.2962	T	13.3679
0.91	16.2585		26.1978

6 PEAKS > AREA/HT REJECT

B4 : GC Peak at 25 Minutes After Injection of Ethylene Glycol.

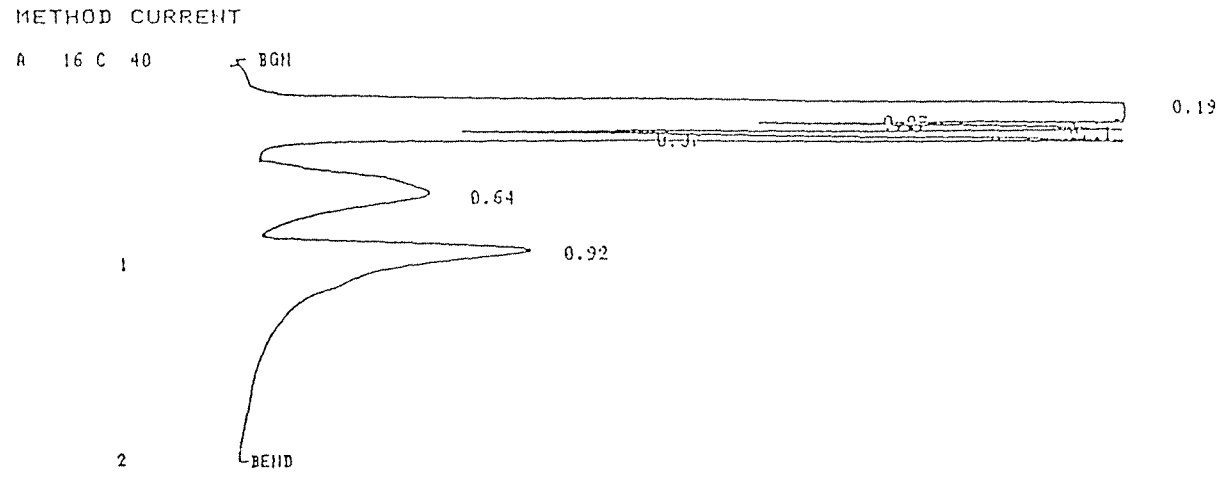

METHOD CURRENT CALCULATION: %

RT	AREA	BC	AREA %
0.19	21.0442	T	35.3535
0.27	6.7681	T	11.3701
0.31	6.3149	T	10.6089
0.37	5.9580	T	10.0092
0.64	7.3891	T	12.4118
0.92	12.0516		20.2465

6 PEAKS > AREA/HT REJECT

B5 : GC Peak at 40 Minutes After Injection of Ethylene Glycol.

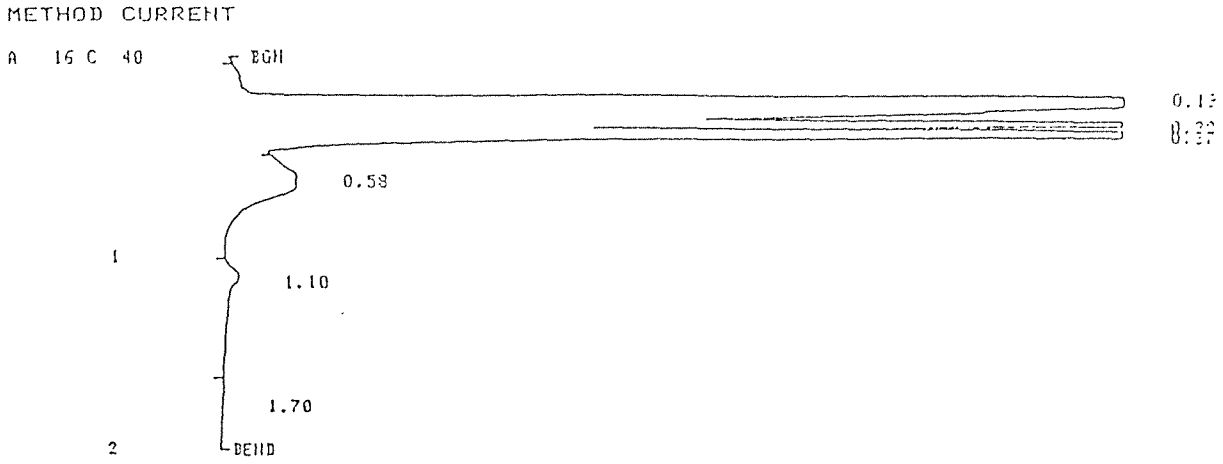

METHOD CURRENT CALCULATION: %

RT	AREA	BC	AREA %
0.19	22.7933	T	45.4070
0.32	8.9769	T	17.8871
0.37	14.5590	T	29.0033
0.58	3.1830	V	6.3409
1.10	0.5579	T	1.1114
1.70	0.1255		0.2501

6 PEAKS > AREA/HT REJECT

B6 : GC Peak at 150 Minutes After Injection of Ethylene Glycol.

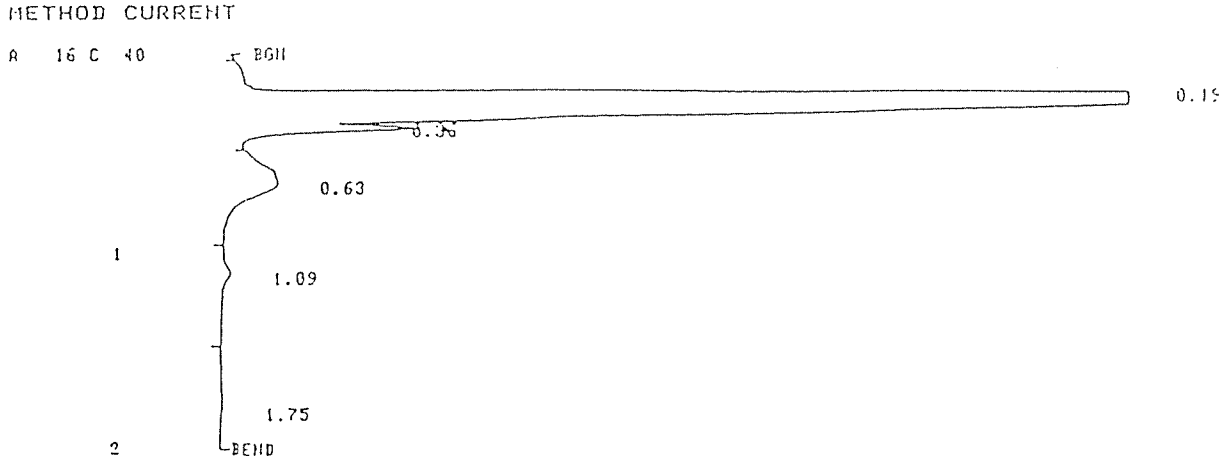

METHOD CURRENT CALCULATION: %

RT	AREA	BC	AREA %
0.19	26.3420	T	87.2546
0.36	1.4483	T	4.7974
0.63	2.1284	V	7.0503
1.09	0.1960	V	0.6493
1.75	0.0749		0.2482

5 PEAKS > AREA/HT REJECT

B7 : GC Peak at 300 Minutes After Injection of Ethylene Glycol.

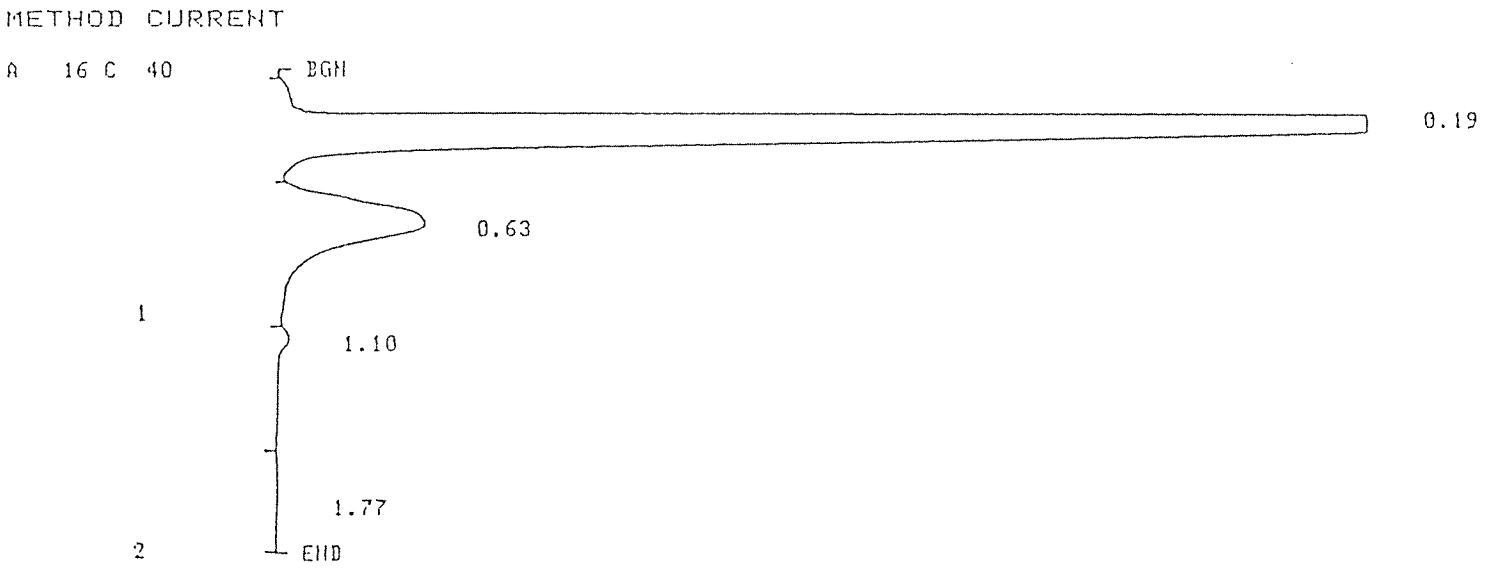

METHOD CURRENT CALCULATION: %

RT	AREA	BC	AREA %
0.19	26.8994	T	84.2261
0.63	4.7610	T	14.9076
1.10	0.2019	V	0.5324
1.77	0.0746	V	0.2337

4 PEAKS > AREA/HT REJECT

B8 : GC Peak After Bioreaction Was Over.

APPENDIX C

Program on Theoretical Substrate and Biomass Concentration Profile

```
C ***********************************************************************
C   THIS IS PROGRAM ON THE THEORETICAL SUBSTRATE
C   CONCENTRATION PROFILE IN THE SYSTEM. THIS IS USED IMSL
C   PACKAGE TO SOLVE  TWO COMBINED ORDINARY DIFFERENTIAL
C   EQUATIONS
C ***********************************************************************
    INTEGER   MXPARM, NEQ
    PARAMETER  (MXPARM=1000, NEQ=2)
C   .
    INTEGER   IDO, ISTEP, NOUT
    REAL      FLOAT, PARAM(MXPARM), T, TEND, TOL, Y(NEQ)
    INTRINSIC  FLOAT
    EXTERNAL   FCN, IVPRK, SSET, UMACH
C
    OPEN(UNIT=6,FILE='[JXJ0772.MODEL]2MMA150.OUT',
   & STATUS='UNKNOWN')
    WRITE (6,1)
1    FORMAT (4X,'ISTEP',5X,'TIME',4X,'SUBSTRATE',4X,'BIOMASS')
C
    CALL UMACH (2, NOUT)
C
C    SET INITIAL CONDITIONS
C
    T    = 0.0
    Y(1) = 150.
    Y(2) = 1750.
C
C    SET ERROR TOLERENCE
C
    TOL = 0.005
C
C    SET PARAM TO DEFAULT
C
    CALL SSET (MXPARM, 0.0, PARAM, 1)
C
C    SELECT ABSOLUTE ERROR CONTROL
C
    PARAM(10) = 1.0
C
```

```
C    PRINT HEADER
C
     WRITE (NOUT,99999)
99999 FORMAT (4X, 'ISTEP', 5X, 'TIME', 9X, 'Y1', 11X, 'Y2')
     IDO = 1
     DO 10  ISTEP=1, 50
       TEND = FLOAT(ISTEP)
       CALL IVPRK (IDO, NEQ, FCN, T, TEND, TOL, PARAM, Y)
       WRITE (NOUT,'(I6,3F12.3)') ISTEP, T, Y
  10 CONTINUE
C
C    FINAL CALL TO RELEASE WORKSPACE
C
     IDO = 3
     CALL IVPRK (IDO, NEQ, FCN, T, TEND, TOL, PARAM, Y)
     END
C
C
     SUBROUTINE FCN (NEQ, T, Y, YPRIME)
     INTEGER    NEQ
     REAL       T, Y(NEQ), YPRIME(NEQ), AKMP, AK, YP
C
     AKMP = 4.244E-3
     AK   = 7.624
     YP   = 0.537
C
C
     YPRIME(1) = - AKMP * Y(1)/YP * Y(2)/(AK+Y(1))
     YPRIME(2) =  AKMP * Y(1) * Y(2)/(AK+Y(1))
     RETURN
     END
C
C
```

APPENDIX D

Program on Kinetic Constants

```
C ***************************************************************
C   THIS IS PROGRAM FOR CALCULATING THE KINETIC CONSTANT, K_M'
C   AND K BASED ON THE EXPERIMENT DATA. THE PROGRAM IS USED
C   IMSL PROGRAM PACKAGE  TO SOLVE NONLINEAR REGRESSION
C   FUNCTION.
C ***************************************************************
C
    INTEGER   LDR, NOBS, NPARM
    PARAMETER  (NOBS=15, NPARM=2, LDR=NPARM)
    INTEGER   IDERIV, IRANK, NOUT
    REAL      DFE, R(LDR,NPARM), SSE, THETA(NPARM)
    EXTERNAL  EXAMPL, RNLIN, UMACH, WRRRN
C
    DATA THETA/7.0E-2, 5.0/
    CALL UMACH (2, NOUT)
C
    IDERIV = 0
    CALL RNLIN (EXAMPL, NPARM, IDERIV, THETA, R, LDR, IRANK, DFE,
   &          SSE)
    WRITE (NOUT,*) 'THETA = ', THETA
    WRITE (NOUT,*) 'IRANK = ', IRANK, '  DFE = ', DFE, '  SSE = ',
   &           SSE
    CALL WRRRN ('R', NPARM, NPARM, R, LDR, 0)
    END
C
C ***************************************************************
C
C   NPARM  :  NUMBER OF UNKNOWN PARAMETERS
C   THETA  :   VECTOR OF LENGTH NPARM CONTAINING PARAMETER
C              VALUE
C   NOBS   :  OBSERVATION NUMBER
C
C ***************************************************************
C
    SUBROUTINE EXAMPL (NPARM, THETA, IOPT, IOBS, FRQ, WT, E,DE,
   &                                IEND)
    INTEGER   NPARM, IOPT, IOBS, IEND
    REAL      THETA(NPARM), FRQ, WT, E, DE(1)
```

```
      INTEGER   NOBS
      PARAMETER (NOBS=15)
      REAL      EXP, XDATA(NOBS), YDATA(NOBS), B, Y
      INTRINSIC EXP
C
      S0 = 150
       B  = 1750.
       Y  = 0.537
C
C     ********* THIS IS  FOR MMA ***************************
C
       DATA YDATA/0.01, 1.0, 2.0, 3.0, 4.0, 5.0, 6.0,
     &          7.0,8.0, 9.0, 10.0, 11.0, 12.0, 13.0, 14.0/
       DATA XDATA/149.0, 137.0, 124.0, 111.0, 98.0, 86.0, 73.0, 60.0,
     &          48.0, 36.0, 25.0, 15.0, 7.5, 2.0, 0.5/
C
C     ************************************************************
       IF (IOBS .LE. NOBS) THEN
          WT   = 1.0E0
          FRQ  = 1.0E0
          IEND = 0
          E    = YDATA(IOBS) - (THETA(1)/(THETA(2)*B))
     &         *ALOG(S0/XDATA(IOBS))-(S0-XDATA(IOBS))/(B*THETA(2))
        ELSE
          IEND = 1
       END IF
       RETURN
       END
C
```

APPENDIX E

Sample Calculation for Oxygen Consumption

1. This calculation is from graphs of the type shown in Figure 5. Defining for activity giving a baseline respiration rate of 1.0 $\frac{nmols}{ml \times \min}$, the dimensions of the y-axis are $\frac{nmols}{ml \times \min \times U}$. The numbers are corrected for the normal fluctuations in oxidative activity of the biobeads over the bioreactor life.

2. Graphical Integration:

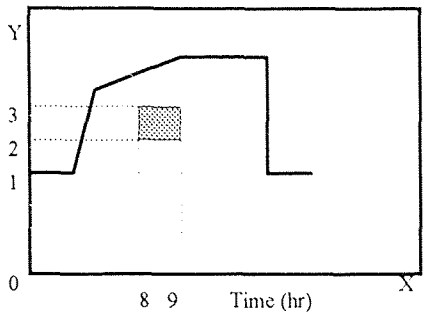

Unit of x-axis = hours, Unit of y-axis = $\frac{nmols}{ml \times \min \times U}$

Values of the square marked above are: $\frac{1.0\,nmols}{ml \times \min \times U} \times 1 \text{ hr} \times \frac{60 \text{ min.}}{1.0\,hr}$.

For a bioreactor of baseline oxygen consumption, $\frac{2.0\,nmols}{ml \times \min}$ before styrene was injected and 2000 ml reaction volume, each square represents oxygen consumed per square, $\frac{60\,nmols}{ml \times U} \times 2.0 \text{ U} \times 2000 \text{ ml}$ $(= 240{,}000\,nmols = 240\,\mu mols = 0.24\,mmols)$

3. Total oxygen consumed per run:

For styrene at 75 ppm, the total number of squares was found to be 28.75 squares.

$$28.75 \text{ squares} \times \frac{0.24\ mmols}{squares} = 6.9 \text{ mmols of } O_2.$$

$$6.9 \text{ mmols of } O_2 \times \frac{32\ mg}{mmol} = 220.8 \text{ mg of } O_2 \text{ consumed.}$$

4. Comparison with theoretical amount of O_2 required. This number is for graphs of the type shown in Figure 6 from equation (6.4).

$$C_8H_8 + 10\ O_2 \longrightarrow 8\ CO_2 + 4\ H_2O.$$

$$\frac{75\ mg}{1000\ ml} \text{ of styrene} \times 2000 \text{ ml} \times \frac{1\ mmol}{104\ mg} \text{ of styrene} = 1.442 \text{ mmols of styrene.}$$

1 mmol of styrene needs 10 mmols of oxygen for bio-oxidation.

$$1.442 \text{ mmols of styrene} \times \frac{10\ mmols\ of\ oxygen}{1\ mmol\ of\ styrene} = 14.42 \text{ mmols of oxygen.}$$

$$14.42 \text{ mmols of } O_2 \times \frac{32\ mg}{mmol} = 461.42 \text{ mg of } O_2 \text{ consumed.}$$

$$\% \text{ of abiotic loss} = \frac{21}{75} = 28\ \%.$$

461.42 mg - (0.28 × 461.62 mg) = 332.22 mg of oxygen should be consumed.

BIBLOGRAPHY

1. Hausser, A., Goldberg, B., and Mertens, J., "An Immobilized Two-Enzyme System (Fungal a-Amylase/Glucoamylase) and Its Use in the Continuous Production of High Conversion Maltose Containing Corn Syrups", Biotech. Bioeng., Vol 25 (1988), pp. 525-539.

2. Lodaya, M., *Biodegradation of Benzene and A BTX Mixture Using Immobilized Activated Sludge*, Doctoral Dissertation, New Jersey Institute of Technology, Newark, NJ, 1989.

3. Lakhwala, F., Sinkar, V., Sofer, S., and Goldberg, B., "A Polymeric Membrance Reactor for Biodegradation of Phenol in Wastewater", Journal of Bioactive and Compatible Polymers, Vol 5 No 4 (1990), pp.439-452.

4. Mattiason, B., *Immobilization Methods in Immobilized Cells and Orgenelles.* Vol.1, B. Mattiason (Ed.), CRC Press, Boca Raton, FL. 1983.

5. Kennedy, J.F., and Cabral, J.M.S., "Immobilized Living Cells and Their Applications", Appl. Biochem. Bioeng. Vol. 4(1983), pp.189-201.

6. Greene, Jr., E., "Immobilized Enzyme Kinetics", AICHE Modular Instruction Series, E5.9 (1978), pp. 68-74.

7. "Facts and Figures", Chem.and Engg. News, Vol 67 (1989), pp.45.

8. Potts, J. E., *The Encyclopedia of Chemical Technology,* John Wiley and Sons, NY, 1982.

9. Baum, B.,and Deanin, R., "Controlled UV Degradation of Plastics" Polymer-Plastic Technology Engineering, Vol.2 (1973), pp.1-28.

10. Guillet, J. ed., *Polymers and Ecological Problems*, Plenum Press, NY, 1973.

11. Jonas, V., *Plastic Ring Decomposition Study,* Oregon Liquor Control Commission, Oregon, November,1986.

12. U.S. Patents 3,860,538 and 3,753,952.

13. Taylor, L., "Degradable Plastics: Solution or Illusion", Chemtech, September (1979), pp. 542-548.

14. Potts, J., *An Investigation of the Biodegradability of Packing Plastics*, The U.S Environmental Protection Agency, EPA-R2-046, NJ, August, 1972.

BIBLOGRAPHY
(continued)

15. Barnothy, M. F., *Biological Effects of Magnetic Fields*, Plenum Press, New York, 1969.

16. Davis, A.R. and Rawls, W.C., *Magnetism and Its Effects on the Living System,* Acres USA, Kansas City, Mo, 1974.

17. Sawyer, C.N., "Milestones in the Development of the Activated Sludge Processes", JWPCF., Vol.37, No.2, (1965), pp.151-162.

18. Dwyer F.D., Krumme M.L., Boyd S.A. and Tiedge J.M., "Kinetic of Phenol Biodegradation by an Immobilized Methanogenic Consortium", Appl. and Env. Microbiol. Vol.52 (1986), pp.345-351.

19. Bettmann, H. and Rehm, H.J., "Continuous Degradation of Phenols by Pseudomonas Putida p8 Entrapped in Polyacrylamide Hydrazide", Appl. Microbiol. Biotechnol. Vol.22 (1985) pp.389 -396.

20. Andrews, S., Attaway, H., Baca, S. and Eaton, D., *Biodegradation of Volatile Organic Compounds Using Immobilized Microbes,* Presented at Haztech International Conference, Cleveland, OH, September 1988.

21. Westmeier, F. and Rehm, H.J., "Biodegradation of 4-Chlorophenol by Entrapped Alcaligenes sp. A7-2", Appl. Microbiol. Biotechnol. Vol.22, (1985) pp.301-308.

22. Sofer, S., Lewandowski, G., Lodaya, M., Lakhwala, L.,Yang, K., and Singh, M., "Biodegradation of 2-Chlorophenol Using Immobilized Activated Sludge", Res. J. WPCF Vol.62 (1990), pp.73-80.

23. Klein, J., Hackel, U. and Wagner, F, F., "Phenol Degradation by Candida Tropicalis Whole Cells Entrapped in Polymeric Ionic Networks", Immobilized Microbial Cells, K. Venkatsubramanian Ed. ACS Symposium Series Vol 106 (1979), pp.101-108.

24. Tanaka, H., Matsumura, M. and Veliky, I. A., "Diffusion Characterics of Substrate in Calcium Alginate Gel Beads", Biotechnol. Bioeng., Vol.26 (1984), pp.53-58.

25. Chien, N.K., and Sofer, S.S., "Flow rate and Bead Size As Critical Parameters for Immobilized-Yeast Reactors", Enzyme Microbiol. Technol., Vol 7 (1985), pp.538.

BIBLOGRAPHY
(continued)

26. Aldercreutz, P., and Mattiasson, B., "Oxygen Supply to Immobilized Cells:Oxygen Supply by Hemoglobin or Emulsions of Perfluorochemicals", Appl. Microbiol. Biotechnol., Vol.16 (1982), pp.165-170.

27. Chen, T., and Humphrey, A., "Estimation of critical Particle for Optimal Respiration of Gel Entrapped and/or Pelletized Microbial Cells", Biotech. Lett., Vol.10(10), (1988), pp.699-702.

28. Gosman, B. and Rehm, H., "Oxygen Uptake of Microorganisms Entrapped in Ca-alginate", Appl. Microbiol Biotechnol, Vol.23, (1986), pp.163-167.

29. Franklin Associates Ltd.,*Characterics of Municipal Solid Waste in the United States, 1960 to 2000*, NY, July 1986.

30. Taylor, L., "Degradable Plastics: Solution or Illution", Chemtech, (1979), pp.542-548.

31. Griffin, G., *Biodegradable Fillers in Thermoplastics*, American Chemical Socity Meeting, Chicago, IL. August 1973.

32. Holmes, P.A., "Applications of PHB - A microbially Produced Biodegradable Thermoplastic", Phys. Technology, Vol.16, (1985), pp. 32-36.

33. Delafield, F.P., Doudoroff, M., Palleroni, N.J., Lustry, C.J. and Contopoulos R., "Decomposition of Poly-β-hydroxybutyrate by Pseudomonads", J. Bacteriol., Vol.90, (1965), pp.1455.

34. Brandl, H., Gross, R.A., Lenz R.W. and Fuller R.C., "Pseudomonas Oleovorans As a Source of Poly-β-hydroxyalkanoates for Potential Applications as Biodegradable Esters", Appl. Environ. Microbiol., Vol.54, (1977), pp.1988.

35. Lageveen, R.G., Huisman, G.W., Preusting H., Ketelaar P., Eggink G. and Witholt B., "Formation of Polyesterrs by Pseudomonas Oleovorans Effect of Substrates on Formation and Composition of Poly-(R)-3-Hydroxyalkanoates", Appl. Environ. Microbiol., Vol.54, (1988), pp. 2924.

36. Macrae, R.M. and Wilkinson, J.F., "Poly-β-hydroxybutyrate Metabolism in Washed Suspensions of Bacillus Cerus and Bacillus Megaterium", J. Gen. Microbiol., Vol.19, (1958), pp.210-222.

BIBLOGRAPHY
(continued)

37. Slepecky, R.A. and Law, J.H., "Synthesis and Degradation of Poly-β-hydroxybutyric Acid in Connection with Sporulation of Bacillus Megaterium", J. Bact., Vol.82, (1961), pp.37-42.

38. Nakata, H.M., "Effects of pH on Intermediates Produced during Growth and Sporulation of Bacillus Cereus", J. Bact., Vol.86, (1963), pp.577-581.

39. Lusty, C.J. and Doudoroff, M., "Poly-β-hydroxybutyrate Depolymerases of Pseudomonas Lemognei", Biochemistry, Vol.56, (1966), pp.960 -965.

40. Oeding, V., and Schlegel, H. G., "β-Ketothiolase from Hydrogenomonas Eutropha H16 and Its Significance in the Regulation of Poly-β-hydroxybutyrate Metaboilsm", Biochem. J., Vol.134, (1973), pp.239.

41. Senoir, P. J., and Dawes, E. A., "The Regulation of Poly-β-hydroxybutyrate Metabolism in Azotobacter Biejerenckii", Biochem. J., Vol.134, (1973), pp.225.

42. Griebel, R. J., and Merrick, J. M., "Metabolism of Poly-B-hydroxybutyrate: Effect of Mild Alkaline Extraction on Native Poly-β-hydroxybutyrate Granules", J. Bacteriol., Vol.108, (1971), pp.782.

43. Nakayama, K., Saito, T., Fukui, T., Shirkura, Y. and Tomita, K., "Purification and Properties of Extracellular Poly(3-hydroxybutyrate) Depolymerases from Pseudomonas Lemoignei", Biochimica et Biophysica Acta, Vol. 827, (1985), pp.63.

44. Merrick, J. M., and Chi Ing Yu , "Purification and Properties of a D(-)-β -hydroxybutyric Dimer Hydrolase from Rhodispirillum Rubrum", Biochemistry Vol.5 No11, (1966), pp.3563.

45. Jurtshuk, P., Manning, S., and Barrera, C. R., "Isolation and Purification of the D(-)-β- hydroxybutyric Dehydrogenase of Azotobacter Vinelandii", Can. J. Microbiol, Vol.14, (1968), pp.775.

46. Omori, T., Jigami, Y., and Minoda, Y., "Isolation, Identification and Substrate Assimilation Specificity of Some Aromatic Hydrocarbon Utilizing Bacteria", Agric. Biol. Chem., Vol.39, (1974), pp.1775.

BIBLOGRAPHY
(continued)

47. Sielicki, M., Focht, D. D., and Martin, J. P., "Microbial Transformations of Styrene an [^{14}C]Styrene in Soil and Enrichment Cultures", Appl. Environ. Microbiol., Vol.35, (1978), pp.124.

48. Katsuhisa, S., and Kenichi, H., "Production of β-Phenethyl Alcohol from Styrene by Pseudomonas 305-STR-1- 4", Agric. Biol. Chem., Vol.43 No7,(1979), pp.1406.

49. Vainio, H., Tursi, F., and Belvedere, G. *What are the significant metabolites of styrene?,* In Cytochrome P-450, biochemistry, biophysics, and environmental implications. E. Hietanen, M. Laitinen, and O. Hanninen (eds). Elsevier Biomedical Press, Amsterdam 1982,

50. Hartmans, S., Smits, J. P., van der Werf, M. J., Volkering, F., and de Bont, J. A. M. "Metabolism of Styrene Oxide and 2-phenylethanol in the Styrene-degrading Xanthobacter Strain 124X", Appl. Environ. Microbiol., Vol.55 No11, (1989), pp.2850.

51. Hartmans, S., van der Werf, M. J., and de Bont, J. A. M., "Bacterial Degradation of Styrene Involving a Novel Flavin Adenine Dinucleotide-dependent Styrene Monooxygenase", Appl. Environ. Microbiol., Vol.56 No5, (1990), pp.1347.

52. Slave, T. , Rev. Chim., Vol 25, (1974), pp.666.

53. Pahren, H. R., and Bloodgood, D. E. , JWPCF Vol 33, (1961), pp. 233.

54. Geating, J., *Literature study of the biodegradability of chemicals in water*, EPA 600/2-81-175, U.S. Environmental Protection Agency, Cincinnati, OH.

55. Wolfe, N. L., Paris, D. F., Stream, W. C., and Bangham, G. L., "Correlation of Microbial Degradation Rates with Chemical Structure", Environ. Sci. Technol. Vol.14, (1980), pp.1143-1144.

56. Vanishnav, D. D., Boethling, R. S. and Babeu, L., "Quantitative Structure Biodegradability Relationships for Alcohols, Ketones and Alicyclic Compounds", Chemosphere Vol.16, (1987), pp. 695-703.

57. Boethling, B. S., "Application of Molecular Topology to Quantitative Structure Biodegradability Relationships", Environ. toxicol. Chem. Vol.5,(1986), pp. 797-806.

BIBLOGRAPHY
(continued)

58. Livingston, A., and Chase, H., "Modeling Phenol Degradation in a Fluidized Bed Bioreactor", AICHE Journal, Vol., 35 No12, (1989), pp. 1980-1992.

59. Antonio O. Lau, Peter F. Storm, David Jenkins, "The Competitive Growth of Floc-forming and Filamentous Bacteria: A Model for Activated Sludge Bulking", JWPCF, Vol.56, (1984), pp.52-61.

60. De Gooijer, C., Hens, H., and Tramper, J., "Optimum Design for a Series of Continuous Stirred Tank Reactors Containing Immobilized Biocatalyst Beads Obeying Intrinsic Michaelis-Menten Kinetics", Biopro. Engg., Vol. 4, (1989), pp 153-158.

61. Chambers R.P. et al., *Enzyme Engineering*, Wiley Interscience, 1972.

62. Sofer, S., Lewandowski, G., Lodaya, M., Lakhwala, F., Yang K., and Singh, M., "Biodegradation of 2-chlorophenol Using Immobilized Activated Sludge", Res.JWPCF, Vol 62, (1990), pp 73-80.

63. Young J. C. and Baumann E. R., "The Electrolytic Respirometer-I Factor Affecting Oxygen Uptake Measurement", Wat. Res. Vol.10, (1976), pp.1031-1040.

64. Carson R. J and Perry R. L., "Use of the Electrolytic Respirometer to Measure Biodegradation in Natural Waters", Wat. Res. Vol.15, (1980), pp.697-702.

65. Berkun M., "Effects of Inorganic Metal Toxicity on BOD-I, Methods for the Estimetations of BOD Parameters", Wat. Res., Vol.16, (1982), pp.559-564.

66. Umbreit W.W., Buris R. H., and Stauffer J. F., *919640 Manometric Techniques* 4th edition, Bargress, Mineapolis.

67. Jan Suschka and Edson Ferreira, "Activated Sludge Respirometric Measurements", Wat. Res. Vol.20, (1986), pp.137.

68. Sollfrank U. and Gujer W., "Simultanuous Determination of Oxygen Uptake Rate and Oxygen Transfer Coefficient in Activated Sludge Systems by an On-line Method", Wat. Res. Vol.24, (1990), pp.725.

69. Riedel K., Lange K. P., Stein H. J., Kuhn M., Ott P., and F. Scheller F., "A Microbial Sensor for BOD", Wat. Res. Vol.24, (1990), pp.883.

BIBLOGRAPHY
(continued)

70. Neurath, P.W., Berliner, M.D. , Hovnanian H.P., Larochelle M.F., *The Growth of Fungi exposed to Static Magnetic Fields*, 2nd Intnatl. Biomag. Symposium, Chicago, Illinois, 1963.

71. Aceto H. Jr., Tobias C.A., Silver I.L., "Some Studies on the Biological Effect of Magnetic Fields", IEEE Trans. Magnetic, Mag-6,(1970) pp.368-373.

72. Blakemore, R.P. "Magnetotactic Bacteria", Science, Vol190, (1975), pp.377-379.

73. Maugh, T. "Magnetic Navigation an Attrative Possibility", Science, Vol 215(1982) pp.1492-1493.

74. Thomas D. Brook, and Michael T. Madigan , *Biology of microorganisms*, Prentice Hall. Englewood Cliffs NJ, 1983.

75. Lowenstam, H. A., "Minerals Formed by Organisms", Science, Vol 211, (1981), pp.1126-1131.

76. Mann, S., "On the Nature of Boundary-organized Biomineralization (BOB)", Journal of Inorganic Chemistry, Vol 28, (1986), pp.363-371.

77. Greenbaum, B., Goodman E., and Marron M., "Effects of Extremely Low Frequency Fields on Slime Mold : Studies of Electric, Magnetic and Combined Fields, Chromosome Numbers and Other Tests. In Biological Effects of Extremely Low Frequence Electromagnetic Fields", Proc. 18th Hanford Life Sciences Symp. pp.117-131.

78. Marron, M., Goodman E., Greenbaum B., and Tipnis P., "Effects of Sinusoidal 60 HZ Electric and Magnetic Fields on ATP and Oxygen Levels in the Slime Mold, Physarum Polycephalum", Bioelectromagnetics Vol 7, (1986), pp.307-314.

79. Watson, J and E. Downes E., "The Application of Pulsed Magnetic Fields to the Stimulation of Bond Healing in Humans", Jap. J. Appl. Physics, Vol 17, (1978), pp.215-217.

80. Fardon, J.C., Poydock, M.E. and Basvito, G., Nature, Vol 211, (1966), pp. 433-434.

81. Shyshlo M. A. and Shimkevich L. L., "The Effect of Static Magnetic Fields on the Oxidative Processes of Albino Mice", Proc, 3rd Internl. Biomagnetic Symp., (1966), pp.16-18.

BIBLOGRAPHY
(continued)

82. Gerencser, V.F., Barnothy M. F., and Barnothy J.M., "Inhibition of Bacterial Growth by Magnetic Field", Nature Vol 196, (1962), pp.539.

83. Brown, F.A. Jr., and Barnwell F. H., "Organismic Orientation Relative to Magnetic Axes, in Response to Week Magnetic Fields", Biol. Bull. Vol 121, (1961), pp.384.

84. Tang Yun, *Isolation and Characterization of a Crude Extracellular Phenol Oxidase from a Recirculation Bioreactor*, Masters Thesis, New Jersey Institute of Technology, Newark, NJ, 1991.

85. Roels, J. A., *Energetics and kinetics in biotechnology*, Elsevier Biomedical Press, New York, 1983.

86. Bailey, J. E, Ollis, D. F, *Biochemical Engineering Fundamentals*, McGraw-Hill, New York, 1977.